Seismic response of steel and composite steel joints with semi-continuous connections.

Parameshwar, Jagalur D

CIVIL AND COMPUTATIONAL ENGINEERING CENTRE

SWANSEA UNIVERSITY

SEISMIC RESPONSE OF STEEL AND COMPOSITE STEEL JOINTS WITH SEMI–CONTINUOUS CONNECTIONS.

PARAMESHWAR. J. D

Supervisor

DR. ROBERT Y. XIAO

SUBMITTED TO THE SWANSEA UNIVERSITY IN FULLFILMENT OF THE REQUIREMENTS FOR THE DEGREE OF MASTER OF PHILOSOPHY

DECLARATION

This work has not previously been accepted in substance for any degree and is not being concurrently submitted in candidature for any degree.

Signed .....(candidate)

Date ..21/03/2008.....

STATEMENT 1

This thesis is being submitted in partial fulfilment of the requirements for the degree of Master of Philosophy.

Signed .....(candidate)

Date ..21/03/2008.....

STATEMENT 2

This thesis is the result of my own investigations, except where otherwise stated. Other sources are acknowledged by footnotes giving explicit references. A bibliography is appended.

Signed .(candidate)

Date ..21/03/2008.....

STATEMENT 3

I hereby give consent for my thesis, if accepted, to be available for photocopying and for inter-library loan, and for the title and summary to be made available to outside organisations.

Signed ...(candidate)

Date ..21/03/2008.....

SYNOPSIS

This research aims to develop an accurate, well-defined finite element model to evaluate and predict behaviour of the semi-continuous composite connection with flush endplate under monotonic and cyclic loading. Connections are most vulnerable area in any structure. A structural engineer has to choose suitable connections considering structural as well as economic factors. Much research have been carried out on experimental investigations with both kind of loading on various connections and presented appreciated results and also suggested to design standards. Finite element method has been extensively used as an effective method in all sectors to predict appropriate results and behaviour of particular location of the structure, which can not be measured from experimental investigation.

In this research, the case studies offer more insight into the 3D- simulation of finite element modelling of flush endplate connection has been developed and compared the results with experimental investigations carried out by Y.Xiao, B.S. Choo & D.A. Nethercot [6] under static loading and J.Y.Richard Liew, T.H.Teo, N.E.Shanmugam [10] under both cyclic and monotonic loading. Comparisons between numerical and experimental data for moment-rotation curves showed satisfactory agreement. Also, in this research, finite element analysis has been carried out on recent flush endplate composite connection tested under monotonic and cyclic loading, which will be tested experimentally in Tongaji University, China. Finite element results are presented in Chapter-5 for further research to compare with available experimental results in future.

ANSYS finite element package has been selected for developing and analysing the 3D finite element modelling. Different parameters have been selected and moment-rotation curve for each case have been evaluated. Initially the bare-steel joint was modelled with hexagonal bolt hole and finally refined with circular bolt hole considering practical situations. The moment-rotation curve and stresses of both cases have been compared and found only 5% to 7 % variations in the results.

ACKNOWLEDGEMENTS

I am very grateful for the support given by my supervisor, Dr. R.Y. Xiao during this work. I would like to thank him for directing me to this challenging and interesting field of research, for the possibilities to introduce the results of the study in many international research forums and his trustful support throughout the work.

I wish to thank Prof. Obey Hasan, Dr. Nityaraju Urs and Dr. Rajesh Ransingh for their advice during initial stage of my course. Also I would like to thank to Prof. J. Bonnet for his assistance and teaching during structural dynamics class.

I am very much grateful to my wife, father-in-law and family for their encouragement and support in both the difficult and the exciting moments of my studies. Also I am very much thankful to my parents and all my family members for their contribution.

I am most grateful to Mrs. G.J. Rao, Branch manager of Corporation Bank, India, for the financial support. Also would like to thanks to Mr. J.D. Nagaraju for his immense help to pursue this study and to Mr. S. Tauffik for help with the development of FE model in this research.

Modern research is reliant on computers and electronics, and users depend on the support staff to keep the computers running. I am most grateful to Mrs. Diana Cook, who helped me for solving problems in my computer system, during my research. Thanks also to Miss. Jacquie for her help and co-operation during my research. I am

also grateful to all the University's staffs and particularly the staffs at the University's Library, for their guidance and co-operation during my research.

Thanks go to those who have provided me advice, information, or publications and papers, including: Tauffik, Fabio, Wahid, Shaarijaan, Chin and other Dr. Xiao's students.

My candidature has been an enjoyable time, and I have made friends amongst my research colleagues. The assistance of my friends made my experience worthwhile. My special thanks goes to Mr. Mazio, who advised me during my research for my personal as well as other problems. Finally I would like to thank all my friends for their help and co-operation during my candidature.

TABLE OF CONTENTS

LIST OF FIGURES

LIST OF TABLES

LIST OF SYMBOLS

M	Bending moment
δ	Deflection
Φ	Rotation
E	Modulus of elasticity
t_{cf}	Thickness of column flange
t_{cw}	Thickness of column web
b_c	Width of column
D_c	Over all depth of column
d_c	Effective depth of column (C/C of flange)
t_{bf}	Thickness of beam flange
t_{bw}	Thickness of beam web
b	Width of beam
D_b	Over all depth of beam
d_b	Effective depth of beam (C/C of flange)
δ_y	Elastic deflection
f_{cu}	Characteristic strength of concrete
E	Young's Modulus
$S_{j,ini}$	Initial stiffness
L	Beam length (i.e. Dist from applied load to face of column)
P	Applied load

$[K]$ Stiffness matrix

$\{q\}$ Vector of nodal field variables (displacements) for elements

$\{q_o\}$ Vector of nodal field variables (displacements) due to initial effects

$\{Q\}$ Vector of nodal field actions (forces) for elements

$\{Q_o\}$ Vector of nodal field actions (forces) due to initial effects

Δ Prefix indicating a finite element increment

CHAPTER 1

INTRODUCTION

Seismic responses to the structures are important in terms of analysis, design and connection detailing. In seismic zones large load reversals may occur. This load reversal will normally require a different approach to the design of the load-resisting structure, leading to different forms of connection. Beam-column connections are essential to the behaviour of moment-resisting frame structures, in their response to earthquake ground shaking. There are two basic functions which these connections must perform. The most basic of these functions is to transfer gravity loads from the beam to the column so that the beam remains attached to the structure. The second function is to provide the stability against lateral sideway and to provide for transfer of sideway related flexural stresses between the beams and columns. The beam-column connection must retain the ability to perform both of these functions for the credible levels of loading likely to be induced by the combined effects of gravity and earthquake-induced loading.

Seismic actions produce deformations with relatively few repetitions of the action. Deformations of fairly large amplitude occur at fairly low speeds. These deformations exhibit cyclic characteristics which may produce low cycle fatigue phenomena of structural elements and connections but rarely their failure. However,

the possibility of damage of element failure due to external cyclic loading such as those produced by earthquakes should be considered in design.

Many researchers reported that, semi-continuous connection is suitable for earthquake resistant structures due to its inherent enough ductility, flexibility, strength, energy absorption and plastic rotation capacity to withstand the seismic forces.

In the case of conventional design, the connections between the beams and columns are treated as nominally pinned or as rigid, resulting in a simple or continuous construction, respectively. But in reality, these connections are not fully characterized with the connection behaviour being between these two extremes. Assuming that the connection is pinned leads to an overly conservative design as no moment transfer can occur at the connection, meaning deeper steel sections required for the beams. Connection design has a major influence on the costs of real structures.

The semi-continuous approach offers a middle course. It is based on designer decision to make use of beam end moment and thereby reduction in cost, as illustrated in Figure 1.1. This end moment is usually set equal to the resistance of a suitable not-too-elaborate connection detail. The beam is then sized for mid-span M $= M_{FREE} - M_{CONN}$. Therefore, such type of connection is key to the semi-continuous frame design. The important features of a connection in semi-continuous framing are that, it is ductile and partial strength.

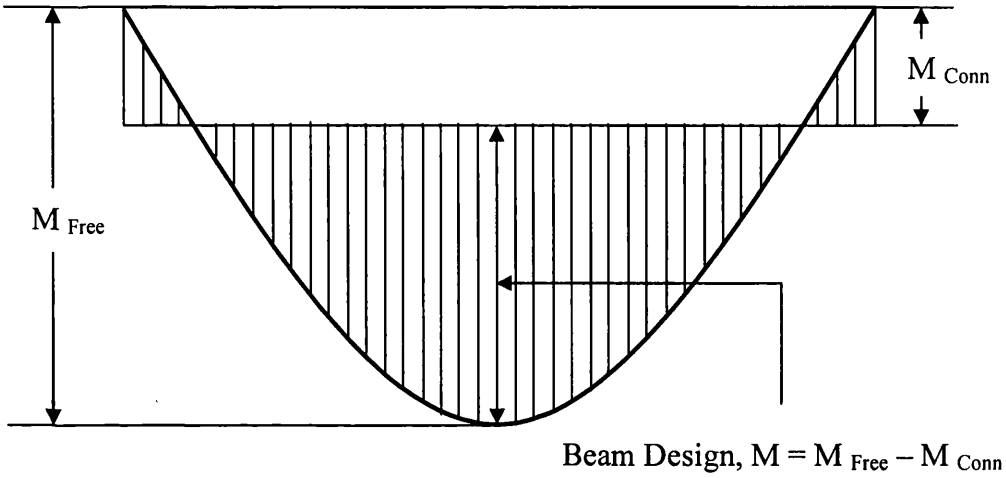

Fig : 1.1. Bending moment diagram for semi-continuous beam

Experiments have shown that the actual behaviour of a connection is nonlinear and lies between the two idealised models. From these models by treating the connection as semi-continuous, it will possible to establish some new design standards for steel frames that utilise semi-continuous connections in terms of strength and deformation capacities.

Also, it offers designer control of the bending moment diagram to optimise overall economy not making additional demands on designer's time otherwise it would be treated as pinned and also by avoiding the stiffness required in rigid connections.

Steel – concrete composite frames are structurally efficient because they exploit the tensile strength of the steel and the compressive strength of the concrete. This efficient use of materials accounts for the success of the structural form in new steel framed multi-storey buildings. Furthermore composite beams in buildings generally are not characterized by a full continuity due to the beam to column connections, thus the analysis and the detailing of such parts in case of gravity and seismic loads have key role in the development of suitable design procedures.

Eurocodes gives a classification for connections as pinned, rigid, or semi-rigid [1, 2]. Connections are usually conservatively designed as pinned, due to the high fabrication costs of rigid connections. However, this allows a simpler frame design process. There have been research efforts in recent years how to classify connection types [4], in which the connections have been classified by strength, stiffness and deformation capacity or ductility.

Eurocode 4 [2] is only for vertical loading as well as horizontal loading patterns on composite steel and concrete structures. On other hand Eurocode 8 [3] deals with design provisions for earthquake resistance to steel – composite structures, but short part is that is devoted to this specific kind of structures due to the lack of knowledge [8].

However, the design guidance and rules of application for the steel-concrete composite connections treated as semi-continuous are now proposed and implemented in design codes. Guidelines for the design of building frames are also available including the connection behavior and methods for the evaluation of the mechanical properties and of the non-linear moment displacement relationship of the connections. Satisfactory design concepts based on semi-continues connection have already been proposed and manuals providing connection capabilities have recently been published for designers [13, 14].

The main aim of this thesis is to investigate the suitability of finite element modeling to compare with the experimental investigation conducted by different authors [6,10] for semi-continuous approach using flush endplate connection subjected to monotonic and seismic loading in the form of cyclic pattern.

1.1 STRUCTURAL PERFORMANCE OF BUILDINGS DURING EARTHQUAKE

Experience has shown that for new structures, the implementation of seismic construction regulations can provide a safeguard against damage from earthquakes. For existing buildings damage will need to be evaluated and then the choice is to repair and strengthen or rebuild. Observations of the structural performance of buildings during an earthquake can identify the strong and weak aspects of their design, as well as suitable materials and construction techniques and site selection.

Damage in earthquakes is caused by four basic effects:

- ground shaking
- ground failure
- tsunamis (seismic sea waves)
- fire after the earthquake.

1.2 AIM OF THE RESEARCH

The primary aim of this research is to develop computational 3D finite element aspects related to the modelling of steel and composite steel joints with semi-continuous connections subjected to static as well as cyclic loading. The ANSYS 8.1 software package has been used to simulate 3D finite element modelling.

1.3 OBJECTIVES

The behaviour of semi-continuous connection at beam-column junction is studied both steel structures as well as in composite structures. The principal purpose is to gain a better understanding of the engineering features of semi-continuous joints under both static and seismic loading and to apply this design knowledge to the structures situated in seismic zones.

In this work, finite element analysis of beam-column connections on bare steel and composite joint is performed and results are validated against the experimental test values. The effects of different parameters like thickness of endplate, bolt diameters are also studied which can significantly influence the over all behaviour of connections. This study emphasize on the moment, rotation and post – failure behaviour.

The research tasks for the study are set as follows:

- Study and investigate the behaviour of semi – continuous connections
- Develop computer simulation of connection modelling using ANSYS -8.1
- Perform finite element analysis on connection modelling by static loading as well as cyclic loading.
- Compare finite element results with experimental investigation conducted by different authors.
- Study on different parameters
- Develop finite element results for further research.

1.4 OUTLINE OF THESIS

The extensive literature review related to semi-continuous connections is presented in Chapter 2 in which the achievements of other researchers are presented and the discrepancies are also discussed. Attention was focused on ultimate moment capacity, rotation and post failure behaviour. Chapter 3 contains general introduction of FEM and application of ANSYS software. The structural details of the new connection configuration developed in this work, the terminology and the methodology of computational approach are described in Chapter 4, in which the connection studied and its components are introduced. The assessment of the finite element analysis results are presented in Chapter 5. The conclusions and suggestions for further research are given in Chapter 6.

In the Appendices, the following information are included:

Appendix I: Calculation procedure.

Appendix II: Input file for finite element analysis using ANSYS.

CHAPTER 2

INTRODUCTION TO SEMI-CONTINUOUS CONNECTIONS AND LITERATURE REVIEW

2.1 INTRODUCTION

This chapter provides an introduction to semi-continuous connections in steel frames, and examines the relevant previous research in this area, including aspects such as moment-rotation capacity and behaviour of joints under static and cyclic loads in steel and composite joints. The discussion is mainly focused on steel and composite steel joints. Emphasize is given on initial stiffness in Moment-rotation, ductility and post failure strength of composite members. The interface between steel and concrete is also reviewed.

The moment-rotation response of a composite joint is mainly influenced by the following factors.

- Deformation of the connecting plates.
- Bolt deformation and slippage.
- Shear deformation of the column web panel.
- Elongation of steel reinforcement in the slab.
- Interface slip of shear connectors.

2.2 BEAM – COLUMN CONNECTION

The design of connections in frames should be based on the satisfactory performance criteria varying from the erection, to the serviceability and ultimate state conditions. The following requirements for the advanced connection system have influenced the design of the connection configuration to meet the best possible performance at all the limit states including the fabrication and erection:

- Simple detailing in steel work.
- Welding on site should be minimized.
- In order to keep composite beam design easy, the steel beam is designed as simply supported during the erection and concreting work. This means that the bare steelwork connections should be designed as hinges and they are employed to resist only vertical shear.
- The moment resistance and flexural stiffness of the composite joint is provided by the tensile action of the slab reinforcement and the balancing compression is transferred to the column by the steel beam. Any contribution of the steel web elements to moment rotation behaviour of the composite joint should be avoided.
- In the composite state, the joint should have sufficient rotation capacity so as to ensure the redistribution of bending moments required by the plastic global analysis of the composite floor beam.

2.3 TYPES OF CONNECTIONS

In the system adopted in Eurocode 3, the joints are classified by two criteria separately: stiffness and strength. Depending on the stiffness of the joints relative to the stiffness of the connected beams, joints are classified as pinned, semi rigid and rigid. Depending on the moment capacity of the joints relative to the connected beams, connections are classified as pinned, partial-strength and full-strength.

The concept of semi-continuous construction requires a statement of the joint behaviour to help the designer to choose a suitable basis on which to carry out the

overall frame analysis. It is necessary to be aware that just as the term rigid is sometimes used loosely to mean nothing more than 'rotation-resistant', the term semi-rigid is sometimes used to describe semi-continuous construction in general. This is unfortunate.

a) PINNED

A nominally free-rotating hinge that prevents any rotational continuity between the connected members.

b) RIGID

No relative rotations occur between the members connected at the joint. Rigid connection is capable of resisting moments with a high stiffness i.e., the connection flexibility/rotation has a negligible influence on the distribution of movements in the frame connections.

c) SEMI-RIGID

The transmitted moment in a joint will result in a difference between the absolute rotations of the two connected members. In this case, connections also need to possess a certain amount of stiffness to reduce deflections at serviceability limit state.

d) FULL-STRENGTH

Joint is stronger than the weaker of the connected members. This type of joint can at least develop the bending strength of the elements it connects.

e) PARTIAL-STRENGTH

The moment capacity of the joint is less the hogging bending resistance of the adjacent beam. The partial strength connections are able to resist the hogging moments at the beam ends. However, they can only be used when the support can resist the applied moment, namely for:

- Connections to the flange of a column
- Connections to the web of a column when there is an opposing beam with a connection of equal strength. This limitation is necessary unless the column is stiffened locally to prevent deformation of the web.

The partial strength connections must be ductile to ensure that they can behave as plastic hinges.

f) CONTINUOUS

The joint ensures a full rotational continuity between the connected members, covering the rigid/full-strength cases.

g) SEMI-CONTINUOUS

The joint ensures only partial rotational continuity between the connected members, covering the rigid/partial-strength, the semi-rigid/full-strength and the semi-rigid/partial-strength cases.

2.4 BASICS OF SEMI-CONTINUOUS CONNECTION

The connection in semi-continuous framing has partial strength and ductility. The ductility of connection is synonymous with rotation capacity (the term used in Eurocode 3), and should not be confused with ductility of a material such as steel. Partial strength of connection has less ability to resist the plastic moment of the beam.

Some merits of semi-continuous construction [13]

1. Depth of beam may be shallower than in simple construction and it leads to reduction in building height and cladding area.

2. It can ease integration of services inside the building

3. Weight of beams may be less as compare to simple construction

4. Connections are less complicated as compared to continuous construction
5. Frames are more robust than in simple construction.
6. It can be achieved between the column of composite frames and slim floor beams and slabs resulting in drastically reduced sections, construction cost and time [14].

In semi-continuous connection, if connection moment capacity increases, the sagging moment for which beam must resist in case of simple connection decreases. The savings in beam weight and depth are possible because of benefits at both the ultimate limit state and serviceability limit state.

Semi-continuous connection has some disadvantages as compare to simple connection viz:

1. Increase in connection cost compared with simplest of simple connection.
2. A slight increase in design complexity.

2.4.1 METHODS OF ANALYSIS

Any frame can be analysed using elastic analysis to determine the moments and shear forces. Plastic analysis can also be used as an alternative option provided that the frame satisfies certain requirements, principally concerning ductility at potential plastic hinge locations.
The following types of analysis can be used in any frame analysis

1. Elastic analysis
2. Plastic analysis
3. Elasto -plastic analysis

1. Elastic analysis:

The stiffnesses of frame members are considered in an elastic analysis. This analysis widely used for simple and continuous frames. But it is not suitable for semi-

continuous design because it requires quantification of connection stiffness, which may prove difficult in practice.

2. Plastic analysis:

In this analysis, strengths of members and connections are considered rather than their stiffness. Connection strength means moment capacity which can be predicted with sufficient accuracy using current methods. Plastic analysis is based on the assumption that the plastic hinges form at critical points in the frame, and rotate to allow redistribution of moments. This rotation requires substantial ductility at these points

3. Elasto -plastic analysis:

In an elasto -plastic analysis, stiffness and strength considerations are both taken in to account. This type of analysis may be used for semi-continuous connections using proper software considering all the connection characteristics, i.e. stiffness, strength and ductility. In this research, ANSYS-8.1 has been used for the analysis of semi-continuous connections.

2.4.2 MOMENT – ROTATION RELATIONSHIP

The rotation capacity of connection is also called as ductility of connection. The behaviour of any type of connection may be fully described by a moment-rotation curve. The three most important characteristics which define such a curve are:

- Stiffness, which is given by the slope of the curve
- Strength (or moment capacity), which is given by the peak value of moment on the curve
- Ductility, or rotation capacity, which is given by the maximum rotation which the connection can undergo before a significant loss in strength occurs.

  The above three characteristics are indicated in Fig 2.1, which shows the moment rotation curve for a typical connection which might be used for semi-continuous construction.

The assumption made in plastic frame analysis and design, namely that, plastic hinges form in the connections requires the connection to be ductile enough to accommodate the necessary rotation without loss of strength. The semi-continuous connections must posses the following [16]

- Strength or moment resistance of the connection is often in the range of 30% to 50% of the plastic moment capacity of the beam.
- The rotation or ductility which the connection must accommodate is varies between 0.02 to 0.04 radians.
- Stiffness (enough to make them at least semi-rigid according to the code definitions for example Eurocode 3, clause 6.4.2.3) [13]

Although connection stiffness has no part to play in plastic analysis, it is worth considered that some stiffness is required to reduce the deflections at the serviceability limit states.

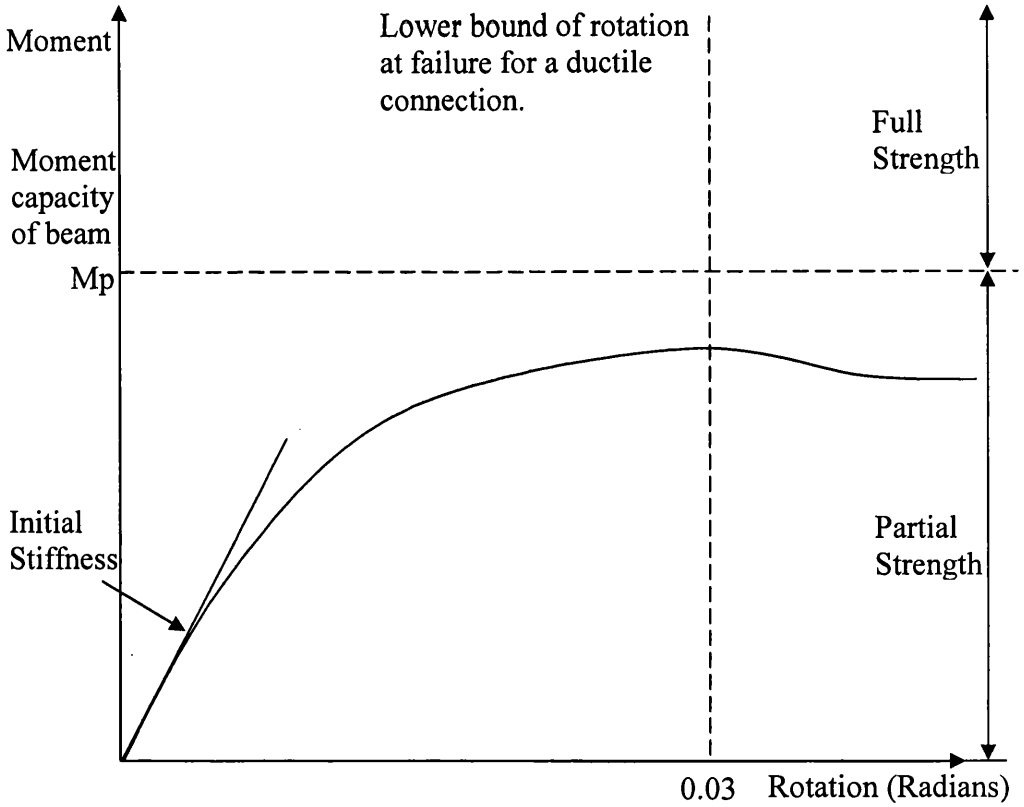

Fig : 2.1 Moment – rotation curve applicable for semi-continuous connection [13].

2.5 RESEARCH IN TO THE SEMI-CONTINUOUS CONNECTIONS (LITERATURE REVIEW)

The research on effects of partial strength and semi-rigid connections has been investigated since the early 1980. Some design rules and regulations of semi-continuous connections have been incorporated in some codes and specifications. However ductility requirements for connections are not properly established in these codes and documents particularly for composite connections which achieve continuity through the use of reinforcement in the slab. Since the modelling of composite connections is very complicated, it can be divided in to three zones as tension, compression and shear [11]. But in this thesis, computational approach using ANSYS software package version 8.1 has been adopted to make modelling of steel and composite connections with due considerations.

The general rule is that the connection moment capacity should be greater than or equal to the applied moment, and the connection rotation capacity should be larger than that required to develop the moments in the beam at the ultimate limit state [12].

The studies discussed are mainly divided in to three parts. In the first part the experimental studies conducted by different researchers on semi-continuous connections have been discussed. In the second part, theoretical approaches on semi-continuous connection studied by different authors have been discussed. And in final part finite element approach used by different publishers on semi- continuous connection studied and discussed.

2.5.1. EXPERIMENTAL STUDIES

Recent experimental study conducted by Y. Richard Liew, T.H. Teo, N.E. Shanmugam [10] includes tests on eight composite joint specimens and one bare-steel joint under reversal of loading. Bolted flush endplate, extended endplate with or without haunch section connection were adopted for test specimens. The columns were either bare steel or reinforced with doubler plate or partially enclosed with concrete. The percentage of steel used in 120mm thick Reinforced Concrete slab is

1.12%. The moment-rotational response of joints was studied subjected to negative and positive bending moment.

The experimental studies concluded that, for flush endplate connection subjected to negative bending, its moment capacity and initial stiffness is higher than the corresponding values when subjected positive bending. This difference can be minimized by providing a stronger steel connection as, extended endplate or haunch section. The cyclic loading requires stronger connections to resist the resultant shear force produced by unbalanced moments.

Provision of doubler plate to the column flange increases shear resistance of panel zone and compressive resistance of column web, which governs the negative moment capacity of composite joint with flush endplate subjected to monotonic and cyclic loading. Positive and negative moment capacities of joint can be enhanced by providing haunch connection without increasing the overall depth of beam. The objective of enhancement is primarily due to increase in the depth of the haunch connection and thus the moment lever arm.

Concrete encasement also increases initial rotational stiffness of joint under both positive and negative bending. The concrete filling in the column web portion performs slightly better results than doubler plate in negative moment region but the effect is the same in case of positive bending.

In 2001, B.M.Broderick and A.W. Thomson [15] has conducted experimental tests to study the seismic behaviour of flush endplate connections under monotonic and cyclic loading conditions. The test specimen consists of eight bare-steel beam-to-column sub-assemblages. The sub-assemblages consisted of a 1 m length of universal beam section connected to a 1 m length of universal column section with different endplate thicknesses of 8 mm, 12mm and 20mm and different bolt diameter of M20 and M16 . The column section used was 203 x 203 x 86 kg/m UC while two different beam sizes were employed (254 x 102 x 22 kg/m UB and 254 x 146 x 37 kg/m UB). The joint consists of an endplate welded to the end of the beam with full strength continuous welds and bolted to the column flange.

The specimen details were selected to display a range of failure modes. They concluded that, comparison with design equations showed a tendency to overestimate joint stiffness and underestimate joint moment capacity, although the mode of failure was usually predicted accurately. The researchers observed that, under cyclic loading, many of the specimens displayed large rotation ductility capacities, and their modes of failure were similar to those displayed with monotonic loads. Where ultimate failure was observed, this was most often due to thread stripping on nuts and bolts.

The performance of the test specimens indicates that this joint type could be applied to earthquake-resistant design—that is they displayed a stable cyclic response up to a determinable rotation limit. However, further investigations are required to determine whether this joint type can be practicably employed in earthquake-resistant frames. These investigations should consist of a series of case-studies to evaluate the seismic resistance of frames already designed to resist wind-loading, employing static inelastic push-over analysis dynamic time-history analysis.

Robert Y.Xiao and C.D. Fisher [20] conducted experimental test on real building in the year 2000, which is constructed with full use of semi-continuous design approach, the first ever in Europe to be designed and constructed. This test was conducted at an academic complex in Southampton city-centre constructed for Southampton Institute. The results of experimental investigations have been validated against finite element approach using ANSYS Software package. The deflection results are or more less alike in both experimental and theoretical approach.

In 1993, Y.Xiao, B.S. Choo & D.A. Nethercot [6], conducted experimental investigations on different types of composite connections like flush endplate, seating cleat, fin plate and etc under static loading. Researchers observed that,

- the flush endplate has the highest moment capacity as compare to seating cleat and fin plate connections with same type of mesh reinforcement.

- the initial stiffness, moment resistance and rotational capacity were dramatically affected by changes to the reinforcement ratio in the slab, metal decking, steel joint type, column web stiffening and moment shear ratio.

- the presence of the column web stiffener not only prevents failure in the column but also increases the moment capacity of the connection without having much influence on the rotation capacity of the beam-column connection.

Hubber[14] used semi-continuous approach in Millennium Tower, which is situated in the north of the centre of Vienna, Austria. The total height of the building is 202m which is tallest building in Austria as shown in Fig 2.2. In this building, the semi-continuous connection was achieved between the column tubes of composite frames and slim floors beams and slabs resulting in drastically reduced sections, construction cost and time. The semi-continuity has been considered in the design at ultimate and serviceability limit states.

The demands for an extremely fast and weather independent erection, very thin slabs (reduced dead load and lower facade costs) with a plane ceiling (easier installation) and very slender columns called for an ingenious solution, which included the following building innovations: Composite slim floor beams fully integrated into the thin slabs, moment-resisting (semi continuous) joints enabling a frame action between the beams and columns and a new type of shot-fired shear connector within the composite columns.

In case of semi-continuous joints, the use of composite slim floor beams in combination with composite columns solves two problems simultaneously which would appear in conventional concrete joints: punching and a low moment resistance combined with a brittle failure due to the limited load introduction of concrete in compression

The composite slim floor beams are built of welded T-shaped steel sections and a concrete slab with minimum sagging reinforcement and a considerable amount of reinforcement in the hogging region within the effective width as shown in Fig 2.3.

The shear connection is provided by headed studs. The actual configuration of a joint between a column and a slim floor beam used at the millennium tower is shown in Fig 2.4.

It was shown that a simple support during erection can easily be transferred into a moment resisting joint with considerable stiffness and resistance at final stage. Activating this frame action between beams and columns enables the realization of very slim floors under observance of ultimate and especially serviceability limit states. In addition the use of shot-fired nails and bolts as shear connectors within the hollow column sections helped speeding up the erection.

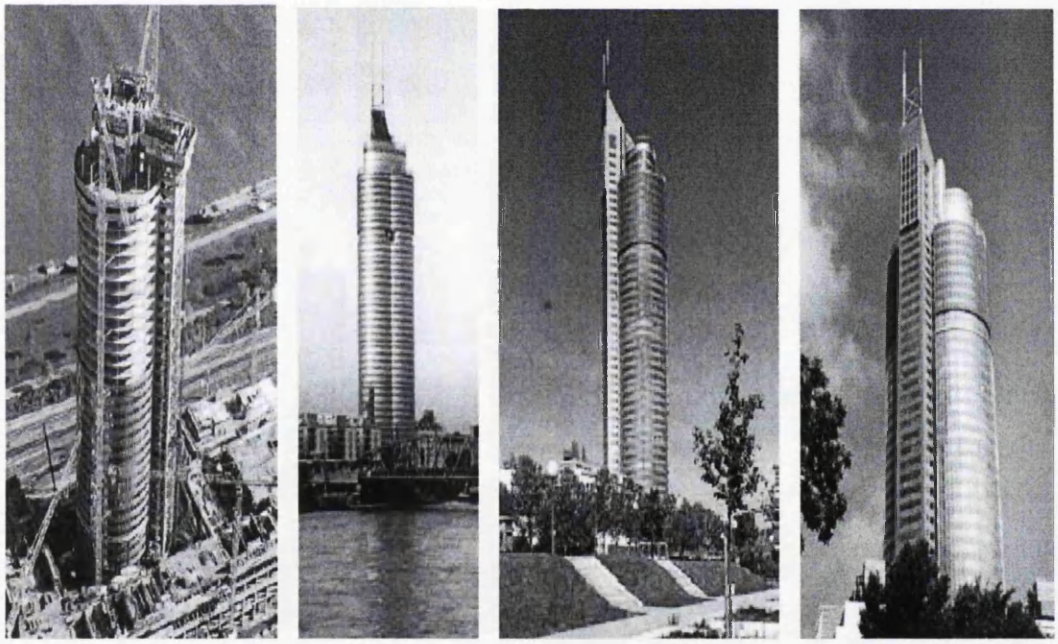

Fig: 2.2– Semi-continuous design approach used in Millennium Tower, Vienna, Austria [14].

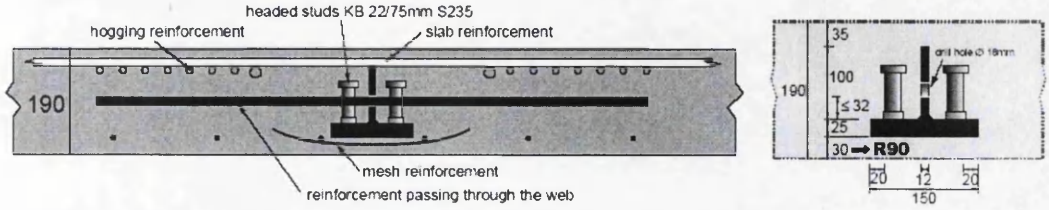

Fig: 2.3 - Composite slim floor beam [14].

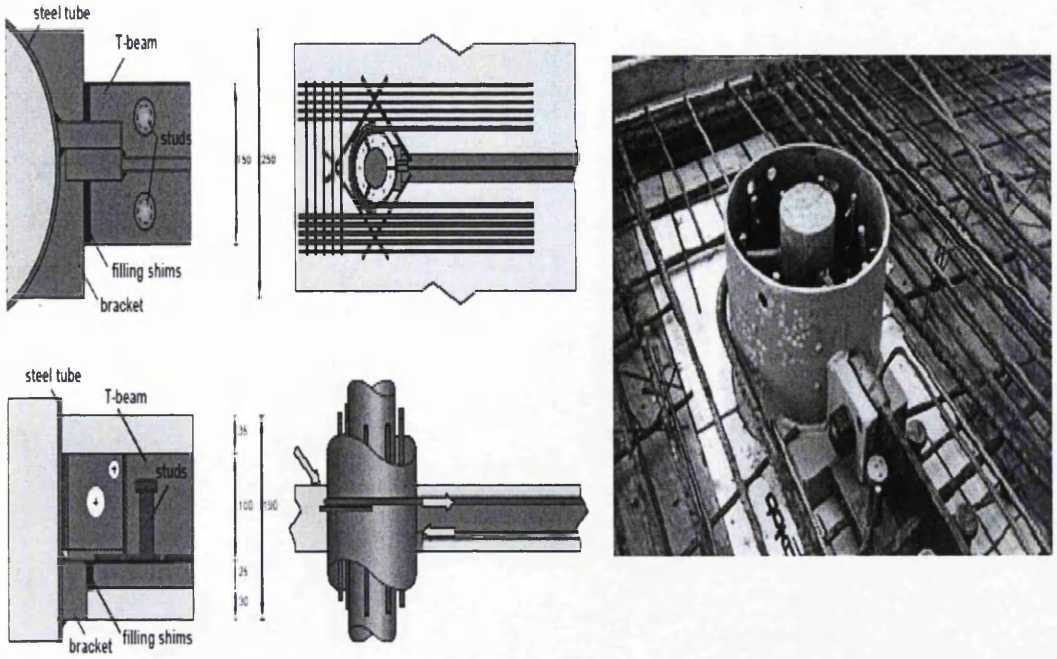

Fig: 2.4- Actual configuration of a joint between a column and a slim floor beam used at the millennium tower [14].

2.5.2. THEORETICAL APPROACH

Y. Richard Liew, T.H. Teo, N.E. Shanmugam [11], also predicted results of moment capacity and initial rotational stiffness of beam-to-column joints obtained from analytical assessments and are compared with the results of experimental tests carried out in part-1. With comparison it is found that, the marginal difference between the both results. However, the rotational stiffness of joint specimens subjected to negative moment is found to be more conservative compared with the Eurocode method.

The formulae for moment capacity, initial rotational stiffness and panel shear resistance of composite joints developed from the component method are presented. Lever arm for different connections is considered for calculating panel shear resistance of joints under reversal of moments. Spring model is considered to derive expressions for calculating initial rotational stiffness under negative and positive moment. The material properties obtained from the experimental tests were used to calculate strength and stiffness. The partial safety factors for materials used in EC3 and EC4 formulae are taken as unity.

Results of initial rotational stiffness obtained from the analytical model also compared with the experimental values reported by Liew et al. for joints subjected to symmetric loading (i.e. both side of the beam-to-column connections subjected to negative moments) to further validate the analytical model.

Following observations were drawn from the comparison of both the experimental and analytical results.

- It is convenient to represent the overall joint behaviour by rotational spring attached to the beam ends while design of composite frames with semi-continuous connections.

- In the unbraced frame, the joint model should take into account the behaviour of column web panel in shear as well as the M-Φ behaviour of relevant connection.

- The procedures for calculating the initial rotational stiffness of joints subjected to negative moments with symmetrical loading followed in Annex.J of EC3 are found to be more conservative. The maximum difference is found to be about 32%.

- The proposed modified EC3 procedure is found to be sufficiently accurate for joints under reversal of loading in which one side of the connection is subjected to positive moment and other side is under negative moment.

- For joints under positive bending, the proposed procedure modified from the EC3 Annex J is adequate to determine the positive moment capacity. The predictions are generally conservative with the maximum deviation of 20%. But based on experimental results, the positive initial rotational stiffness may be determined with reasonable accuracy by taking the lever arm distance between tension bolt rows to centre of concrete slab thickness in compression zone.

Fabbrocino.G. Manfredi.G, Cosenza.E [8], developed computational analysis related to the modelling of composite flexural members with reference to the continuous and semi-continuous structural systems. Authors presented the approach, which is a generalisation of the well known Newmark's kinematic model of the composite cross section and the computational problems related to local (cross section) and global non-linear analysis. At local level, the main attention has been focussed on the definition of a generalised moment-curvature relationship and at the global level solution of simple structural schemes has been analysed. This computational model is very effective to obtain parameters such as rotations, deflections as global parameters and slips, curvature, interaction forces and rebar strains as local parameters both in case of continuous and semi-continuous connection.

In 1998, Gizejowzski. M.A., Papangelis.J.P. and Parameswar.H.C. [7], presented stability design procedures for semi-continuous steel frames by direct and indirect methods. The direct design procedure is based on the concept of advanced analysis which assumes the same partial safety factors for load components and sectional strengths as those used in the conventional limit states design method. The indirect design procedure is related to the strength of individual members through the effective length factor. The difference between the direct and indirect design procedures is that the resistance in the former refers to the complete structural systems, whereas the resistance of each individual component is considered in the latter. A new set of member stiffness equations for the effective length chart. The indirect design procedure of semi-continuous frames conforms to the EC3 Standard (European Code ENV-1993-1-1 1992) which gives detailed routines for the calculation of the initial stiffness, strength and rotation capacity for a variety of welded and bolted steel connections in Annex J for semi-rigid connections.

In 1994, Y.Xiao, B.S. Choo & D.A. Nethercot [19], developed mathematical model to study the behaviour of different types of connections and validate the results with experimental results conducted by different authors. From this mathematical model, authors observed that, connection moment capacity (M con) can reach the composite beam hogging moment (M hog) when the reinforcement ratio and/or slab depth is increased sufficiently for composite flush endplate connections.

2.5.3 FINITE ELEMENT APPROACH

There are a few research papers that use the finite element method to predict the behavior of different types of steel connections under static loading. In fact, there are several that consider only moment endplate connections. However, the limitations of these works are readily apparent and can be listed as general limitations present in most current research on this topic. First, the endplate behavior, and not bolt forces, is the prime concern. The endplate strength for most endplate configurations has been well defined in the literature. However, most bolt force prediction schemes have been shown to be impractical for design applications. Almost all the papers use truss elements to represent the entire bolt and the results are extremely limited. Second, all of the papers on this topic only consider small endplate configurations (i.e., flush or four-bolt extended). The main reason for this is that these smaller connections provide more flexibility than larger ones. This is needed for efficient partially restrained (PR), sometimes called semi-rigid connection design applications. Finally, the theme of most papers is the adequacy of the finite element method in determining the connection's behavior. Very few applications are made.

Mohammed R. Bahaari & Archibald N. Sherbourne (1996) [18] uses the ANSYS finite element program to develop a 3D simulation of bolted connections to unstiffened columns with extended moment endplate connections. Eight–node isoparametric solid elements i.e. STIFF 45 was used for modeling the bolt head and nut. Bolt head and nut areas were considered as hexagons and therefore standard dimensions of the cross flat and height specified. The bolt shank was modeled using six 3D spar elements connecting farthest corner nodes of head and nut to each other. The 3D interface elements, i.e. STIFF 52, modeled the boundary between the column flange and endplate with a co-efficient of friction equal to 0.5 were defined for sliding resistance while the interface is closed.

In case of moment – rotation behavior of connection, the authors used expression to find the rotation of connection in order to make direct comparison between analytical and finite element studies as follows.

$$\phi = \frac{U_t - U_c}{D_b - t_{bf}} \qquad [2.1]$$

U_t & U_c are relative displacements of the endplate at the locations of the beam tension and compression flanges. Where D_b is the depth of beam and t_{bf} is the thickness of the beam flange. Authors observed that, the moments and rotations are in the same range as the test data and the general trends of the curves are similar.

Recently, Y.I. Maggi, R.M. Goncalves, R.T. Leon & L.F.L. Ribeiro,[22] studied parametric analyses on the behaviour of extended endplate connections using finite element modelling. The authors predicted that, how the interaction between the endplate and the bolts changes the connections' behavior. ANSYS version 6.0 was used to develop finite element modelling on extended endplate connections with SOLID and contact elements (SOLID45, TARGE170 and CONTACT173). Six numerical models, and associated experimental specimens, were discussed relating to overall stiffness, displacements of the endplate and axial forces in the bolts.

Different aspects were presented for the modeling, and the numerical results demonstrate the feasibility of the FE models to simulate the connection behavior and to capture behavioral changes as consequence of geometric variations. The numerical results were found to be in good qualitative agreement with the actual connection behavior.

Ahmed and Nethercot [23] have carried out analytical studies with Finite Element Method by using ABAQUS and proposed a method to calculate the initial stiffness of the flush endplate connections based on a simple force mechanism.

Cheng-chih chen, Shuan-Wei Chen, Ming-Dar Chung, Ming- Chih Lin [24], studied experimentally and analytically on cyclic behaviour of the beam – to-column welded moment connections used in steel moment – resisting frames. The ANSYS finite element program was used in the analytical studies. ECCS loading procedure was adopted to carry out the experimental investigation on cyclic loading. The symmetry in the plane of the beam and the column webs was such that only half of the

specimen was modelled and analysed to reduce computational effort. An eight-node, three –dimensional solid element solid element with 24 nodal degrees of freedom was used to model the structural steel. Bilinear material properties for steel section with strain hardening 4% of modulus of elasticity were used in finite element analysis.

To verify the analytical model, the predictions of the finite element analysis were compared with experimental results in terms of load and deformation relationships. The results are consistent with each other.

There are several other papers that consider topics dealing with finite element modeling of moment endplate connections, or finite element modeling of steel connections for seismic design.

In this research, the approach for developing finite element model is different as compared to previous researchers by using different element types as mentioned in section 4.3 of Chapter 4. Fig 4.6 to 4.10 shows pattern of meshing in all components of connection.

A finite element analysis program ANSYS-8.1[17] was used to develop the 3D computer modelling of flush endplate connections. In order to model the prototype connection, the finite element program should include the effects of material and geometric non-linearity, and local buckling. The element types were considered to develop finite element model explained in Section 4.3.2.

CHAPTER 3

METHOD OF FINITE ELEMENT ANALYSIS

3.1 INTRODUCTION

Finite element analysis techniques have been introduced in to structural elements since the 1960's. Today, particular element types tailored for the analysis of structural steel and reinforced concrete can be found in most popular commercial FEA packages. Since the nonlinearity, variability and other failure modes of structural elements are assessed as complex, application of FEA techniques to structural steel and concrete structures is still limited to some extent, especially in the analysis of large and complex three dimensional components and structures. Investigations for details of the modelling techniques in this area are essential. A standardisation of FEA techniques for bare steel and composite connections is aimed to be established in the present research.

A series of prerequisites are required for any finite element analysis. These prerequisites will be the basis of standardisation. Normally the prerequisites include choice program, simplification of the analysed system, design and generation of model, treatment of particular problems, and selection of solution method.

This chapter introduces choice of these items. Once the items have been determined, they will be kept unchanged and applied to all of the modelling in the present work. The items selected for particular applications described in Chapter -4.

3.2. NONLINEAR FINITE ELEMENT ANALYSIS

Nonlinear finite element analysis is an essential component of computer-aided design. Testing of prototypes is increasingly being replaced by simulation with non-linear finite element methods because this provides a more rapid and less expensive way to evaluate design concepts and design details.
Nonlinear analysis consists of the following steps:

1. Development of a model
2. Formulation of the governing equations
3. Discretization of the equations
4. Solution of equations
5. Interpretation of the results.

The solution of nonlinear problems by the finite element method is usually attempted by one of three basic techniques: incremental or stepwise procedures, iterative or Newton methods, and step-iterative or mixed procedures. Considering only the nonlinear equilibrium equation for a single element the equation can be written as:

$$[K]\{q\} = \{Q\} \qquad [3.1]$$

Where the nonlinearity occurs in the stiffness matrix [K], which is a function of nonlinear material properties [C(σ)]. We can indicate that the material parameters in [K] are no longer constants by writing

$$[K] = [K(\{q\},\{Q\}] \qquad [3.2]$$

The symbolic nonlinear relationship between {Q} and {q} is shown in Fig 3.1(a) Fig 3.1(b) shows the non-linear stress-strain curve corresponding to the load,{Q}, and displacement, {q}, in Fig 3.1. It is on the basis of this stress-strain or constitutive law that we determine the variable matrix [C($\bar{\sigma}$)] for the nonlinear analysis.

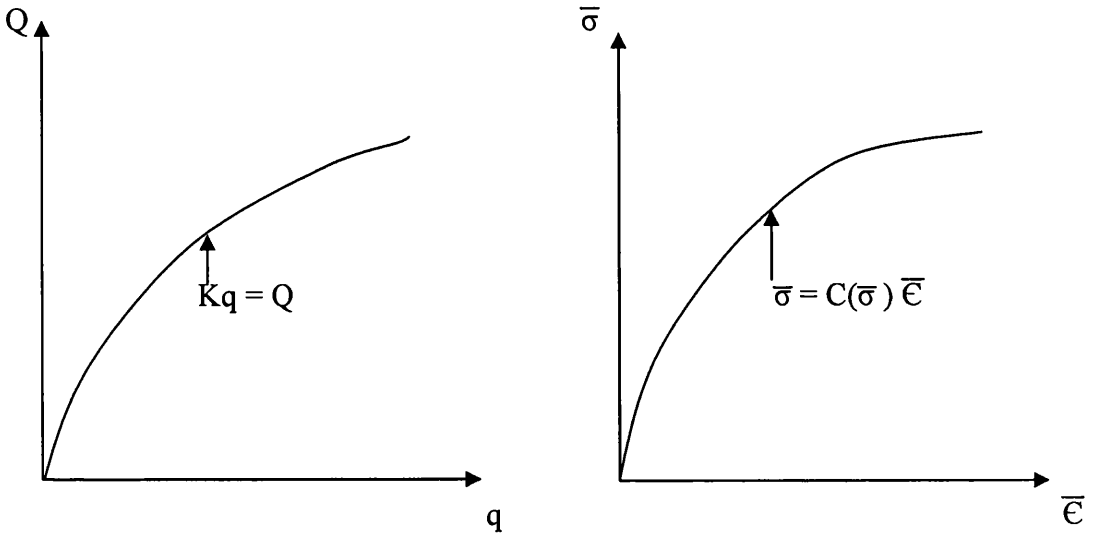

a) Symbolic load – displacement curve b) Stress – Strain curve

Fig 3.1: Non-linear curves.

The basis of the incremental or stepwise procedure is the subdivision of the load into many small partial loads or increments. Usually these load increments are of equal magnitude, but in general they need not to be equal. The load is applied one increment at a time, and during the application of each increment the equations are assumed to be linear. In other words, a fixed value of [K] is assumed throughout each increment, but [K] may take different values during different load increments. The solution for each step of loading is obtained as an increment of the displacements {q}.

These displacement increments are accumulated to give the load displacement at any stage of loading, and the incremental process is repeated until the total load has been reached.

In writing equations for the incremental method, let the initial or reference state of the body be given by the initial loads and displacements, $\{Q_o\}$ and $\{q_o\}$. Usually, $\{Q_o\}$ and $\{q_o\}$ are null vectors because of undeformed state of the body. However, they can specify any initial equilibrium state of $\{Q_o\}$ and $\{q_o\}$. Total load can be divided in to M increments, so the total effective load is

$$\{Q\} = \{Q_o\} + \sum_{j=1}^{M} \{\Delta Q\, j\} \qquad [3.3a]$$

Where the Δ notation is used to indicate a finite element increment. Hence, after the application of the i^{th} increment, the load is given by

$$\{Qi\} = \{Q_o\} + \sum_{j=1}^{i} \{\Delta Q\, j\} \qquad [3.3b]$$

Where $\{Q_M\} = \{Q\}$. Adopt a similar notation for the displacements, so that after the i^{th} step the displacement are

$$\{q_i\} = \{q_o\} + \sum_{j=1}^{i} \{\Delta q_j\} \qquad [3.4]$$

To compute the increment of displacements, a fixed value of the stiffness, which is evaluated at the end of the previous increment, is shown in the equation below.

$$[K_{i-1}] \{ \Delta q_{i-1}\} = \{\Delta Q\, i\} \qquad \text{for } i = 1,2,3, \ldots\ldots, M \qquad [3.5a]$$

Where

$$[K_{i-1}] = [K_{i-1}(\{q_{i-1}\}, \{Q_{i-1}\})] \qquad [3.5b]$$

and where $[K_o]$ is the initial value of stiffness. $[K_o]$ is computed from the material constants derived from the given stress-strain curve at the start of the loading. Equation [3.5] give the basic incremental method, and equations [3.3] and [3.4] are essential auxiliary relations. The incremental procedure is schematically indicated in Fig 3.2.

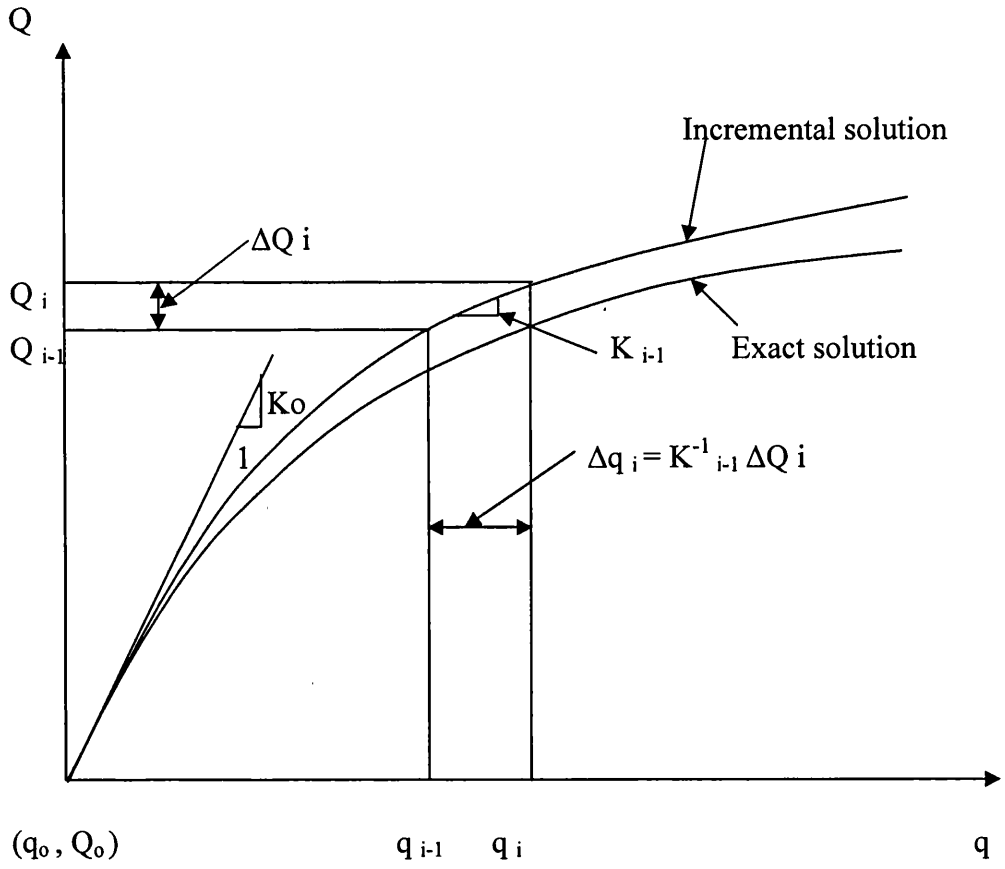

Fig 3.2: Basic incremental procedure

Usually, in the incremental procedure the tangent modulus are used to formulate $[C(\sigma)]$ and to compute the stiffness matrix [K] in equation [3.5]. This matrix is often referred to as the tangent stiffness matrix.

The incremental method is analogous to the numerical methods used for the integration of systems of linear or non-linear differential equations, such as the Euler method and Runga-Kutta techniques.

The accuracy of incremental procedure can be improved by taking smaller increments of load, say by adopting half of the load increment. However, since a new incremental stiffness matrix $[K_{i-1}]$ must be computed for each step, we see that the increased accuracy is purchased at the cost of additional computational effort.

ANSYS employs the "Newton-Raphson" approach to solve nonlinear problems. In this approach, the load is subdivided into a series of load increments. The load increments can be applied over several load steps.

3.3 THE *ANSYS* PROGRAMME

Today, possessing the latest finite element analysis and design technology, ANSYS is widely used by researchers and engineers. ANSYS is a general purpose finite element modelling package for numerically solving a wide variety of mathematical problems in all kinds of subjects. For structural engineering analysis, it can deal with static, dynamic, buckling, etc. problems in both linear and non-linear states. Mainly because of these features, the ANSYS program (version 8.1) is chosen as a basic tool for the present research.

The ANSYS program consists of two basic levels. One is the begin level that act as a gateway of the program. The other is the processor level containing several processors. Each processor serves a special purpose, from pre-processing, loading and solving, to post-processing. ANSYS offers a library of over 100 standard elements including many specialised elements that can be used for most kinds of structural engineering analyses.

There are over 800 commands in the program, each act as a specific function. ANSYS can be run either in interactive mode or batch mode. The program works with one large database that stores all input data and out put data in an organised fashion. Thus it is quick and easy to list, display, modify, or delete any specific data item. Details of characteristics of the program can be found in the ANSYS user's manual [17].

3.4 TYPE OF MODEL

Finite element model may be categorised as being 2D or 3D. Choice of model dimensionality and related element types will often determine which method of model generation will be most practical for particular problem. ANSYS has different type of models such as, line models, 2-D solid models, 3-D shell models and 3-D solid models.

a) Line models

These models can represent 2-D or 3-D beam structures, as well as 2-D models of 3-D axisymmetric shell structures. Solid modelling usually does not offer much benefit for generating line models; they are more often created by direct generation methods.

b) 2-D solid models

These type of models are used for thin planar structures (plane stress), infinitely long structures having a constant cross section(plain strain), or axisymmetric solid structures.

Although many 2-D analysis models are relatively easy to create by direct generation methods, they are usually easier to create with solid modelling.

c) 3-D shell models

3-D shell models are used for thin structures in 3-D space. Although some 3-D shell analysis models are relatively easy to create by direct generation methods, they are usually easier to create with solid modelling.

d) 3-D solid models

These models are used for thick structures in 3-D space that have neither a constant cross section nor an axis of symmetry. Creating a 3-D solid analysis model by direct generation methods usually requires considerable effort. Solid modelling always makes the job easier.

3.5 MODEL GEOMETRY

One of the fundamental decisions taken when planning an analysis is how to present and simplify the geometry of the model of the model. The basic rules recommended for the analyses of the problem within this research programme are:

i) Main dimensions of the components must be represented as exactly as possible because they will significantly control the mechanical behaviour of a model. Herein the main dimension means extents of section and length or height of components, such as beam, columns, bolts, endplates, etc of the analyzed specimen.

ii) When both the geometry and the loading have common axis of symmetry, it should be used to simplify the problem. Frequently only half, a quarter, or even one eighth of specimen needs to be modelled, if there are one, two, or three axes of symmetry, respectively. This will significantly save both space and time required to run the model.

iii) Dimensions of less significant components which affect the mechanical behaviour of an analysed specimen slightly, but exact representation of their geometry will cause the whole modelling process to become much more complex. Some simplifications are necessary for these components. For example, both the main reinforcements and links will be modelled by spar elements that can only be subjected to axial forces in either compression or tension. Details of the elements are described in Chapter-4.

3.6 MESH GENERATION

The ANSYS programme provides two ways to generate meshes for models. The first is solid modelling with which the program generates all the nodes and elements automatically following the described geometric boundaries, using the established size and shape of elements. The second method is direct generation by which the location of every node, the size, shape and connectivity of every element is determined manually. Although solid modelling is an easy way to generate mesh for models, sometimes uses large amount of CPU time, and fails to generate a valid mesh under certain circumstance. In order to control accurately the meshing of a model, direct generation is selected as the preferred method for the present work.

3.7 LOADING

Load was applied on the top of flange of the composite beam as a point load. Care was taken for the convergence of the analysis due to the complex nature of both geometry and material non-linearity. Due to the limited linear response of concrete material (Fig. 4.9) provided by the ANSYS load was applied very slowly by using small load steps to avoid divergence in the analysis.

The load was applied in ten load steps in case of static analysis and five/ten load steps in one iteration of cycle (i.e. total 20 load steps/40 load steps in one complete cycle). The cyclic load analysis was carried out till the analysis has been terminated due to failure of one of the joint component. The procedure of cyclic loading is explained in Section 5.3.2 of Chapter 5.

3.8 PRE and POST PROCESSING

ANSYS requires an input file which defines the nodes, elements, material properties, boundary conditions and loadings. The typical input file is described in appendix-II. The user input parameters such as dimensions, mesh size, imperfections, and material properties are stored in ANSYS input file i.e. batch file. It was possible to create many files quickly, in order to investigate the effects of various parameters efficiently and easily.

It was possible for the output to contain full details of deformations, stresses and strains in each direction for each node during every increment. Only a fraction of the available output was required to obtain the moment - curvature relation for the beam being analysed.

A small post processor was written to extract the particular values from the ANSYS output file (*.dat), into a form which could be easily inserted into a spreadsheet. A macro within Microsoft Excel processed the extracted data into a moment -curvature plot and calculated the rotation capacity.

3.9 CONVERGENCE TOLERANCES

Several choices of convergence for successive iterations are offered in the ANSYS program. The convergence of a solution can be controlled by tolerances based on forces, moments, displacements, or rotations, or on any combinations of these items.

The force-based convergence serves as an absolute measurement of convergence, while displacement-based convergence provides only a relative measurement of apparent convergence. Additionally, for a modeling of a system including concrete elements, after crushing occurs at an integration point the strain of concrete at that point increases intensively. This may invalidate displacement–based convergence checking. Consequently, the force-based convergence checking is adopted as the convergence criteria. The values of the criteria are determined for each particular model.

CHAPTER 4

3D SIMULATION OF FINITE ELEMENT MODELLEING

4.1 INTRODUCTION

A great effort of research on the behaviour and design of connections subjected to seismic load has been conducted over the past few years. The primary areas of research have been on welded connections and on finding alternative connections that provide adequate ductility. The end-plate connection is one alternative that has been investigated.

The finite element analysis determined similar trends as observed experimentally, namely that the rotation capacity was a function of both the flange and web slenderness, and that for a given aspect ratio, the relationship between web slenderness and rotation capacity was non-linear, and the slope of the line describing the relationship increased as the web slenderness decreased.

Numerical or finite element analysis provides a relatively inexpensive, and time efficient alternative to physical testing. It is vital to have a sound set of experimental data upon which to calibrate a finite element model. It is then possible

to investigate a wide range of parameters within the model. Several authors studied on 3D finite modeling of connections and they achieved the fairly good results when compare to experimental results.

The objective of this study was to predict the behaviour of steel and composite steel joints under static load and cyclic load through an accurate, well-defined finite element model. In this chapter, the developments of finite element model on different endplate connections are presented. The endplate connections consist of a plate that is connected to the beam by means of shop weld and then bolted to the column flange. The connections are primarily used to connect a beam to column or to link two beams together.

The eight bolt flush endplate connection consists of four rows two bolts and its configuration as shown in Fig 4.2 and the four bolt flush endplate connections consists of two rows of two bolts and its configuration as shown in Fig 4.3(a).

4.2. CONNECTION DETAILS

4.2.1. EXPERIMENTAL DETAILS

Different types of cases considered to study the behaviour of connections using 3D computer simulation of finite element analysis. In this study only flush endplate connection details have been considered and validate the results with experimental results conducted by different authors.

Case A) Experimental specimen details carried out by Y.Xiao, B.S. Choo & D.A. Nethercot [6] on composite connection in steel and concrete subjected to static loading – Part 1.

Y.Xiao, B.S. Choo & D.A. Nethercot [6], performed experimental investigation on different types of connections. All specimens were tested in a cruciform configuration.However, the flush endplate test is considered in this study and its

experimental set up is illustrated in Fig 4.1 and 4.2. It consists of two universal beams of 305 x 165 x 40 UB connected to the column 203 x 203 x 52 UC through flush endplate. The com floor 46 metal decking was used as permanent shuttering with welded shear studs. Experimental specimen details considered for finite element study as shown in Table 4.1. The material properties of experimental investigation are listed in Table 4.5.

Two loads were applied symmetrically at 1.5 m from the column flange through two hollow section load spreaders. The main experimental observations were included moment resistance, rotational stiffness and rotational capacity of connections. Additional detailed information and results may be found in [6].

Table 4.1 : Experimental specimen details

Specimen	Joint type	Web stiffening and specimen shape	Reinforcement ratio (%)
SCJ4	Flush endplate	Cruciform None	T12 rebar (1.0%)
SCJ5	Flush endplate	Cruciform Web Stiffener	T12 rebar (1.0%)

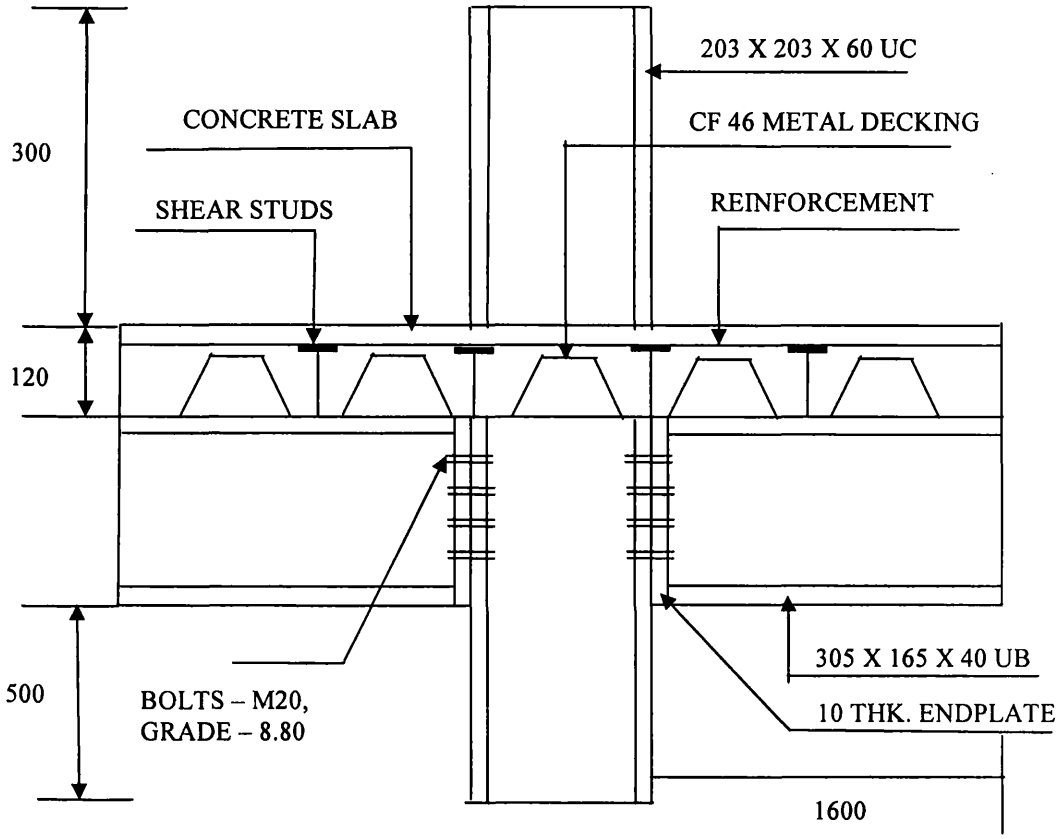

Fig. 4.1. Cruciform arrangement of flush endplate composite connection.

(All dimensions are in mm.)

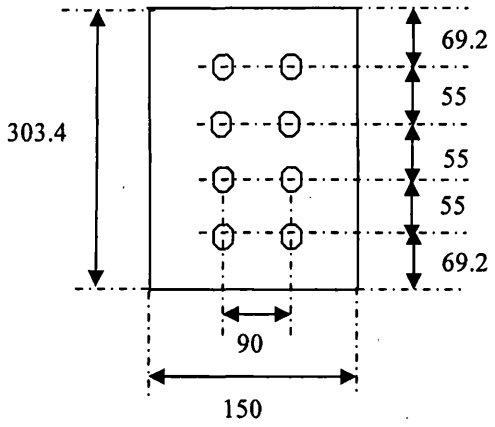

Fig. 4.2. Typical flush endplate details.

(All dimensions are in mm.)

Case B) Experimental specimen details carried out by J.Y. Richard Liew, T.H. Teo, N.E. Shanmugam [10] on composite joints subject to reversal of loading – Part 1: Experimental study mentioned in Table 4.2 and Fig – 4.3.

The following details were commonly used for all test specimens:

Type of connection	-	Flush endplate
No of Bolts	-	Four
Bolt grade	–	M20 Grade 10.9 bolts
Thickness of endplate	–	12 mm
Grade of Steel	–	S275
Thickness of Slab	–	120 mm
Reinforcement ratio	–	1.12% (2010 mm^2)

The reinforcement type used is high yield deformed bars.

Longitudinal reinforcements of 16 mm diameter bars (T16) were distributed in one layer with equal spacing over the width of slab besides the column section. Two layers of 10 mm diameter deformed bars were supplied as transverse reinforcement to prevent longitudinal splitting failure of concrete slab. The longitudinal spacing of transverse reinforcement and shear studs of 130 mm were used to achieve full composite action between the slab and steel beam. Additional detailed information and results may be found in [10].

Table 4.2: Specimen details considered for finite element modeling.

Specimen	Universal column size	Universal Beam Size	Loading Condition	Connection
SJ1	305x305x97	305x165x54	Cyclic	Flush endplate
CJ1	305x305x97	305x165x54	Monotonic	Flush endplate
CJ2	305x305x97	305x165x54	Cyclic	Flush endplate

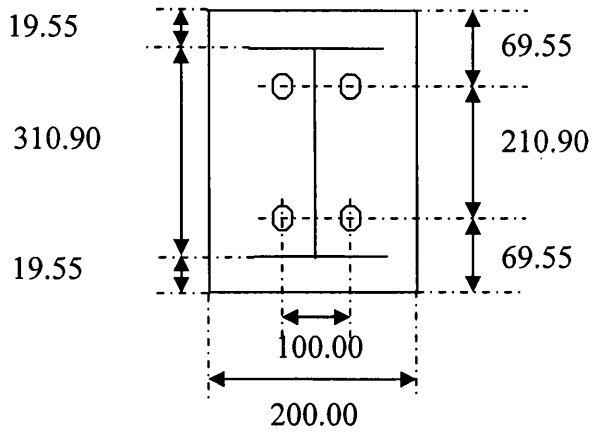

a) Flush endplate

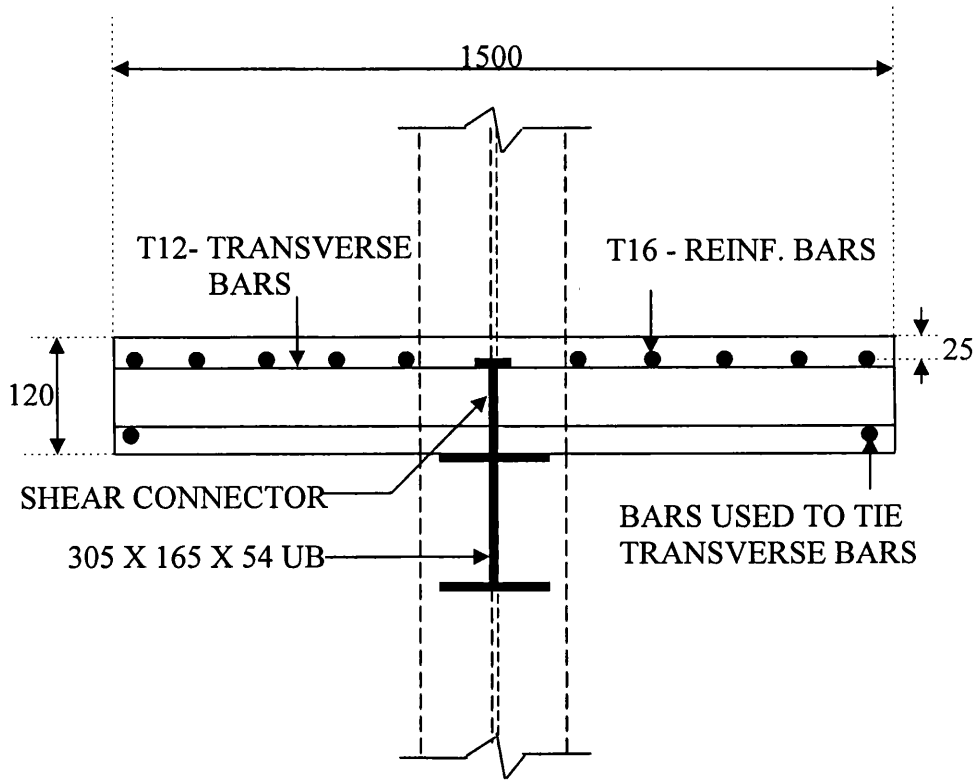

b) Cross-sectional details of composite beam

Fig 4.3 – Showing experimental set-up details

(All dimensions are in mm.)

The material properties of experimental investigation are listed in Table 4.6.

Case C) Experimental specimen details of Tongji project studied by finite element analysis to compare with experimental results for further research.

The following details were commonly used for all test specimens:

Type of connection	-	Flush endplate
No of Bolts	-	Eight
Bolt grade	–	M20 Grade 10.90 bolts
Thickness of endplate	–	10 mm
Grade of Steel	–	S345
Size of web stiffener	-	176mm x 71mm x 10mm
Shear studs	-	One per trough
Thickness of Slab	–	130 mm
Main reinforcement	–	8 – 16mm diameter

The reinforcement type used is high yield deformed bars.

One layer of 12 mm diameter deformed bars was supplied as transverse reinforcement at top of concrete slab. The DP688 metal decking was used as permanent shuttering with welded shear studs. The longitudinal spacing of transverse reinforcement and shear studs were kept same to achieve full composite action between the slab and steel beam. In this experimental study all the beam and column sections will be the built-up sections assembled through welding.

Table 4.3: Experimental specimen details.

Specimen	Built up column size (mm)	Built up Beam Size (mm)	Loading Condition	Connection
Type 1	200x200x8x12	300x150x6x10	Monotonic	Flush endplate
Type 2	200x200x8x12 (Dx bx t_w x t_f)	300x150x6x10 (D x b x t_w x t_f)	Monotonic	Flush endplate With web stiffener
Type 3	200x200x8x12	300x150x6x10	Cyclic	Flush endplate

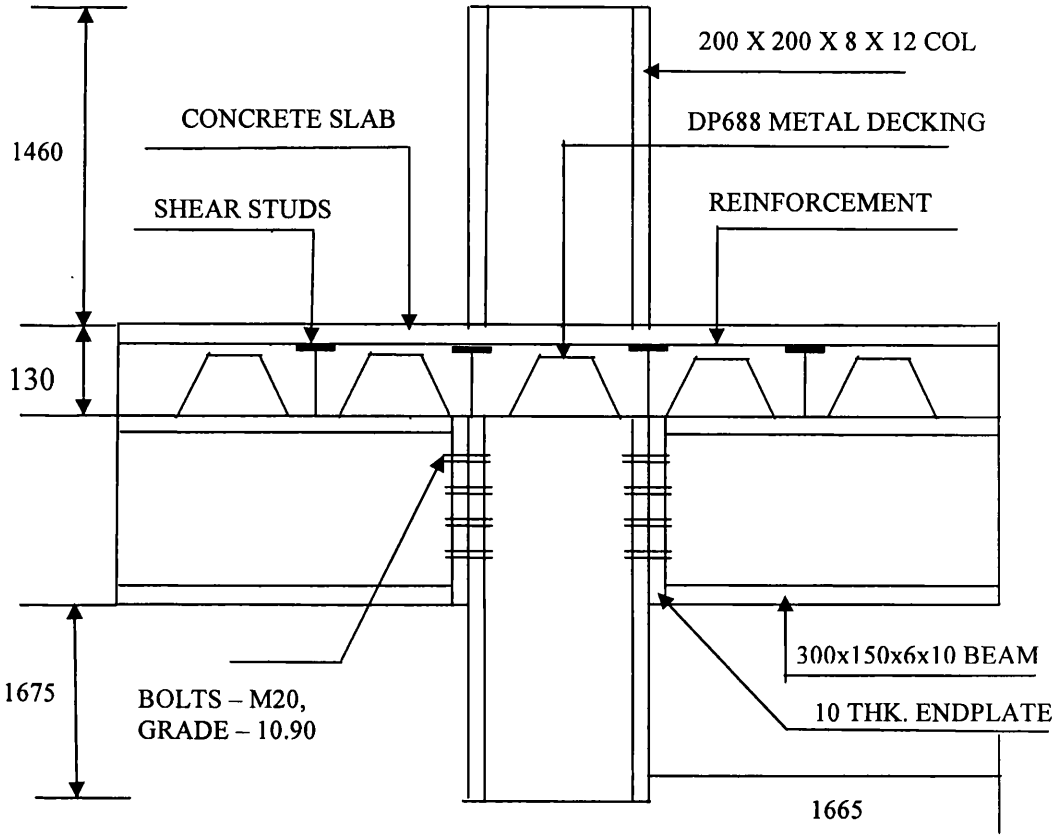

Fig. 4.4: Cruciform arrangement of flush endplate composite connection for Tongji project

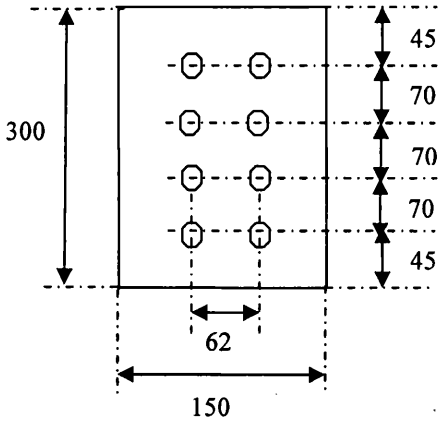

Fig. 4.5: Typical flush endplate details.

(All dimensions are in mm.)

The characteristic values of material properties are considered and given in Table 4.7.

4.3 DEVELOPMENT OF FINITE ELEMENT MODELLING

4.3.1 MODELLING OF CONNECTION CHARACTERISTICS

The proper use of finite element model may provide a viable procedure to the basis for justifying a connection configuration for seismic design use. A finite element approach is the appropriate solution to examine this possibility and the results compared to results from several tests conducted by different authors.

Several connection components are modelled to achieve the following aims:

1. Examine the accuracy of the mechanical model for both steel and concrete and suitability of their application in the ANSYS programme.

2. Check the applicability of the selections for finite element analyses such as element types, mesh generation, loading and solutions.

3. Investigate the behaviour of some well known connections which are tested by other researchers, so that reliability of the modeling in the present work can be verified.

4. Finally, based on the above work, standardization of FEA techniques for both steel and concrete can be completed.

After the detailed discussion of all validation tests performed, two representative cases shown in Figs. 4.1 to 4.3 are described to demonstrate the accuracy of finite element modeling. Specimen brief details and results are reported here. Additional detailed information and results may be found in [6] and [10].

A finite element analysis program ANSYS-8.1 was used to develop the 3D computer modelling of steel and composite steel joints. In order to model the prototype connection, the finite element program should include the effects of material and geometric non-linearity, residual stresses, and local buckling. The boundary

conditions and element types considered to develop finite element model explained in sections 4.3.2 and 4.3.3.

4.3.2 CHOICE OF ELEMENT TYPE

ANSYS finite element analysis package [17] has several element types suitable for numerical analysis: solid two and three dimensional elements, 2D and 3D spar (truss) elements, beam elements, shell elements, contact elements and etc. The major aim of the analysis was to predict the formation of inelastic local instabilities in a cross section and the corresponding moment - rotation capacity.

4.3.2.1 ELEMENT TYPES FOR CONNECTIONS MODELLING

Beam, membrane and truss elements are not appropriate for the buckling problem. Solid three dimensional elements may be suitable, but the solid elements have only translation degrees of freedom at each node, but Solid 65 element is suitable for concrete elements. The following element types were used to develop finite element modeling of joints.

i) Shell 143

ii) Solid 185

iii) Solid 65

iv) 3D – Spar (Link 8)

v) Contact 52

The brief descriptions of suitability of selected elements have been explained below. Fig 4.6 shows a typical finite element modeling of semi-continuous flush endplate composite connection. There were number of zones in the connection, each with different mesh densities. The most important zone is in the endplate and endplate portion in the column flanges. The mesh density was highest in the endplate potion, as it was important to be able to model the formation of the local buckle. The length of column flange and web below and above endplate portion were of less important in the model, and the mesh density was reduced in those zones and the same pattern

of meshing is considered in beam flanges and web. Fig 4.7(a) & (b) shows the mesh distribution around the cross-section of bolt and nuts.

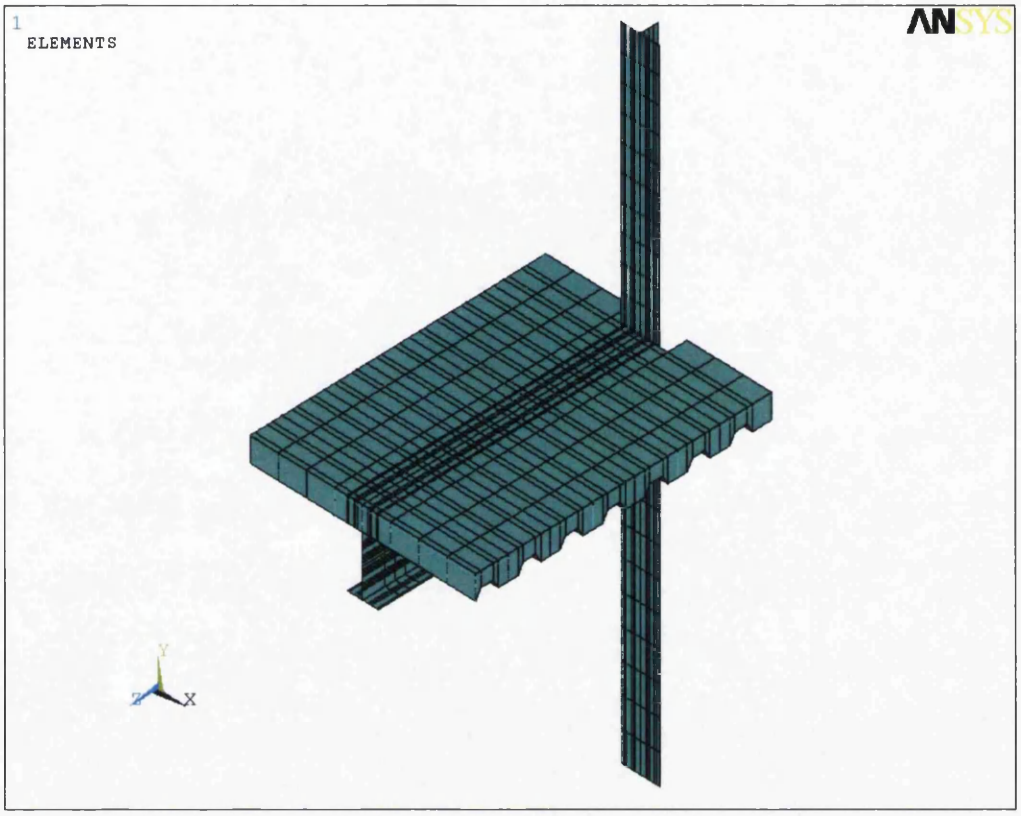

Fig 4.6 : Finite element modeling of flush endplate composite connection.

i) Shell 143

This type of element is well suited to model non-linear, flat or warped, thin to moderately thick shell structures. The element has six degrees of freedom at each node: translations in the nodal x, y, and z directions and rotations about the nodal x, y, and z-axes. The deformation shapes are linear in both in-plane directions.

The element has plasticity, creep, stress stiffening, large deflection, and small strain capabilities. The flanges and web of universal columns and universal beams were modeled with this type of element. Also endplates were modeled with same type of element. The typical mesh densities in shell elements as shown in Fig 4.7

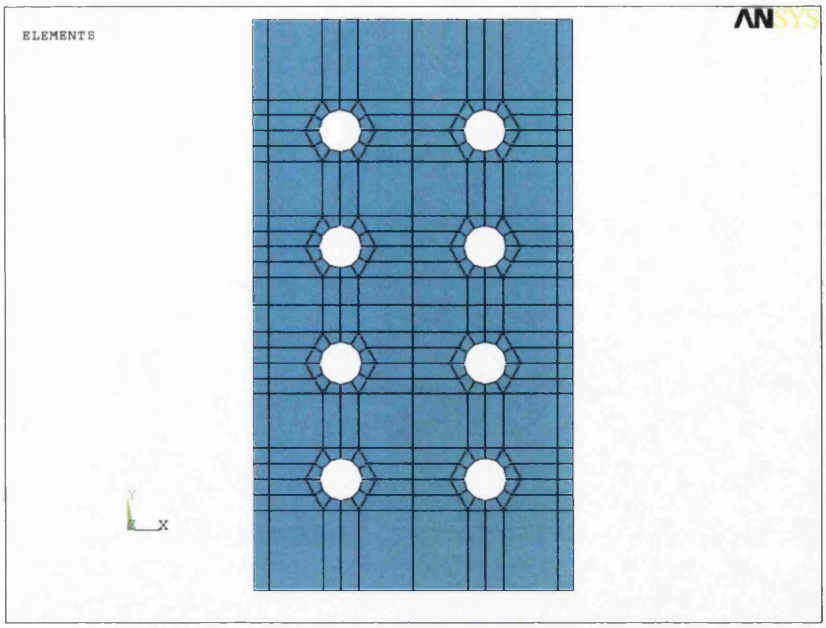

a) Finite element meshing of endplate

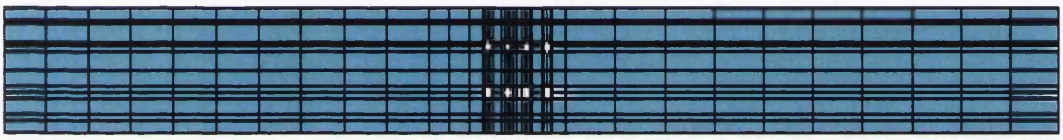

b) Finite element meshing of column flange

c) Finite element meshing of column web

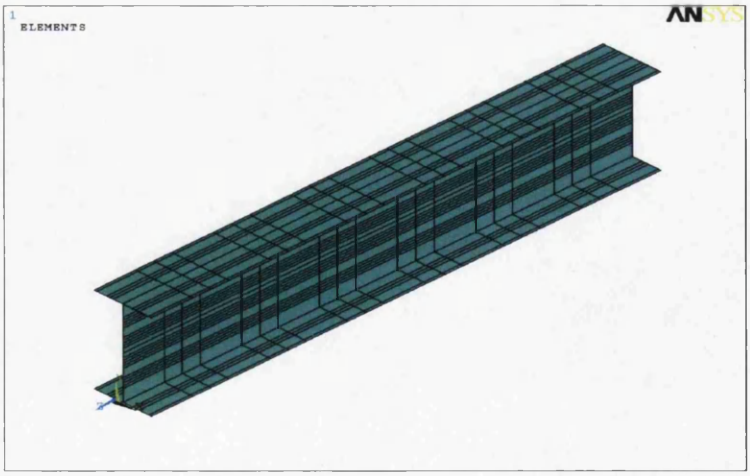

d) Finite element meshing of beam flange and web.

Fig 4.7 : Finite element modeling of shell elements.

ii) Solid 185

Bolt head and nut are idealized using solid elements. The bolt shank was modeled using twelve 3D spar (Link) elements connecting the farthest corner nodes of head and nut to each other. The effective area of the bolt is split equally among the twelve spar elements.

This element is defined by eight nodes having three degrees of freedom at each node: translations in the nodal x, y, and z directions. This element has plasticity, hyper elasticity, stress stiffening, creep, large deflection, and large strain capabilities. The typical configuration of element connectivity is shown in Fig. 4.8

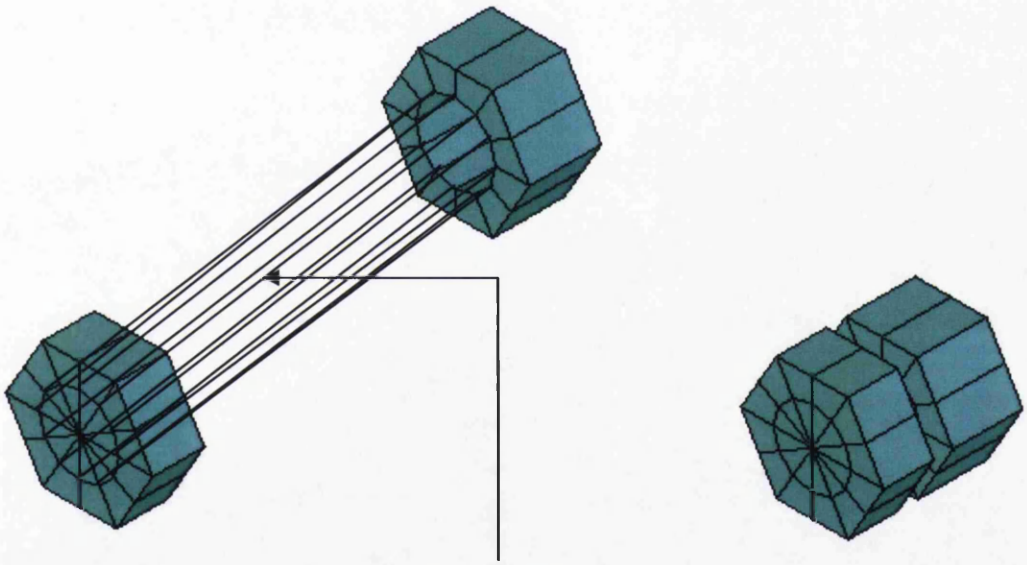

Fig 4.8 : Finite element modeling of bolts, nutts & shank elements.

iii) Solid 65

Concrete has properties of cracking in tension and crushing in compression and it has non-linearity behaviour in its stress-strain relationship. The ANSYS programme provides special three –dimensional element, which is SOLID65 for modeling of concrete elements.

This type of elements used for the 3-D modeling of solid concrete core with or without reinforcing bars (rebar). It is capable of cracking in tension in three orthogonal directions and crushing in compression. The element has plasticity, creep, swelling, stress stiffening, large deflection and large strain capabilities. In concrete applications, for example, the solid capability of the element may be used to model the concrete while the rebar capability is available for modelling reinforcement behaviour. The element is defined by eight nodes having three degrees of freedom at each node: translations in the nodal x, y, and z directions. Up to three different rebar specifications may be defined in this case of element.

The rebar capable of tension and compression, but not shear. They are also capable of plastic deformation and creep. The reinforced concrete slab elements over the flanges of universal beam were modelled with this type of element as shown in Fig 4.9

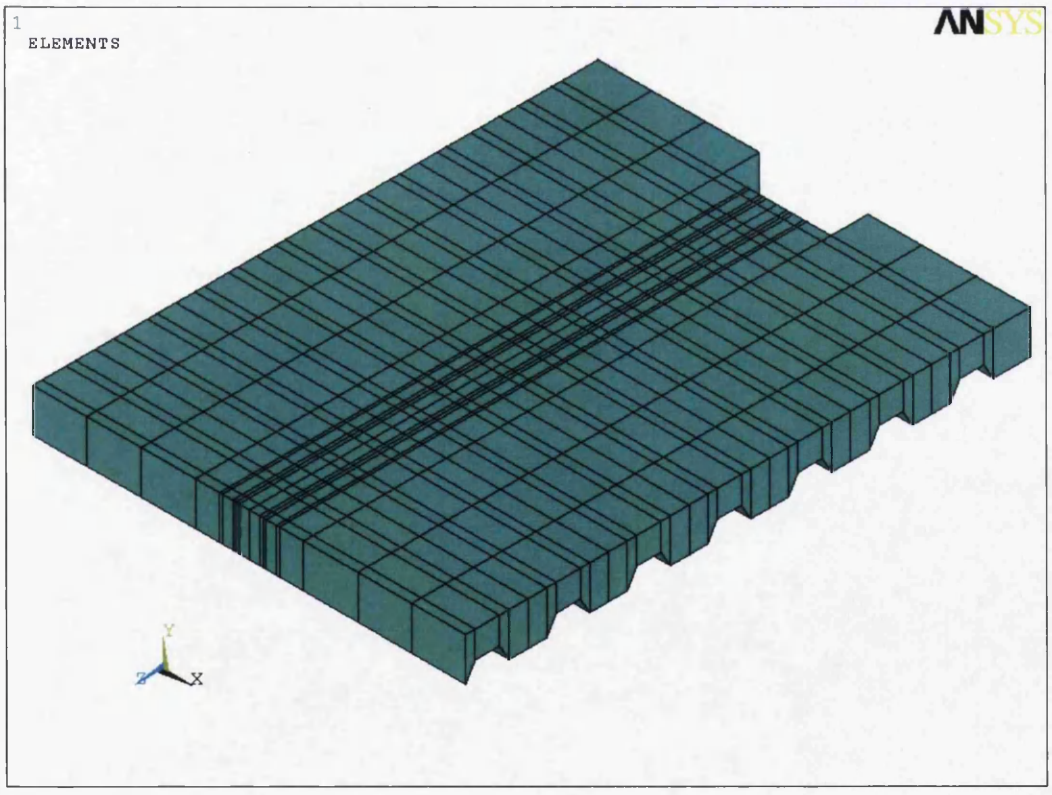

Fig 4.9 : Finite element modeling of concrete elements.

iv) 3D – Spar (Link 8)

The bolt shank was modeled using twelve 3D spar (Link 8) elements connecting the farthest comer nodes of head and nut to each other. The effective area of the bolt shank is divided equally among the twelve spar elements.

The 3-D spar element is a uniaxial tension-compression element with three degrees of freedom at each node: translations in the nodal x, y, and z directions. The element has plasticity, creep, swelling, stress stiffening, and large deflection capabilities. The typical configuration of element is shown in Fig. 4.8 & 4.10 (a).

Also this type of element was used to model the reinforcement in both directions as well as shear studs as shown in Fig. 4.10 (b). In finite element analysis, the reinforcements in concrete can be modelled in three approaches. One is to use two or three dimensional solid elements. The second one is to add reinforcement as smeared material in anything up to three directions. The third is to add spar elements along the centre line of the reinforcement. In the first method, full stress distribution can be modeled. Additionally, slip characteristics between reinforcement and concrete, and dowel action of reinforcement can be modeled. Also this method is suitable for the special local behaviour analysis, and requires more elements. In the last two methods it is assumed that bond between the reinforcement and surrounding concrete is complete, and the reinforcement is subjected only to axial tension or compression so that the modeling is simplified. The third approach is preferred because spar elements are more accurate in modeling the reinforcement and shear studs behaviour in complex stress situations than the smeared material capability of the element. The smeared material option for modeling reinforcement has been found to be accurate only if the member is acting primarily in bending.

The principle contribution of main reinforcements and shear studs is to resist axial forces. This can be best represented by using the three-dimensional spar element LINK 8 in ANSYS [17]. Only two nodes on the reinforcement axis are required to define this element geometrically, and these nodes coincide with corner nodes of the surrounding concrete element.

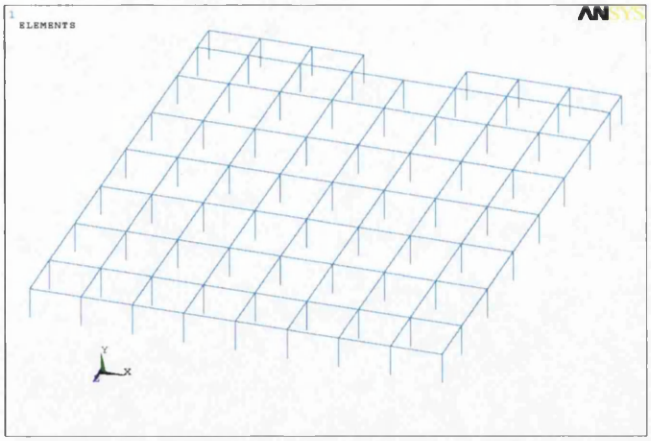

a) Bolt shank elements **b) Reinforcement and shear stud elements**

Fig 4.10: Finite element modeling of 3-D Spar (Link-8) elements.

v) Contact 52

The 3D interface elements i.e.CONTACT 52 were introduced between the endplate and the column flange to model movement of endplate away from the column flange. The gap or contact problems need to be modelled by using contact elements. The coefficient of friction equal to 0.5 is defined for sliding resistance while the interface is closed.

The ANSYS programme [17] provides several choices for contact elements which transfer load only when the materials are in contact at the gap interface. Normally, these contact elements are used to connect point to point or point to surface either with two or three degrees of freedom. In plane problems, contact elements with two degrees of freedom can be used, while in 3D space frame problems contact elements with three degrees of freedom can be used. In the present research, three dimensional point to point contact element, CONTACT 52 is chosen.

This element represents two surfaces which may maintain or break physical contact and may slide relative to each other. The element is capable of supporting only compression in the direction normal to the surfaces and shear (Coulomb friction) in the tangential direction. The element has three degrees of freedom at each node: translations in the nodal x, y, and z directions. The element may be initially preloaded in the normal direction or it may be given a gap specification.

The element is defined by two nodes, two stiffnesses (normal stiffness, KN and horizontal stiffness, KS), an initial gap or interference (GAP), and an initial element status (START). The orientation of the interface is defined by the node locations, or by a user-specified gap direction. Most interfaces between adjoining components are initially in contact with each other, that is, the initial gap is zero. Zero gap, however, is not applicable to element CONTACT 52. A value of 10^{-5} mm is used when the gap between the contact surfaces is zero. If the value is less than 10^{-5} mm, the value will be treated as 0.000 by the programme.

A specified stiffness acts in the normal and tangential directions when the gap is closed and not sliding. The stiffness of contact elements will not affect the results significantly. The higher the stiffness value, the more accurate results, but it takes more time to execute the program.

4.3.3. BOUNDARY CONDITIONS

The size of a finite element model can be reduced significantly by using symmetry in the body being analyzed. There was symmetry along the length of the column web (the Y - axis in the finite element model). The loading was symmetric about the middle of the column flange. The support conditions were almost symmetric along the middle longitudinal section of the column web perpendicular to X-axis and Z-axis. It was possible to consider only half of the model, and apply the boundary conditions to all nodes along the middle section of the column web i.e. symmetry about a vertical plane is utilized and only half of the structure is analyzed.

The column flange is assumed to be rigid and the nodes along the back of the flange are fixed against all translations. Finally, nodes along the symmetrical surface are fixed against lateral translations. The boundary conditions used in finite element modeling of connections are tabulated in Table 4.4.

Table 4.4: Boundary conditions used for the development of connection modeling

Sl No.	Location	Material	Restrained Dof 's
1	At column bottom	Steel	Ux, Uy, Uz, ROTx, ROTy, ROTz
2	At column top	Steel	Ux, Uy, Uz, ROTx, ROTy, ROTz
3	At flush endplate bottom	Steel	Uy
4	At beam end	Steel	Ux
5	At concrete top, At reinforcement at end of cantilever	Concrete/ Reinforcement	Ux
6	At concrete top, At reinforcement near column flange/endplate	Concrete/ Reinforcement	Uz
7	Along the centre line of flush endplate	Steel	ROTx, ROTz

The model presented in Fig. 4.6 is in the global coordinate system where x, y and z axes are parallel to the lines. Symbols used in the Table 4.4 are in terms of U and ROT which are translation and rotation respectively. For example, Ux and ROTx represent restriction of translation and rotation respectively against the X-axis.

Due to symmetrical configuration along the centre line of column web, a half model (Fig 4.6) was analysed by incorporating necessary boundary conditions as mentioned in Table 4.4.

4.3.4 MESH REFINEMENT

Mesh refinement is extremely important. If the mesh is too coarse, results can contain serious errors. If the mesh is too fine, it will waste computer resources, experience excessively long run times and model may be too large to run on the computer system. To avoid such problems, always address the issue of mesh density before begin the model generation.

The accuracy of any complex finite element program is limited by the mesh refinement. Therefore, for all validation tests, a coarse and a fine mesh are considered. The terms "coarse" and "fine" are nominal and represent relative mesh refinement (i.e., the coarse mesh has half the number of elements as the fine mesh). The coarse and fine meshes are shown in Fig. 4.6, 4.7, and 4.9 respectively. The coarse mesh results are within 2% of the fine mesh results and the initial coarse mesh was considered adequate. However, in this research, mesh refinement was considered in critical areas (endplate and column flange at endplate portion).

4.4 MATERIAL PROPERTIES

In finite element analysis, material properties are extremely important to understand the constitutive relationships and failure modes of the model. In this research, the material properties for universal beam, universal column, endplate, bolts and nuts, shear stud, metal decking, reinforcement and concrete elements has been considered.

In any structure, failure normally occurs in the connections and surrounding concrete, while bond failure between the reinforcement and the surrounding concrete seldom happens. Thus the full interaction between concrete and universal beam flange through metal decking has been considered in the finite element model.

The material properties used for steel and concrete in the finite element analysis were taken from the results of material conducted by different authors mentioned in the following table

Table 4.5: Material properties considered for finite element modeling in CASE – A [6]

Element Type	Yield Strength (N/mm^2)	Density (N/mm^3)	Young's Modulus, E (N/mm^2)	Ultimate tensile strength (N/mm^2)	Poisson's ratio
Column flange	289.8	7.85×10^{-5}	2×10^5	458.80	0.30
Column web	317.4	7.85×10^{-5}	2×10^5	485.90	0.30
Beam flange	314.0	7.85×10^{-5}	2×10^5	514.80	0.30
Beam web	377.40	7.85×10^{-5}	2×10^5	496.90	0.30
Endplate	275 *	7.85×10^{-5}	2×10^5	458.80 *	0.30
Reinforcement					
For T 12 rebar	497	7.85×10^{-5}	2×10^5	870	0.30
For T 10 rebar	504	7.85×10^{-5}	2×10^5	622	0.30
Concrete		2.50×10^{-5}	34785		0.25

* - For endplate, minimum values have been considered for the analysis.

For concrete, $f_{cu} = 40\ N/mm^2$ is considered.

Young's modulus of concrete is calculated as per BS: 8110 -1-1997.

Table 4.6: Material properties considered for finite element modeling in CASE – B [10].

Element Type	Yield Strength (N/mm^2)	Density (N/mm^3)	Young's Modulus, E (N/mm^2)	Ultimate strength (N/mm^2)	Poisson's ratio
Column flange	387.2	7.85×10^{-5}	2×10^5	527.1	0.30
Column web	403.0	7.85×10^{-5}	2×10^5	536.5	0.30
Beam flange	284.4	7.85×10^{-5}	2×10^5	458.7	0.30
Beam web	308.20	7.85×10^{-5}	2×10^5	469.1	0.30
Endplate	265.3	7.85×10^{-5}	2×10^5	438.1	0.30
Reinforcement					
For T 16 rebar	495	7.85×10^{-5}	2×10^5	-	0.30
For T 12 rebar	488	7.85×10^{-5}	2×10^5	-	0.30
Concrete		2.50×10^{-5}	30125	0	0.25

For concrete, $f_{cu} = 30$ N/mm^2 for CJ1 and 40 N/mm^2 for CJ2 is considered.

Young's modulus of concrete is calculated as per BS: 8110 -1-1997 for CJ1.

Table 4.7: Material properties considered for finite element modeling in CASE – C. Nominal values were considered in this case.

Element Type	Yield Strength (N/mm^2)	Density (N/mm^3)	Young's Modulus, E (N/mm^2)	Tangent Modulus (%)	Poisson's ratio
Column flange	345	7.85×10^{-5}	2×10^5	1.0	0.30
Column web	345	7.85×10^{-5}	2×10^5	1.0	0.30
Beam flange	345	7.85×10^{-5}	2×10^5	1.0	0.30
Beam web	345	7.85×10^{-5}	2×10^5	1.0	0.30
Endplate	345	7.85×10^{-5}	2×10^5	1.0	0.30
Reinforcement					
For T 16 rebar	460	7.85×10^{-5}	2×10^5	0	0.30
For T 12 rebar	460	7.85×10^{-5}	2×10^5	0	0.30
Concrete		2.50×10^{-5}	30125	0	0.25

For concrete, $f_{cu} = 30$ N/mm^2 is considered.

Young's modulus of concrete is calculated as per BS: 8110 -1-1997.

4.5 MATERIAL STRENGTH

The material strength used in the finite element analysis, which is applicable to both steel and concrete described here. Material strength is the most important, sensitive and dominate factor among the material properties, viz strength, ductility, durability, toughness, etc. Usually the yield stress or proof stress is used to define strength for steel and the cube or cylinder strength is used to define strength for concrete.

Several material strengths have been chosen according to the purpose of application. These are sample strength, mean strength, characteristic strength and design strength. Sample strength can only be obtained after a physical sample test. This value cannot be used to predict the material strengths of an analysed model because of the randomness of material properties. Mean strength normally considered as the average value of at least three standard tested samples. It is a statistical value with 50% of failure possibility. Characteristic strength is a statistical value based on large amount of physical test results with 5% possibility of failure, and is a standard value widely used in engineering standards and codes. Design strength is a one used in design work, with much smaller failure possibility and large safety factor. In finite element modelling on the behaviour of engineering structures, normally test results should be matched firstly. The safety of the recommended design methods can be considered afterward. Therefore, the standard value of characteristic strength is used as the basic input strength for any kind of material in this research, unless particular stress states are considered.

CHAPTER 5

ASSESMENT OF FINITE ELEMENT ANALYSIS RESULTS

5.1 INTRODUCTION

This research is focused on the behaviour of beam-column joint through flush-end plate connections in a building frame subjected to static and cyclic loadings. The principal purpose was to gain a better understanding of the engineering features of semi-continuous connections with steel and composite joints.

The objectives achieved during this research were set as:

1. To study the behaviour of semi-continuous bare-steel and composite joints by using flush end plate connections subjected to static loading.

2. To study the behaviour of semi-continuous bare-steel and composite joints with flush end plate connections subjected to Cyclic loading.

5.2 VALIDATION OF FINITE ELEMENT RESULTS WITH EXPERIMENTAL VALUES UNDER STATIC LOADING.

In order to evaluate the capability of the 3D finite element model, together with understanding the behaviour of connection, the experimental program reported by Y.Xiao, B.S. Choo & D.A. Nethercot [6] was examined analytically.

In order to make a direct comparison between the analytical and experimental studies, the results of the finite element analysis of the connections is presented as moment versus rotation as shown in Fig 5.1. The load was applied at the end of the cantilever and the connection moments were obtained by multiplying the recorded load, P by the length of lever arm, the distance measured from the centre of the load at the tip of the beam to the surface of the column flange. The typical calculation of rotation value is presented in Appendix – I.

The results of finite element model and the experimental investigation of SCJ4 and SCJ5 are in fairly good correlation with each other with marginal difference of 5 to 10% as shown in Fig 5.1.

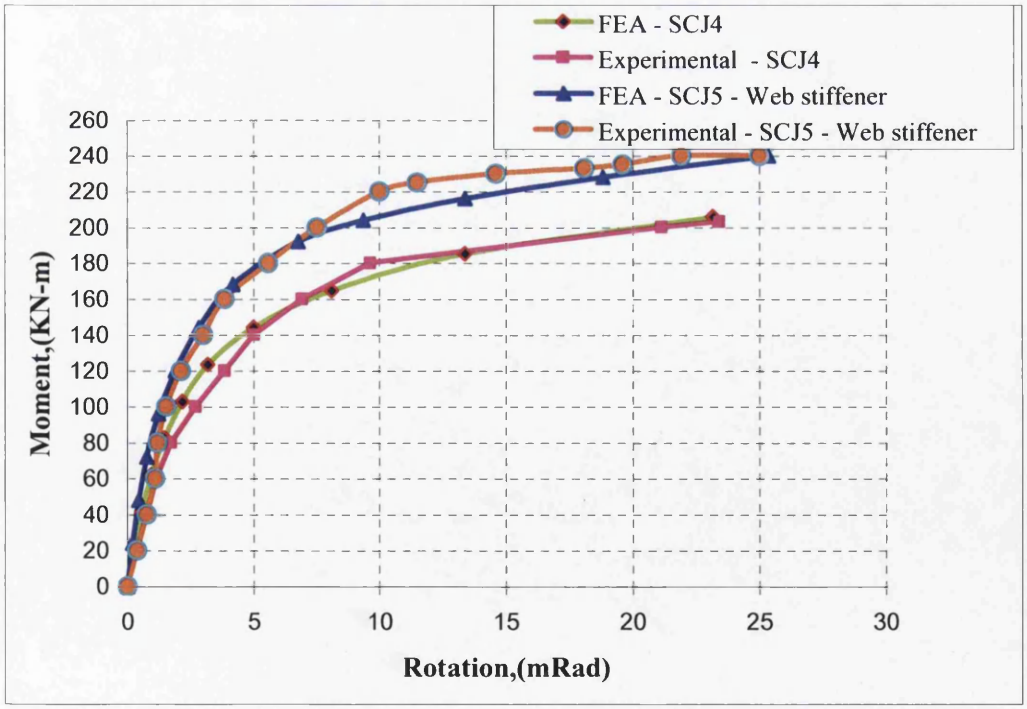

Fig: 5.1: Moment – rotation curve comparison between exp [6] & FEA results.

In the graph presented in the figure 5.1, it can be observed that initial stiffness of the both connection of 3D model showed slight deviation from the experimental. However, the results of the 3D model are consistent in all the above connections. Also, the moments and rotations are in the same range as the test data and the general trends of the curves are similar.

In figure 5.2, the moment vs. rotation curves of the SCJ4 and SCJ5 observed with the yielding sequence of several components during FE study. It is clearly noticed that in SCJ4 column web yields earlier than end plate, column flange and other components, where as this trend is entirely different in case of SCJ5 because of web stiffener. In this case, yielding of column web takes place with higher initial moment capacity of 165 Kn-m as compare to SCJ4 i.e. 95 Kn-m. However in both the cases, yielding of beam bottom flange and bolts are in last order.

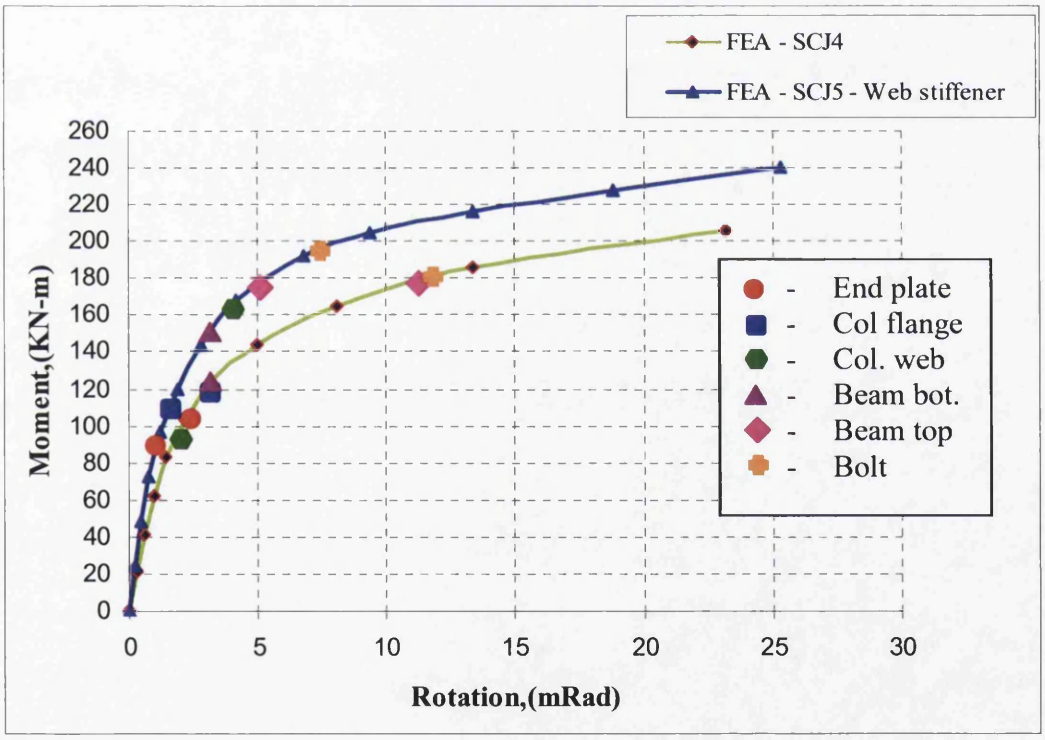

Fig: 5.2: Moment – rotation curve with yielding sequence of components in FEA study.

Also it is observed that the waiving of column web stiffeners is not advisable because their absence causes premature failure in the column web. This consequently leads to a drastic drop in moment and rotation capacities. The increase in moment capacity with web stiffener is about 15 to 20%.

The moment vs. rotation curves with different plate thickness and their yielding sequences are presented in fig 5.27 and 5.29 in section 5.5. It is clearly observed that if thickness of end plate lesser than the thickness of column flange and higher than the column web, the yielding of column web is prior to end plate. As thickness of end plate increases higher than the column flange (i.e. up to 40%) the trend of yielding sequence is entirely different.

Increasing the thickness of endplate from 10 mm to 20 mm increases both the moment capacity and rotation with almost the same percentage in the range of 20% to 30%. But trend of the curves in all the cases follows the same with marginal increase in initial stiffness. In case of thickness of plate almost twice than the column flange, it is found that no advantage will be gained to increase the moment capacity of connection for S275 grade steel due to excessive deflection of the column flange and web.

However, marginal increase in moment capacity can be achieved by increasing grade of steel to S355 for column section only.

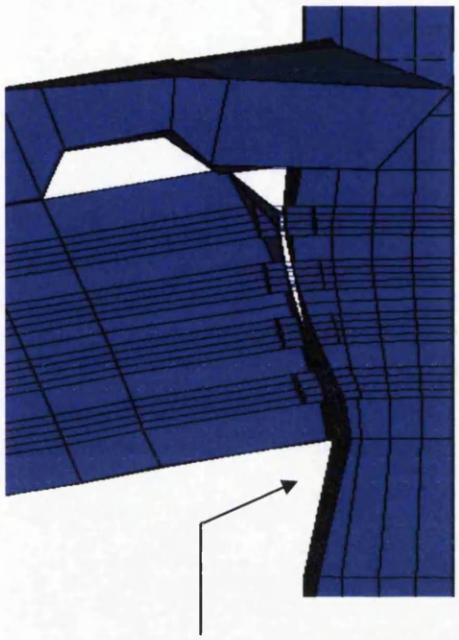

Buckling of column flange & web.

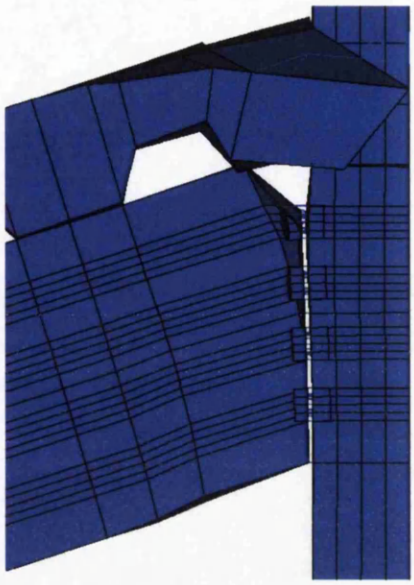

Buckling of beam flange & web.

a) SCJ4 – with out web stiffener

b) SCJ5 – with web stiffener

Fig: 5.3: showing failure modes of connections.

From the fig 5.3, it clearly reveals that the failure modes of SCJ4 and SCJ5 exactly follow the same trend of experimental investigation [6].

5.3 CORRELETION OF FINITE ELEMENT RESULTS WITH EXPERIMENTAL VALUES UNDER CYCLIC LOADING.

The previous section of this chapter examined the effectiveness of the finite element method predicting the behavior of test specimens subjected to static loading, where emphasis was placed on correlating the moment – rotation values with two experimentally tested flush end plate configurations.

This section presents some of the findings of an ongoing study to correlate test results of flush end plate connections under cyclic loading with the results of finite element investigations.

5.3.1 ECCS CYCLIC LOADING

The finite element modeling of flush endplate connections have been considered for the cyclic loading analysis following the ECCS loading procedure [21]. The procedure for assessing the behaviour of structural steel elements under cyclic loads recommended by the ECCS can be applied to plane or three dimensional tests and may include preliminary monotonic displacement tests. This procedure is designated the complete testing procedure. If monotonic tests are omitted it is designated the short testing procedure.

5.3.2 COMPLETE TESTING PROCEDURE

This procedure includes three tests performed on different specimens. The first and second tests impose displacement increasing monotonically in the tension and in the compression range respectively. The positive and the negative reference elastic load F_y and the corresponding reference elastic displacement δ_y are obtained from the recorded force-displacement curve. The reference elastic load is defined as the intersection between the tangent modulus E_t at the origin of the force-displacement curve and the tangent that has a slope of $E_t/10$ as indicated on Fig 5.4.

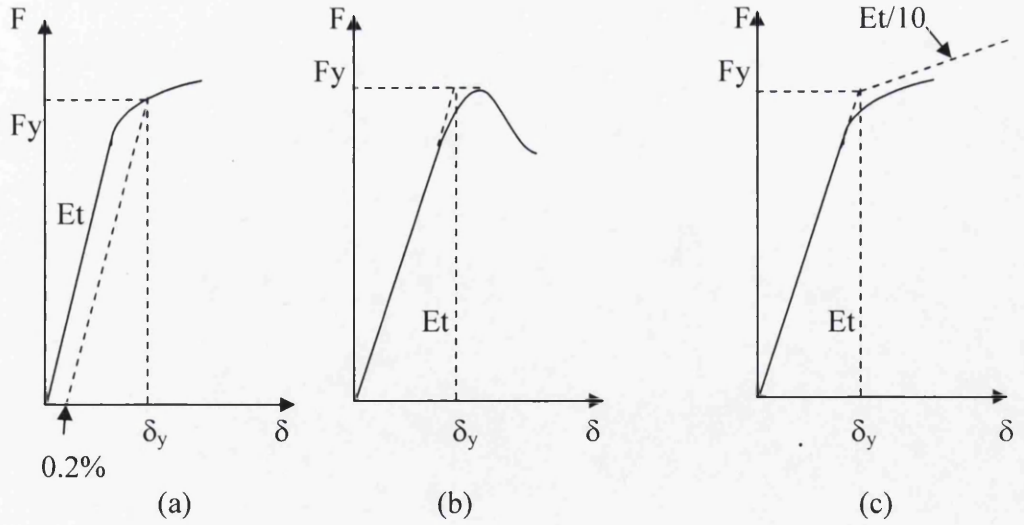

Fig: 5.4: Reference elastic force Fy and the corresponding reference elastic displacement δy for cyclic loading.

Other conventional definitions of F_y may be used, such as (a) the value corresponding to the 0.2% offset load at some point in the tested specimen (Figure 5a), or (b) the maximum load (Figure 5b). Definition (a) ignores the post-elastic reserves of the specimen and definition (b), in spite of its interest in the buckling context, may correspond to exaggerated deformation of the flexural behaviour of beams or joints. The definition of F_y recommended by the ECCS (Figure 5c) covers many cases and types of behaviour and avoids some disadvantages of the definitions (a) and (b).

The third test is a cyclic test with increasing displacement as follows:

- one cycle in the interval $[+\delta_y/4 \; ; -\delta_y/4]$,
- one cycle in the interval $[+2\delta_y/4 \; ; -2\delta_y/4]$,
- one cycle in the interval $[+3\delta_y/4 \; ; -3\delta_y/4]$,
- one cycle in the interval $[+\delta_y \; ; -\delta_y]$,
- three cycles in the interval $[+(2+2n)\delta_y \; ; -(2+2n)\delta_y]$ with $n = 0,1,2,3...$

The end of the test is not defined beforehand. For research purposes the test will probably be continued as far as possible in order to obtain the maximum information.

A cyclic displacement history as shown in fig 5.5 was applied to the beam tip. Displacement amplitudes were specified in multiples of δy, which represents the displacement at the cantilever end when the beam reached its yield moment capacity. The specimens were subjected to displacement amplitudes of 0.25, 0.5, 0.75, 1.0, 2.0, 4.0, 6.0, 8.0δy and so on as shown in fig 5.5 until the analysis is not converged.

The envelopes of the M- Φ curves from the cyclic loading were almost identical to the M- Φ curve from monotonic test, indicating that the ECCS cyclic loading procedure did not affect the monotonic M- Φ curves behaviour of the composite joint. The differences of the peak moment capacities were less than 12% [10].

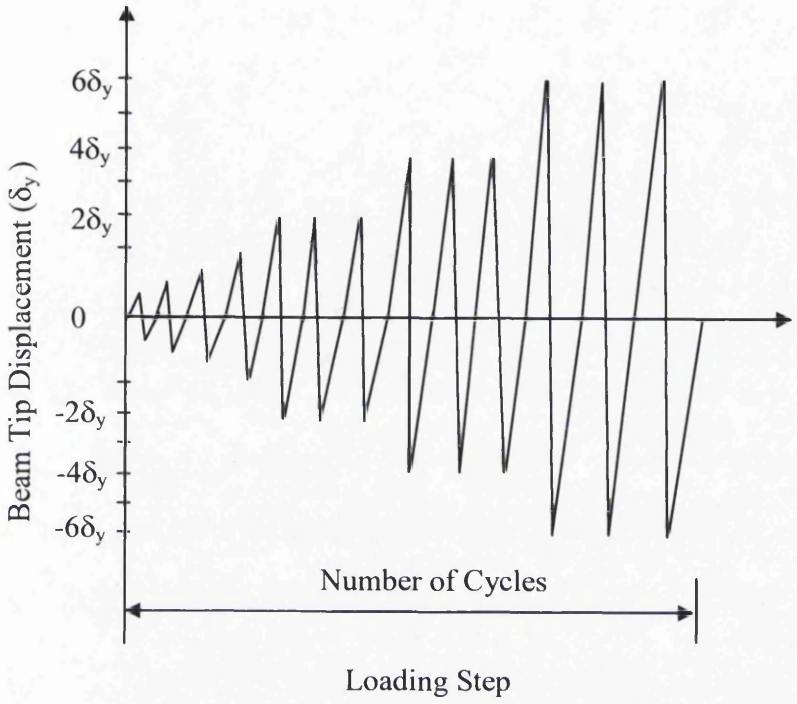

Fig: 5.5: ECCS loading procedure

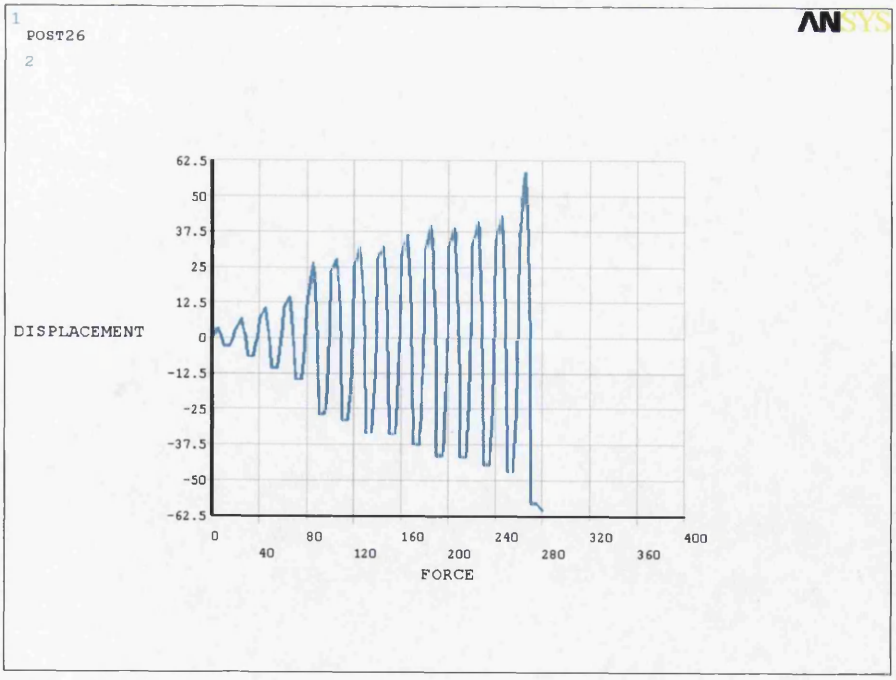

Fig: 5.6: Shows typical pattern of cyclic loading applied in ANSYS.

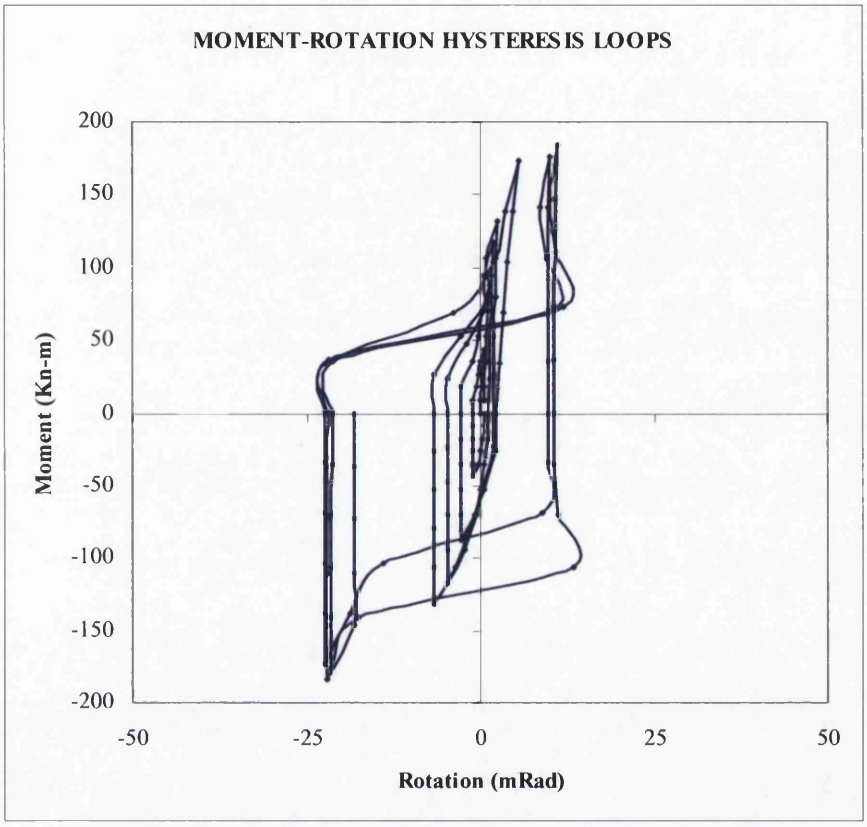

Fig: 5.7: Moment – Rotation hysteresis loops for specimen SCJ4 from FEM analysis

From the fig 5.7, it can be observed that rotation values from monotonic and cyclic tests were almost identical and the maximum moment capacity in case of cyclic load test is about 183.75 Kn-m, where as in case of monotonic test the maximum moment capacity is nearly 205 Kn-m. The difference between the both maximum moment capacities is works out to be 10.5% which is less than 12% [10]. The cyclic loading analysis was not converged beyond this moment capacity.

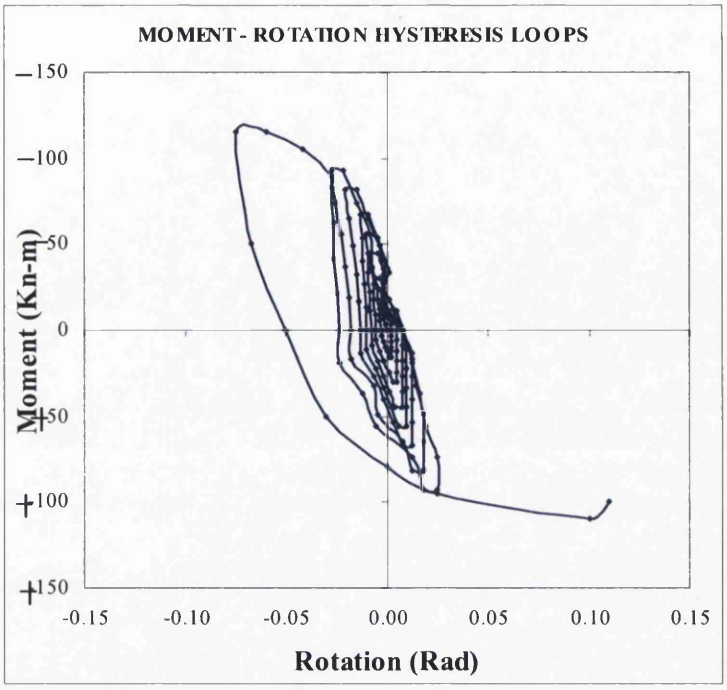

Fig: 5.8: Moment – Rotation hysteresis loops for specimen SJ1 from experimental investigation [10].

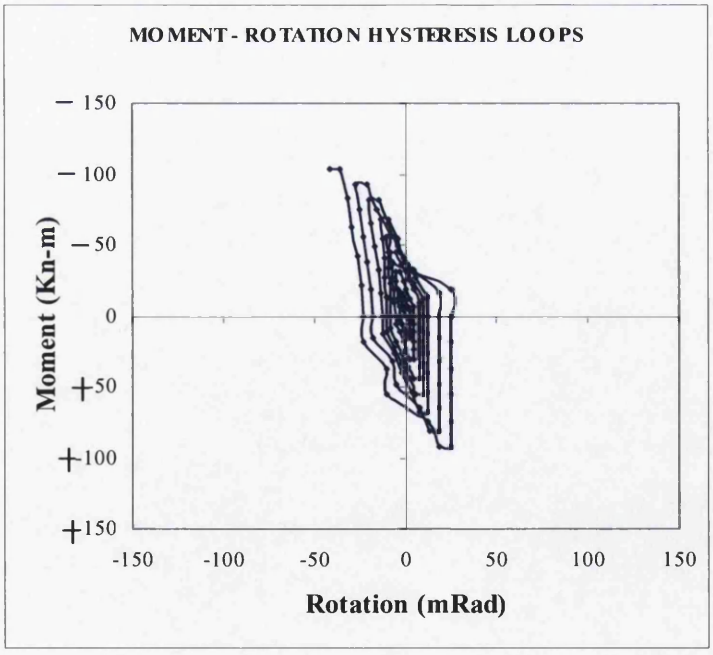

Fig: 5.9: Moment – Rotation hysteresis loops for specimen SJ1 from FEM analysis.

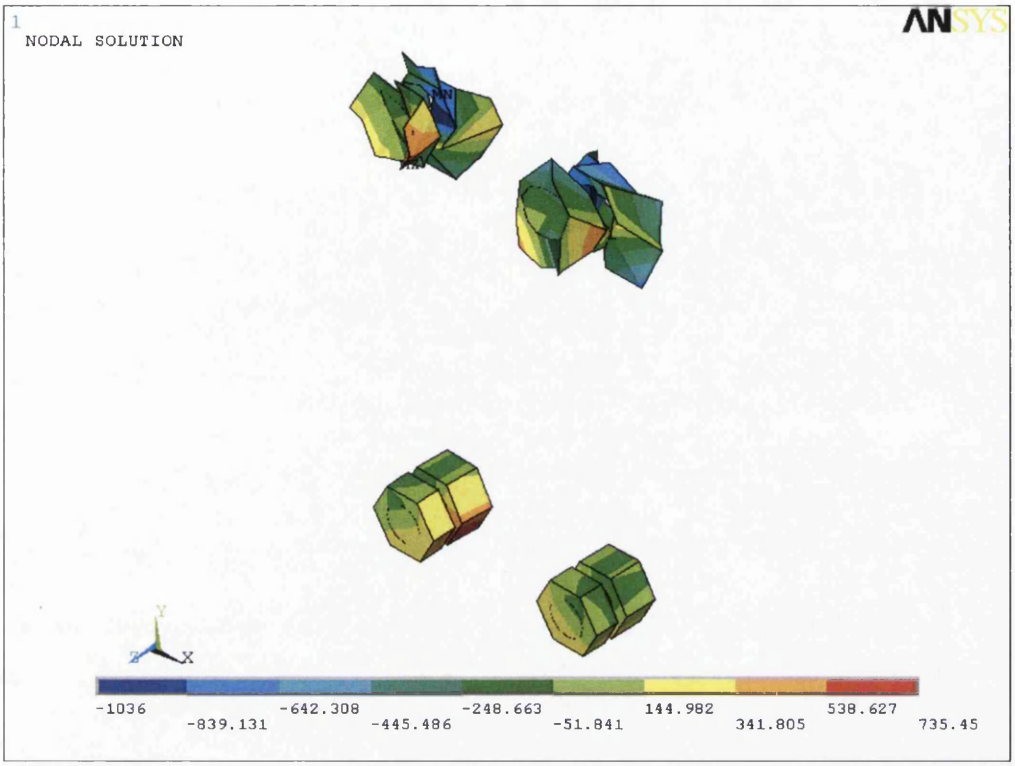

Fig: 5.10: Bolt fracture of connection at last cycle of analysis.

Typical input of cyclic loading in the ANSYS is shown in Fig 5.6. This Fig shows graph of displacement V/S number of cycles applied through point load at the end of cantilever beam tip. In this Fig, X-axis represents force in terms of number of load sub steps i.e. each cycle has one force value and it has applied in cyclic pattern with four iterations. Single iteration has five load sub steps, therefore twenty load sub steps per each cycle. Y- Axis represents, displacement results corresponding to each load sub step.

The results of finite element analysis were compared with the experimental results in terms of moment-rotation hysteresis loops to verify the analytical model. Figure 5.8 and 5.9 plots the moment versus rotation curves for specimen SJ1 as determined by experimental investigation and finite element analysis. The joint's moment rotational responses of FEM analysis follows the same trend of experimental investigation as shown in Fig 5.9, which are almost identical in both the positive and negative moment regions because of symmetry of the connection to the mid depth of beam section.

It is observed that the moment capacity (i.e 95 KN-m) in both the cases is the same, where as the rotation value at the last cycle of experimental investigation before failure is almost the same as finite element investigation as shown in Figs 5.8 and 5.9. After a number of plastic excursions, when the analysis is not converged at the last cycle (i.e. in the first cycle of $+ 8\delta_y$) due to increase in moment to 104 KN-m, one or more joint components such as endplate, column flange and column web deformed excessively and bolts fracture occurred as shown in Fig 5.10.

It is also observed that during the cyclic load analysis, the stresses are getting relieved (dissipated energy) in joint components due to failure of one of the joint components. This is shown in Fig 5.32 to 5.37 in Section 5.6, stress distribution of endplate before and after failure of joint. It is clearly seen that stress distribution pattern is entirely different before and after failure of the joint. But difference between the values of stresses in each component of the joint due to energy dissipation showed in Table 5.1. From the table, it can be noted that the difference of decrease in percentage (i.e. energy dissipation) is higher in the column flange as compare to endplate, column web and beam. But in case of bolts, there is a marginal increase in stresses which is about 6.0%. During cyclic analysis, stresses in both the + ve and – ve ranges were almost similar. Whereas, after the failure of joints the stress values were more or less same as monotonic loading(in the range of 15 to 20% variation) as shown in Fig 5.32 to 5.43 in Section 5.6. The stresses in the endplate attain the maximum values earlier than the column flange both in the case of cyclic loading as well as monotonic loading.

From the Table 5.2, it can be observed that in case of composite joints the difference of decrease in percentage (i.e. energy dissipation) is higher in the column web as compare to endplate, column flange and beam. But in case of bolts, there is a considerable increase in stresses which is about 28.21%.

Table 5.1: The values of stresses before and after failure of joint during cyclic loading (energy dissipation) - SJ1.

Sl. No.	Component	Max stresses in N/mm2		% of difference
		Before failure	After failure	
1	End Plate	481.253	441.458	-8.26
2	Column flange	506.198	399.39	-21.1
3	Column web	335.39	265.06	-20.96
4	Beam	285.26	257.94	- 9.58
5	Bolts	976.25	1036	+6.12

Table 5.2: The values of stresses before and after failure of joint during cyclic loading (energy dissipation) - CJ2.

Sl. No.	Component	Max stresses in N/mm2		% of difference
		Before failure	After failure	
1	End Plate	470.629	437.37	-7.07
2	Column flange	503.398	406.871	-19.18
3	Column web	360.549	242.272	-32.80
4	Beam	294.446	232.187	- 21.14
5	Bolts	1010	1295	+28.21

- Decrease in percentage. + Increase in percentage.

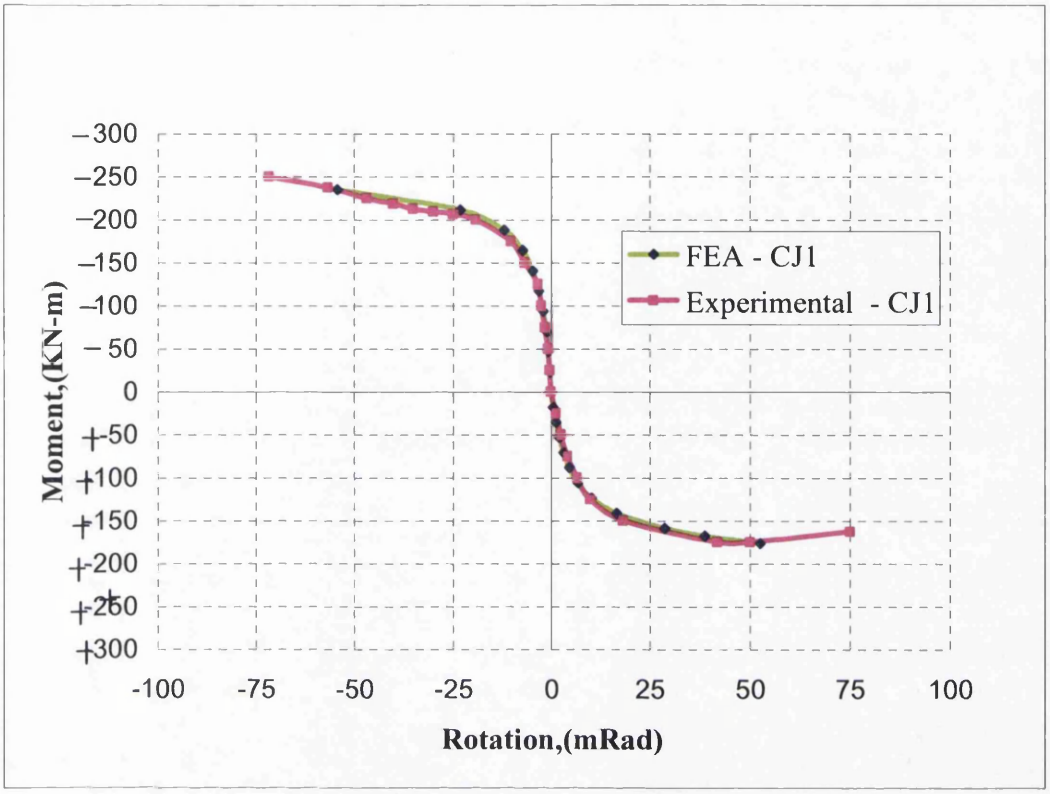

Fig: 5.11: Moment – rotation curve comparison between exp & FEA results [10].

Figure 5.11 illustrates the comparison of specimen CJ1 with finite element analysis results. The above Fig shows that the initial stiffness of both the cases is almost identical in positive and negative moment region, but there is a marginal difference in plastic region. In the experimental investigation, it is observed that there is slight dip at negative moment 210 KN-m and further proceeded till 250 KN-m. Where as, in positive moment region the peak value is 170 KN-m. In finite element analysis it is found that the stresses are with in the limit at peak values of moment. The results of finite element model and the experimental investigation of CJ1 are in good agreement with marginal difference of 5 to 10% as shown in Fig 5.11.

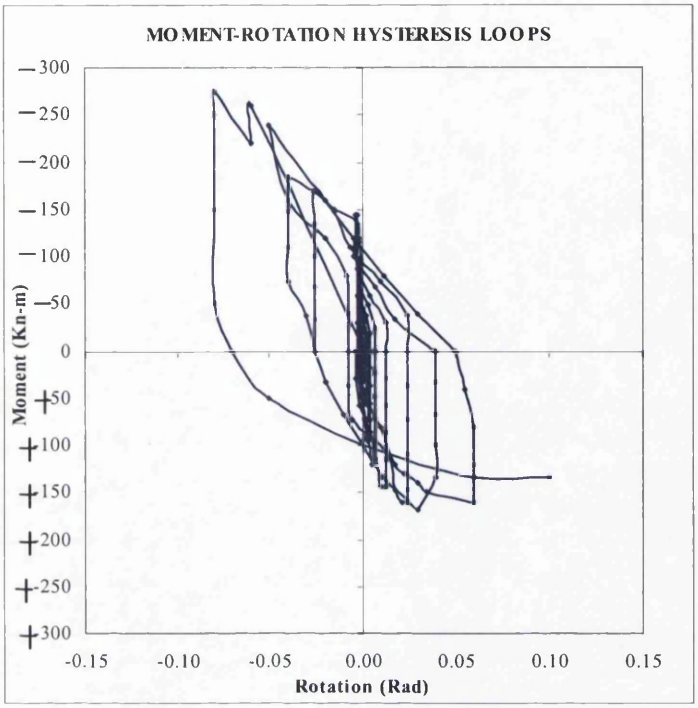

Fig: 5.12: Moment – Rotation hysteresis loops for specimen CJ2 from experimental investigation [10].

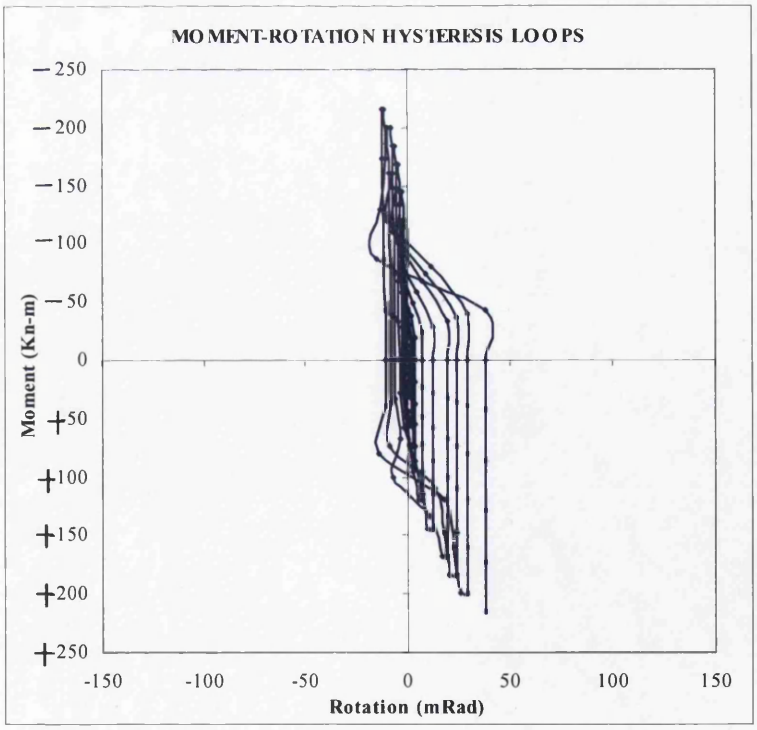

Fig: 5.13: Moment – Rotation hysteresis loops for specimen CJ2 from FEM analysis.

The specimen CJ2 which has composite format was also modelled to compare the finite element analysis results with the results from experimental investigation as shown in Fig 5.12 and 5.13 in terms of moment-rotation hysteresis loops. The curves from numerical analysis have a higher initial stiffness than the curves obtained from the experimental test specimens probably due to stiffness of concrete and metal deck. The variation in the results of ultimate moment and rotation is in the order of 10 to 15%. The differences between the results from the two approaches are small and considered acceptable for adoption of this technique in the analysis of larger and more intricate joints.

The behaviour of composite joint is entirely different from the bare-steel joint. In case of bare-steel joint, the joint's moment rotational responses is almost identical in both the positive and negative moment regions because of symmetry of the connection to the mid depth of beam section as shown in Fig 5.8 and 5.9. But composite joints exhibit different moment – rotational responses when they are subjected to positive and negative moments under a reversal of loads as shown in Fig 5.12 and 5.13.

In case of composite joint, the results in negative region are higher than the positive region because of increase in stiffness due to composite action as shown in Fig. 5.11 to 5.15. It is also observed that the composite joint has more initial stiffness than the bare-steel joint. In case of CJ2 the analysis was not converged due to fracture of bolts. The difference between the values of stresses in each component of the joint due to energy dissipation is shown in the Table 5.2. The Fig. 5.14 and 5.15 shows comparison of equivalent von mises stress distribution of the specimen CJ2 and SJ1 at last cycle before failure of joint.

In experimental and finite element investigation, most of the hysteretic M-Φ curves follow more or less the same loading/unloading path during the cyclic loading history (except in the last cycle). This shows that the joint stiffness is not affected heavily by three load cycles. During experimental investigation, the shake down effect may only be observed when more load cycles are applied [10]. It can be correlated in finite element investigation that after three or four cycles M-Φ curve starts propagates in the plastic region.

Table 5.3 summarizes the results of the finite element analysis for three specimens and compares with test data. The first column specifies the test number and the second column shows the maximum moment reported in the test. The third column of the table shows the analytical moment capacity and column 4 shows their relative percentage of difference to assess the accuracy of the results between both the approaches. Also Table 5.3 compares the values of initial stiffness of both the approaches.

Table 5.3: Summary of Strength Results: Experimental vs FE analysis.

Specimen	Mu (Kn-m) Experimental		Mu (Kn-m) FE analysis		% of difference	
	Negative	Positive	Negative	Positive	Negative	positive
SJ1	125	110	104	95	16.8	13.6
CJ1	268	176	235	176	12.3	0.0
CJ2	273	167	220	200	19.4	12.0

Table 5.4: Summary of stiffness Results: Experimental vs FE analysis.

Specimen	$S_{j,ini}$ (Kn-m/rad) Experimental		$S_{j,ini}$ (Kn-m/rad) FE analysis		% of difference	
	Negative	Positive	Negative	Positive	Negative	positive
SJ1	13,103	13,091	11,104	11,104	15.25	15.17
CJ1	28,784	17,043	30,390	18,403	5.6	7.4
CJ2	27,648	16,987	30,390	18,403	9.9	8.34

It is observed that failure modes in finite element analysis follow the experimental investigation.

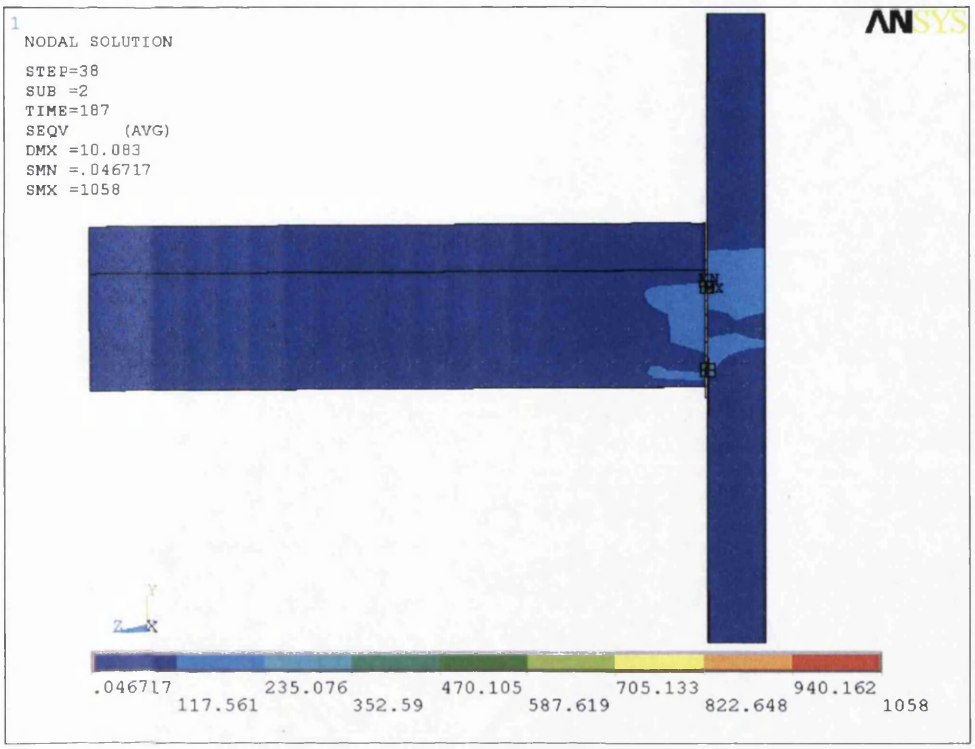

Fig: 5.14: Equivalent von mises stress distribution of the specimen CJ2 [10].

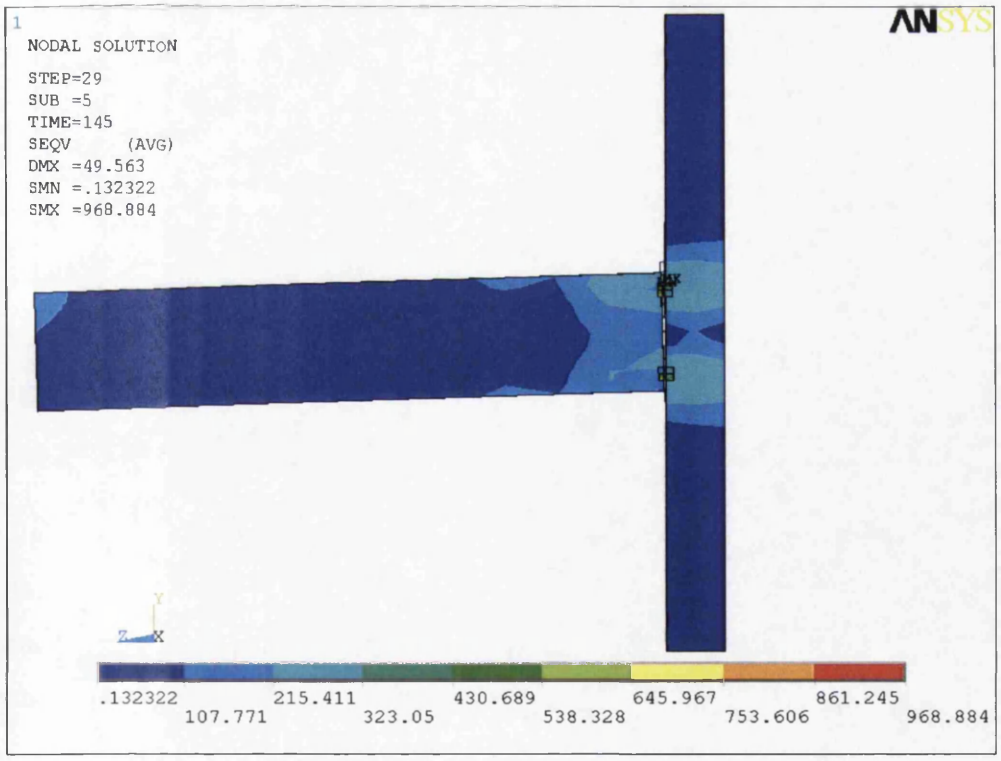

Fig: 5.15: Equivalent von mises stress distribution of the specimen SJ1 [10].

5.4. FINITE ELEMENT RESULTS FOR FURTHER RESEARCH

In this research, finite element analysis has been carried out on new flush end plate connection configuration which will be tested experimentally in Tongaji University, China. The details of connection configuration explained in chapter 4. Finite element results are furnished in this section for further research to compare with available experimental results in future.

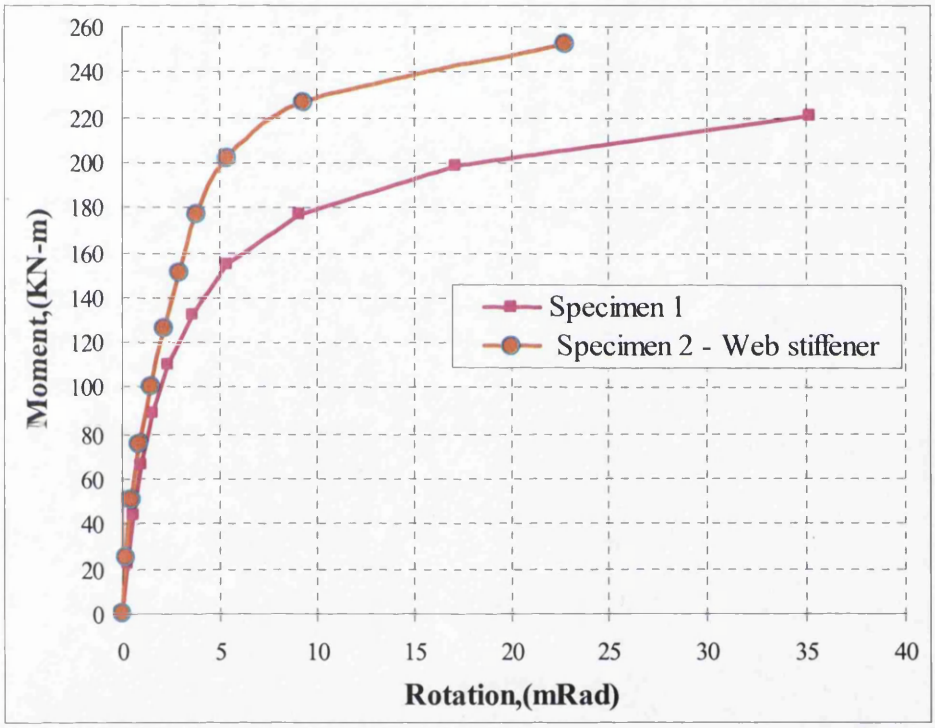

Fig 5.16: Moment – rotation curve of Tongaji project with monotonic load by FEA results.

The figure 5.16 demonstrates that it follows the same trend as appeared in figure 5.1, but the short fall is observed in case of rotation value corresponding to connection with stiffener. However, connection with column web stiffeners is advisable because their presence increases moment capacity up to 20%.

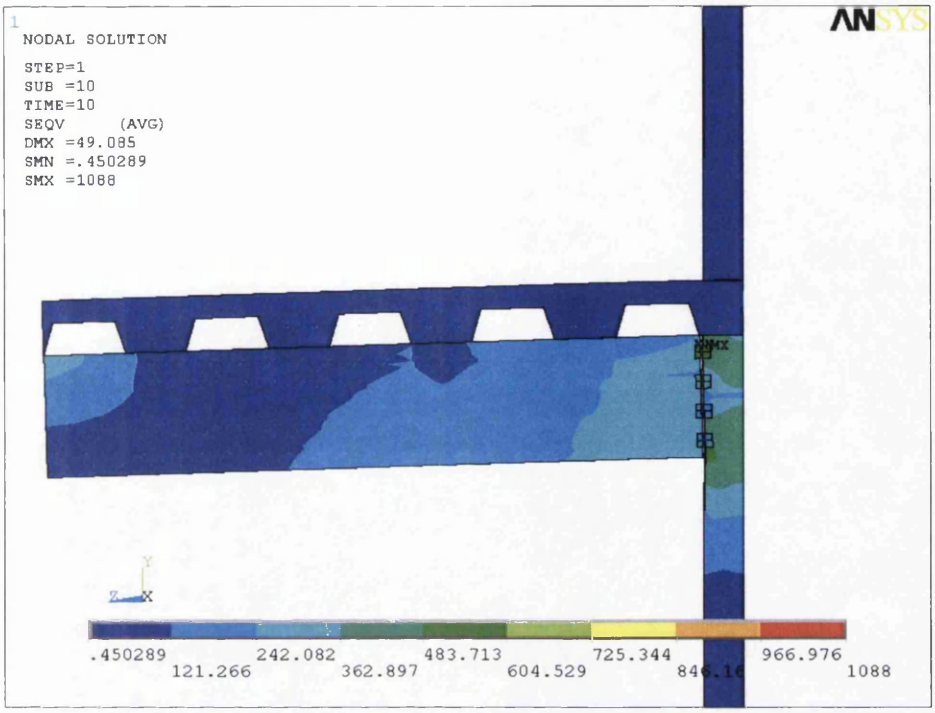

Fig: 5.17: Equivalent von mises stress distribution in Tongaji project specimen with out web stiffener- monotonic load.

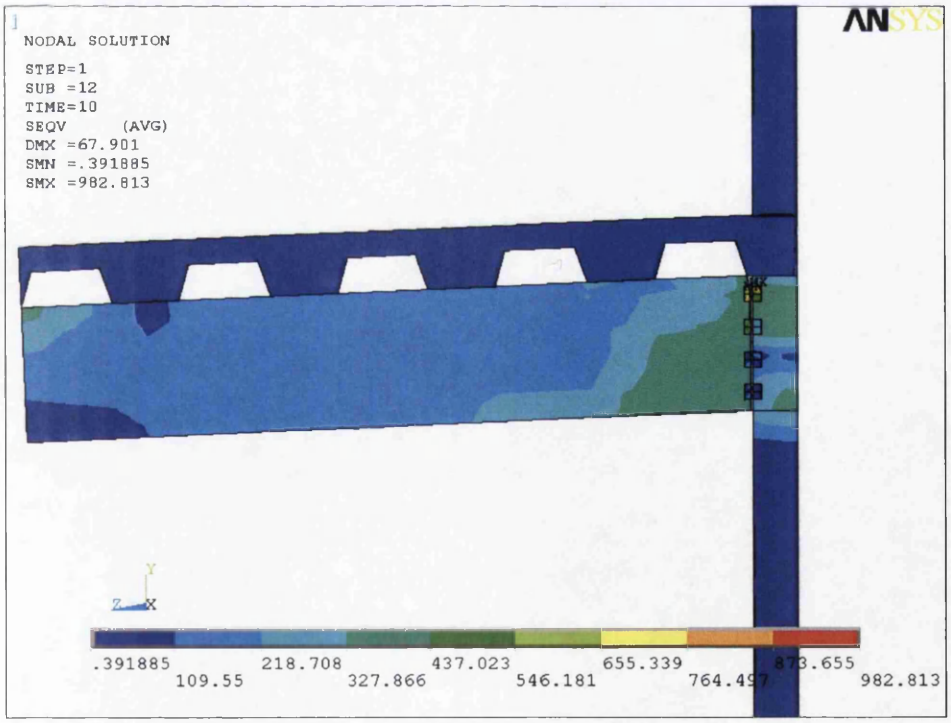

Fig: 5.18: Equivalent von mises stress distribution in Tongaji project specimen with web stiffener- monotonic load.

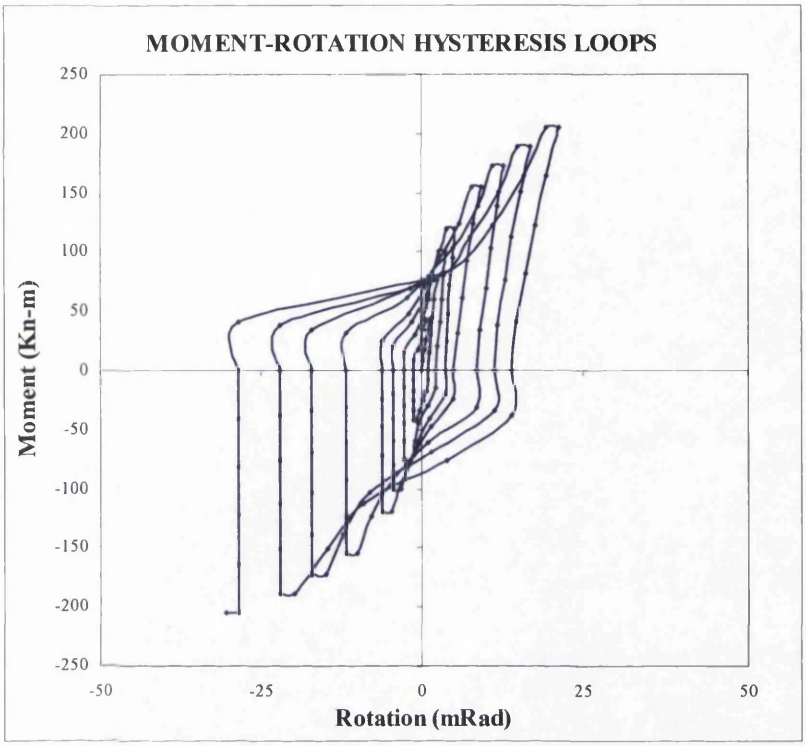

Fig: 5.19: Moment – rotation curve of Tongaji project with cyclic load by FEA results.

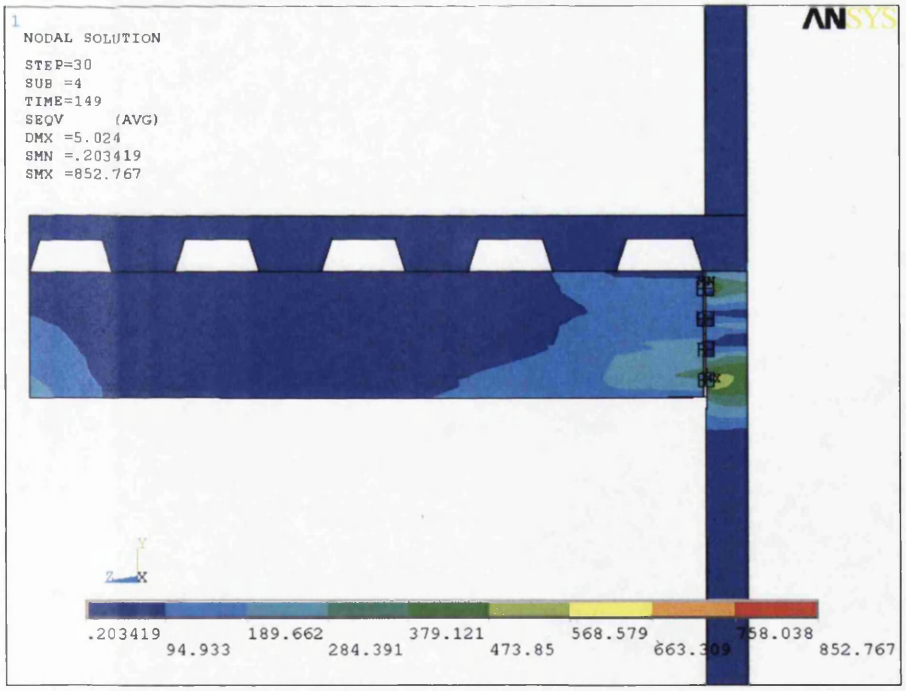

Fig: 5.20: Equivalent von mises stress distribution in Tongaji project specimen with out web stiffener- Cyclic load.

In figures 5.16 and 5.19, it can be seen that rotation values from monotonic and cyclic tests were more or less same and the maximum moment capacity in case of cyclic load test is about 205 Kn-m, where as in case of monotonic test the maximum moment capacity is nearly 220 Kn-m. The difference between the both maximum moment capacities is works out to be 7.3% which is less than 12% [10]. The cyclic loading analysis was not converged beyond this moment capacity. It is observed that, cyclic loading produces much more deterioration of the resistance of the connection than the monotonic loading.

5.5 PARAMETRIC STUDY

The finite element analysis has been carried out to compare several other parameters in terms of moment capacity viz, shape of bolt hole (hexagonal & circular), bare-steel and composite connections, no of bolt rows, diameter of bolts, different plate thickness and different percentage of reinforcement ratio.

To achieve the exact finite element modelling, initially the bare-steel joint has been modelled with hexagonal bolt hole and finally refined with circular bolt hole considering practical situations. The moment-rotation curve and stresses of both the case is compared and found only 5 to 7 % variations in the results as shown in Figs 5.21 – 5.23.

It is concluded that the moment carrying capacity of composite joint is about 60% to 75% higher than the bare steel joint as shown in Fig 5.24. The Fig 5.25 shows moment – rotation relationship between two and four rows of bolts. There is about 20% increase in moment capacity in case of four rows of bolts as compare to two rows. In Fig 5.26, comparison made between different bolt diameters and it shows that, there is not much difference in moment capacity for bolt diameters M20 and M22. Fig 5.27 shows moment-rotation curves of different plate thickness. Increasing the thickness of endplate from 10 mm to 20 mm increases both the moment capacity and rotation with almost the same percentage in the range of 20% to 30%.

Figure 5.28 compares the moment- rotation curves of specimen SCJ4 with different slab reinforcement percentage of 0.5%, 1.0%, 1.2%, & 1.5% respectively. This Fig clearly indicates that enhancement of reinforcement ratio in the slab, increases the capacity of the connection in terms of moment-resistance, initial stiffness and rotation. It is observed that increase in moment is considerable (about 30%) as reinforcement ratio increases from 0.5% to 1.5% and ductility of connection in terms of rotation increases almost double. If the percentage of reinforcement ratio is increase to 2.0%, ultimate stresses increases beyond the limit due to excessive deflection of column web, flange and endplate. Initial stiffness of all the curves follows the similar nature. Yielding sequence of joint components with different plate thickness was carried out and shown in Fig 5.29

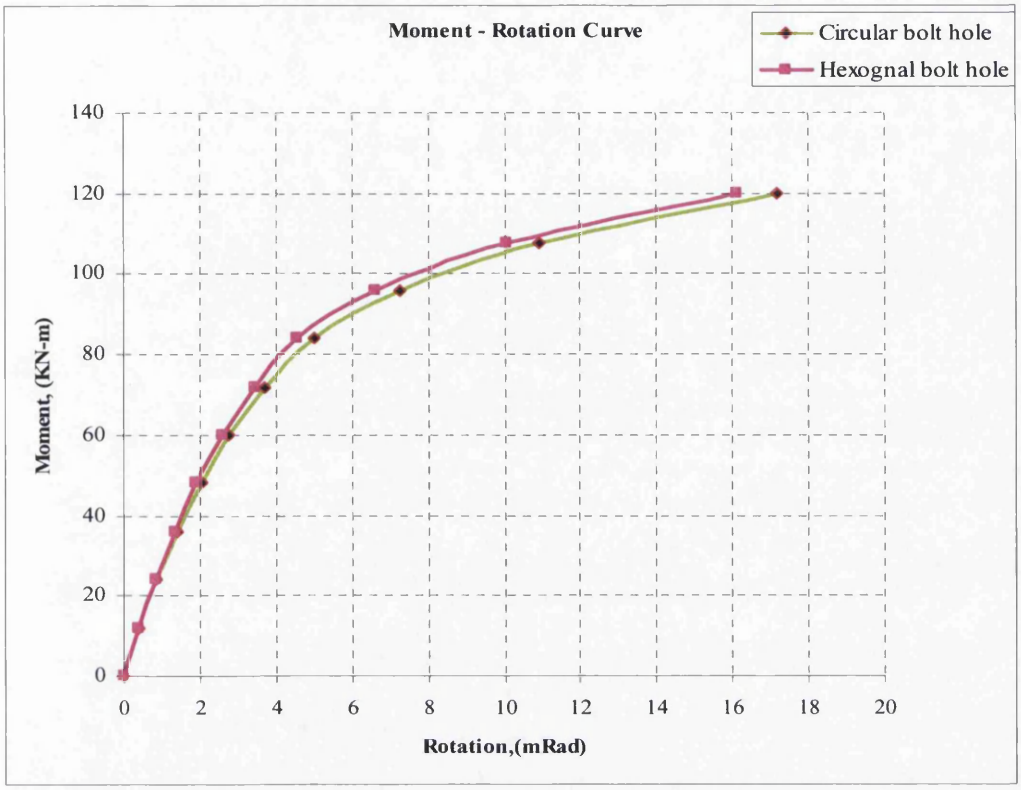

Fig: 5.21: moment vs. rotation curve of circular and hexagonal bolt holes

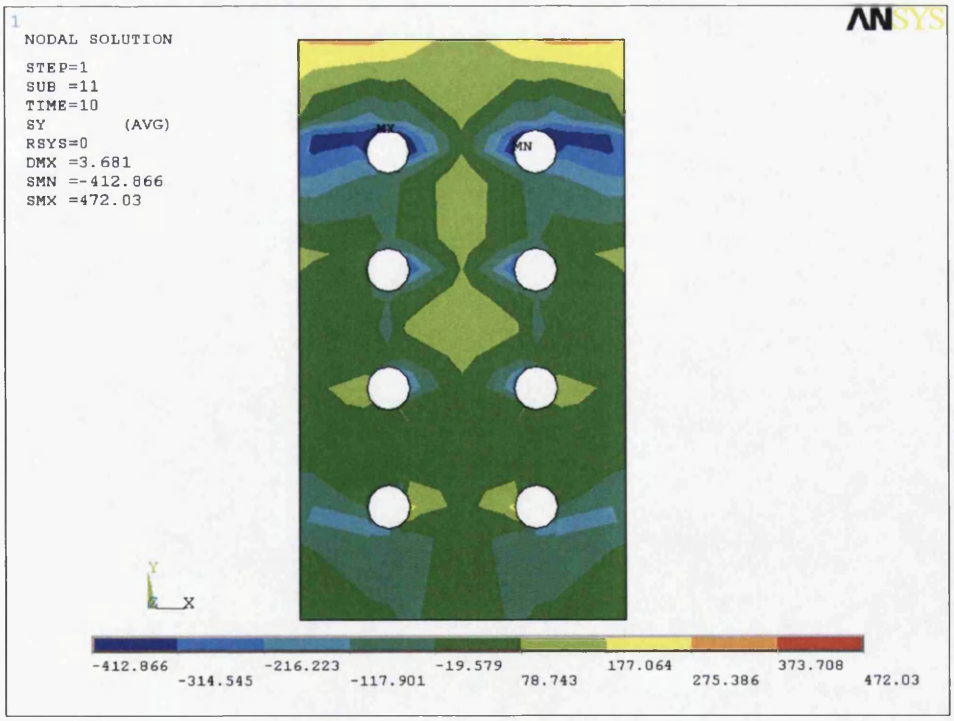

Fig: 5.22: Stress contours in end plate with circular bolt hole

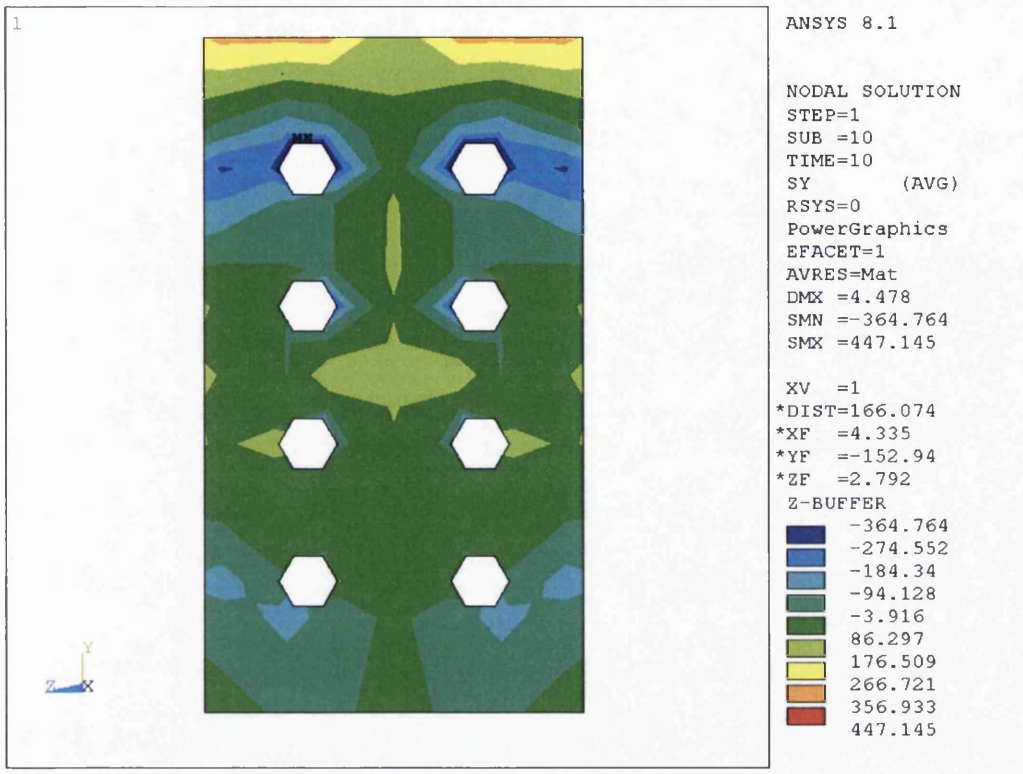

Fig: 5.23: Stress contours in end plate with hexagonal bolt hole

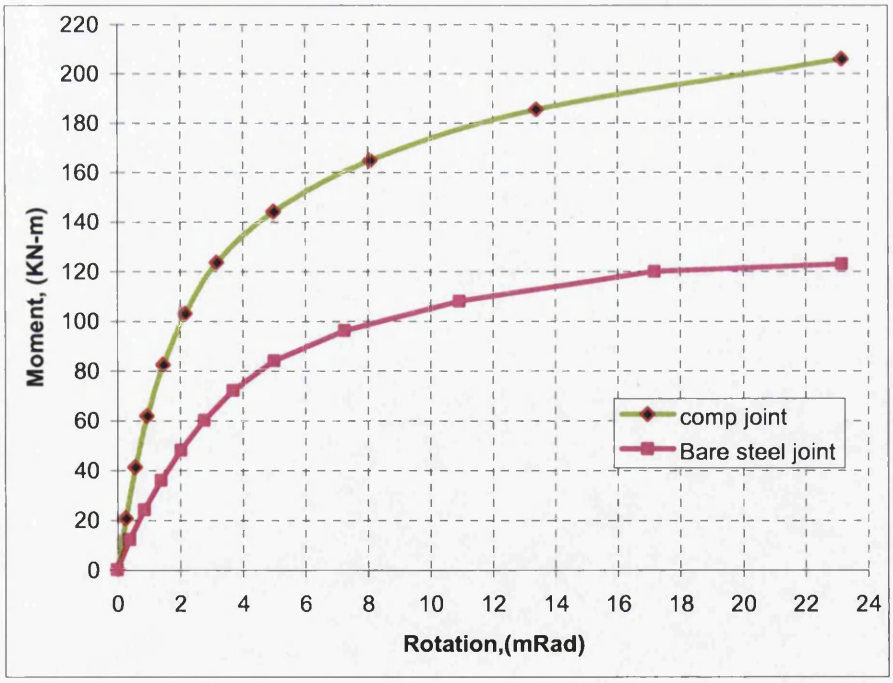

Fig: 5.24: Comparison of moment – rotation curves between composite & bare-steel joint.

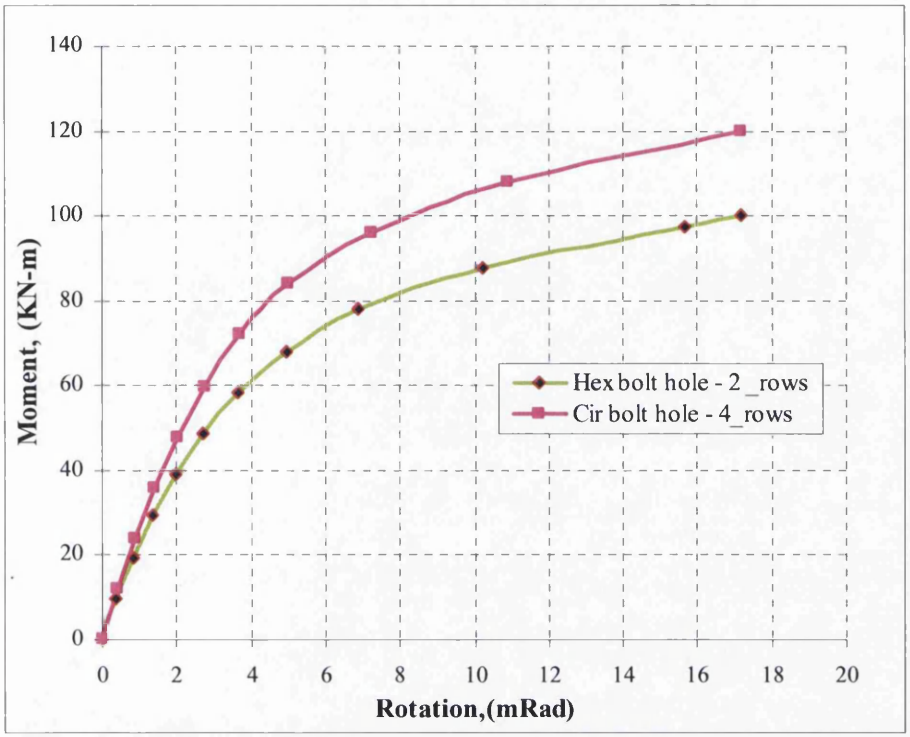

Fig: 5.25: Comparison of moment – rotation curves with different number of bolt rows

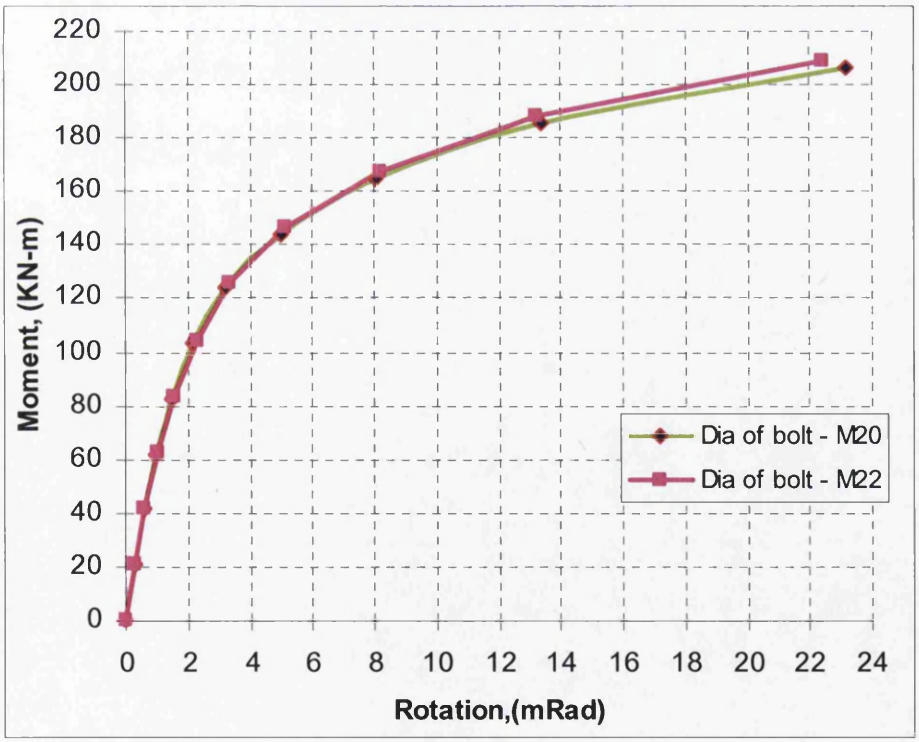

Fig: 5.26: Comparison of moment – rotation curves with different bolt diameters.

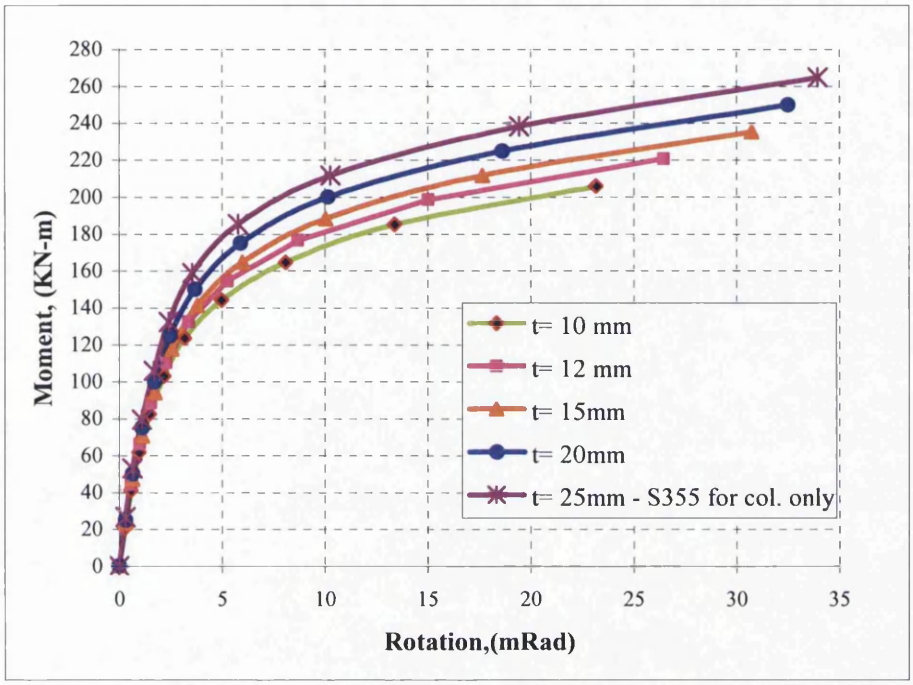

Fig: 5.27: Comparison of moment – rotation curves with different plate thickness

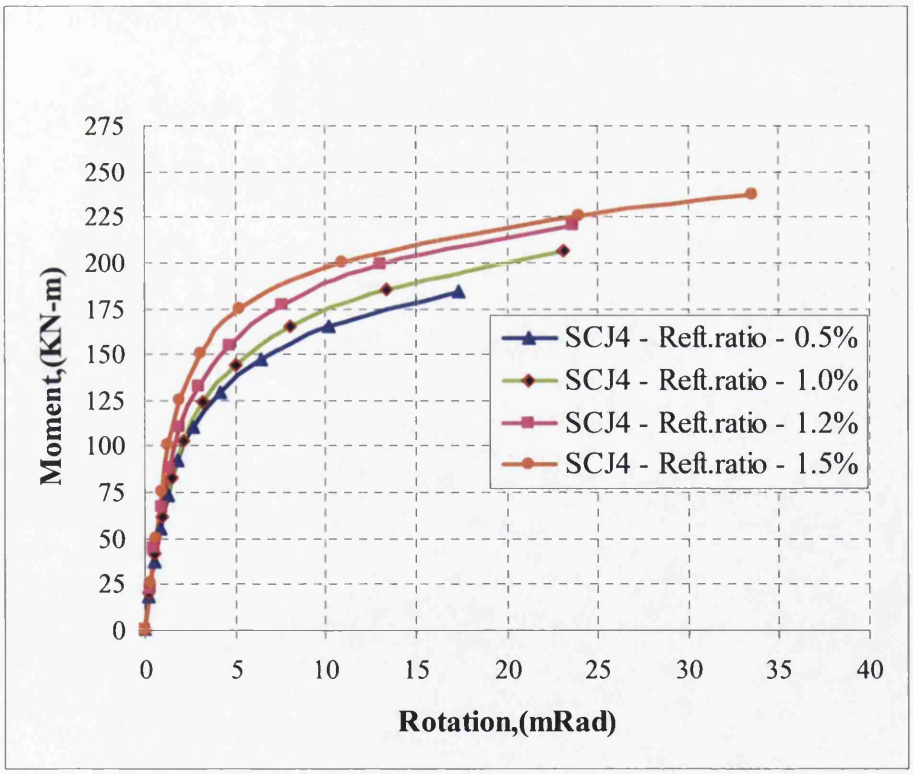

Fig: 5.28: Comparison of moment – rotation curves with different reinforcement ratio.

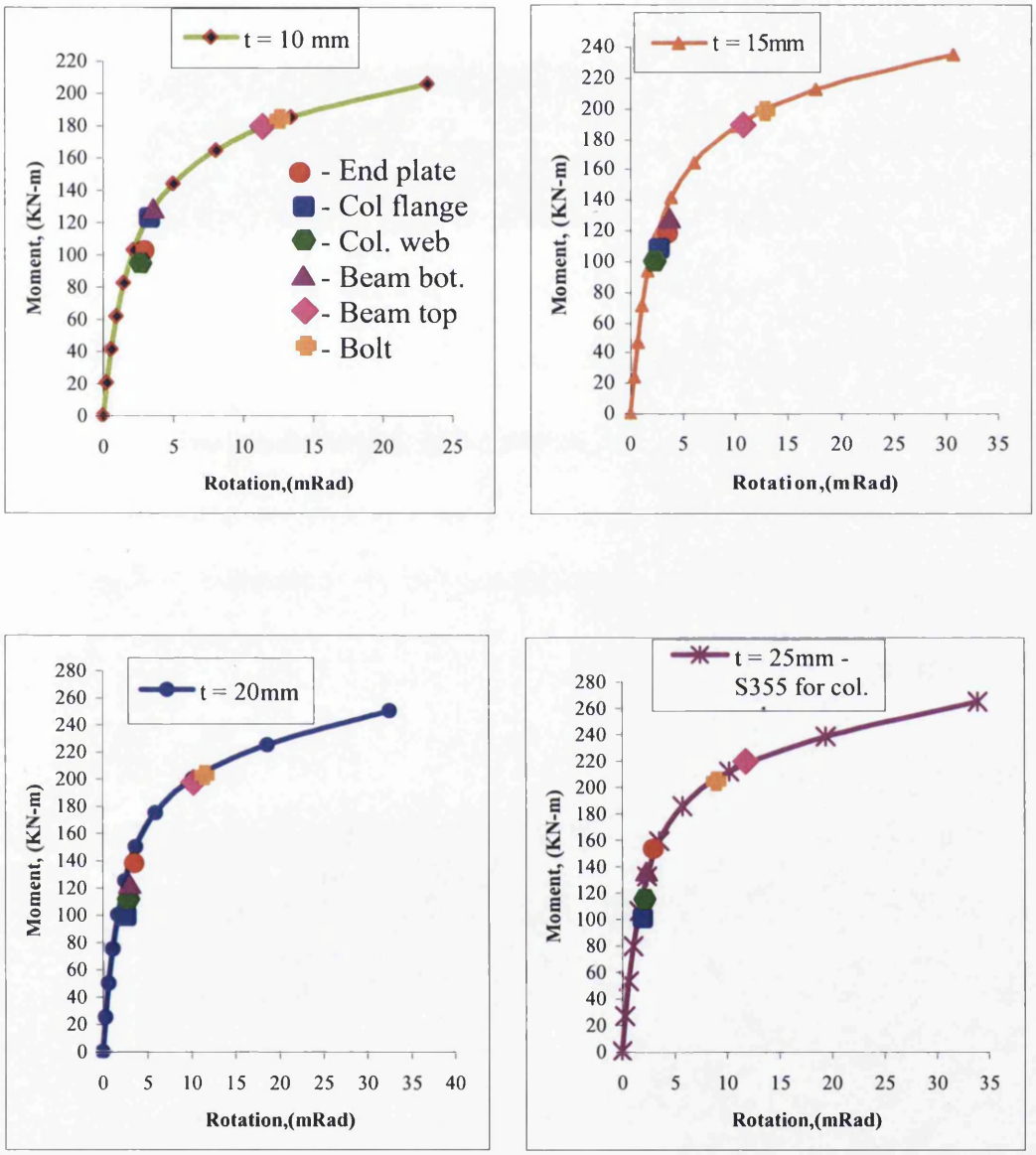

Fig: 5.29: Moment – rotation curve with yielding sequence of components with different plate thickness

5.6 STRESS CONTOURS AND OTHER FIGURES

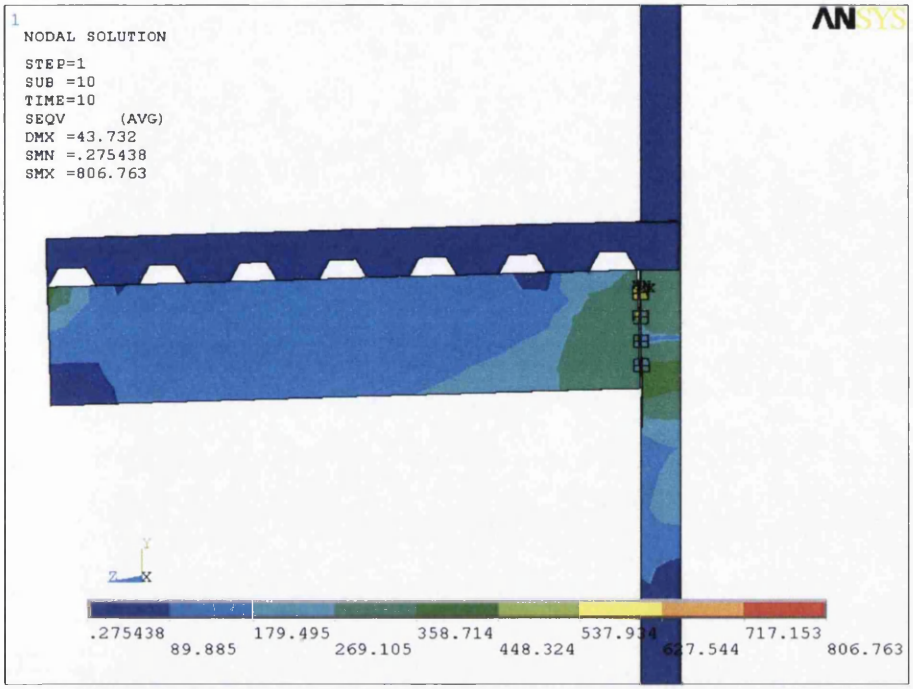

Fig: 5.30: Equivalent von mises stress distribution of the specimen SCJ4 [6].

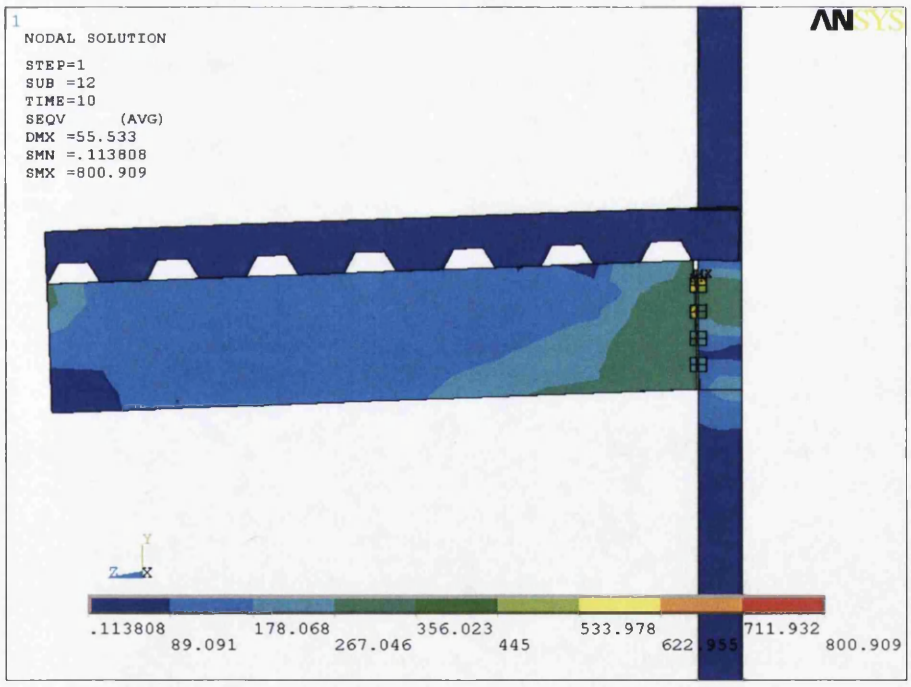

Fig: 5.31: Equivalent von mises stress distribution of the specimen SCJ5 [6].

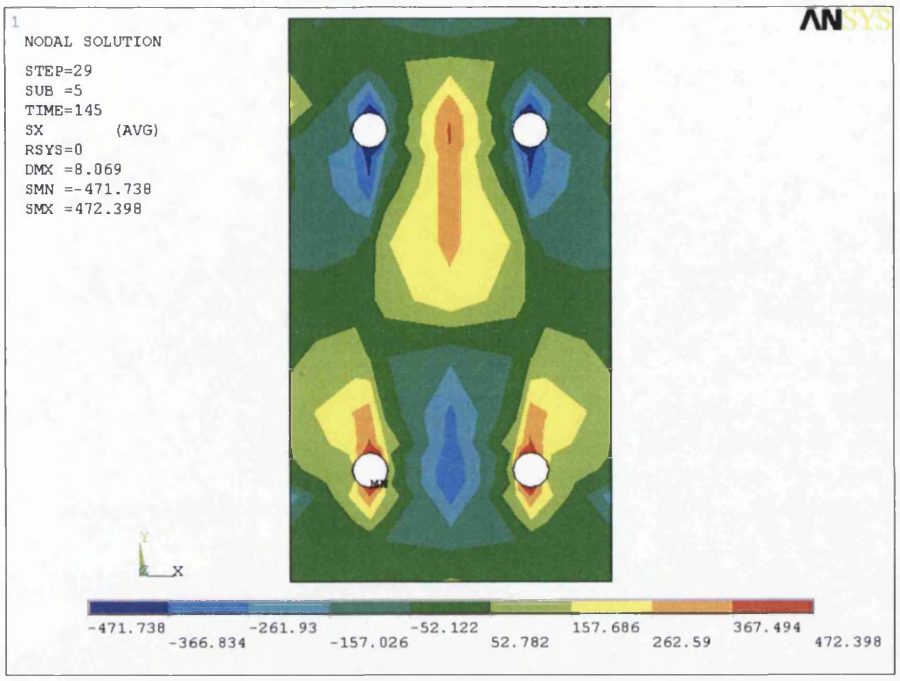

Fig: 5.32: Stress distribution of end plate in x- direction before failure of joint – SJ1 with cyclic loading.

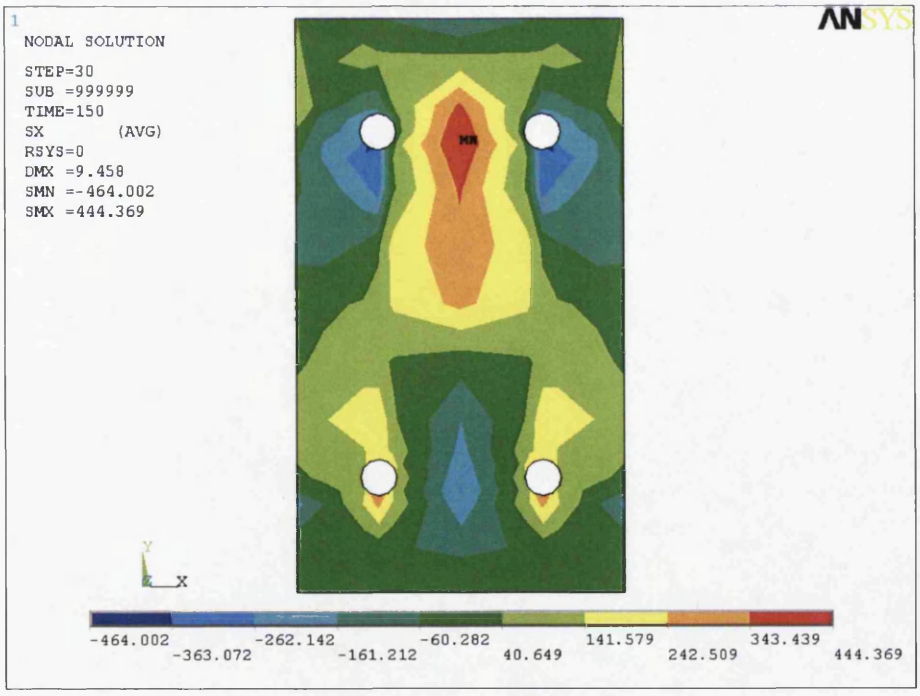

Fig: 5.33: Stress distribution of end plate in x-direction after failure of joint – SJ1 with cyclic loading.

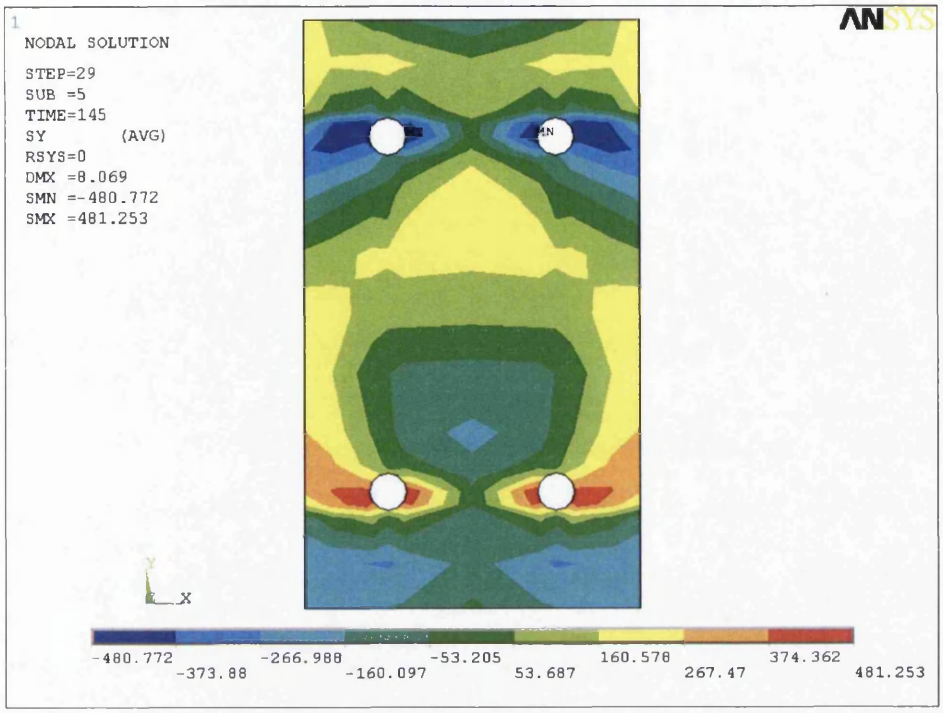

Fig: 5.34: Stress distribution of end plate in y- direction before failure of joint – SJ1 with cyclic loading.

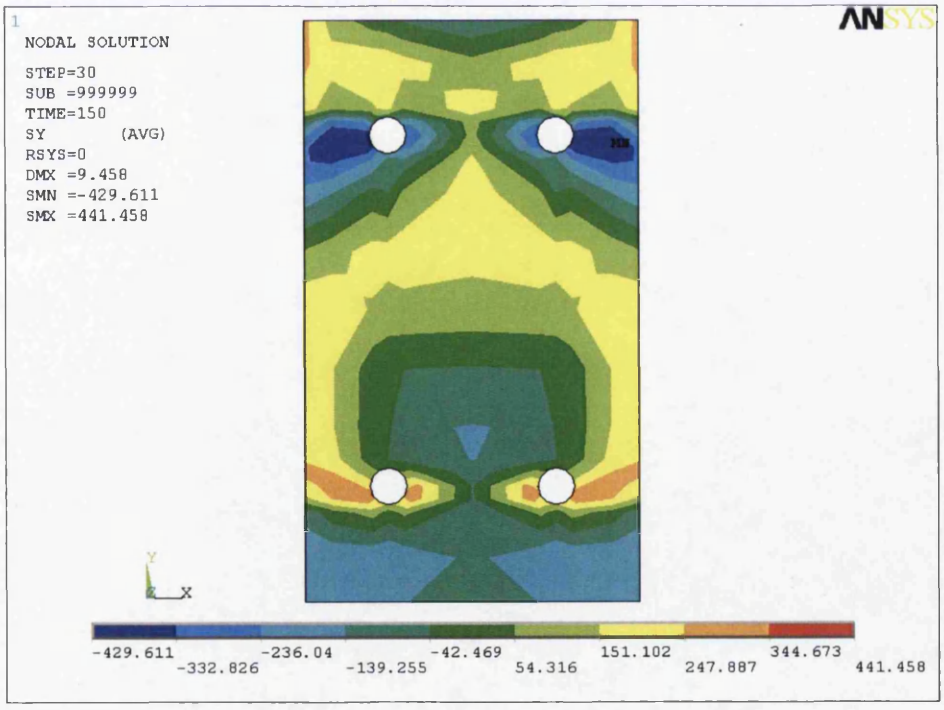

Fig: 5.35: Stress distribution of end plate in y-direction after failure of joint – SJ1 with cyclic loading.

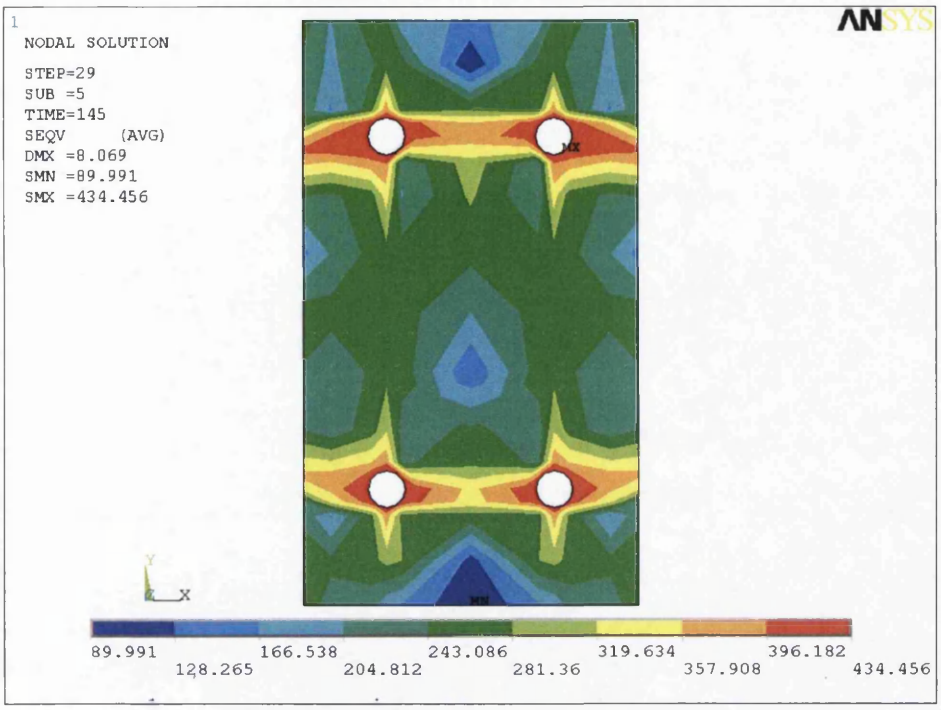

Fig: 5.36: Equivalent von mises stress distribution of the end plate before failure of joint - SJ1 with cyclic loading.

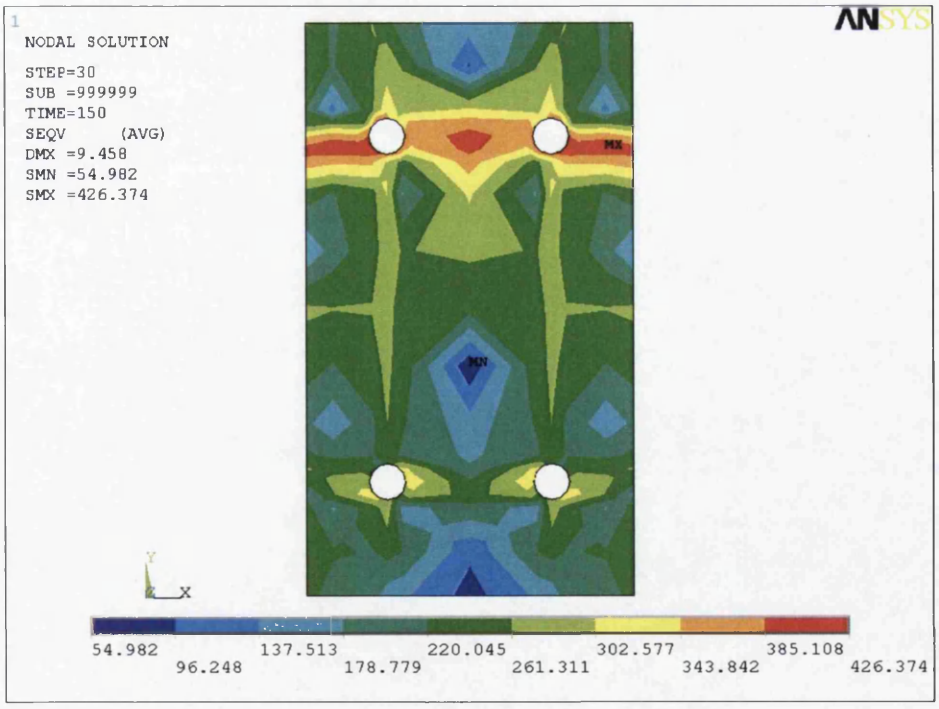

Fig: 5.37: Equivalent von mises stress distribution of the end plate after failure of joint SJ1 with cyclic loading.

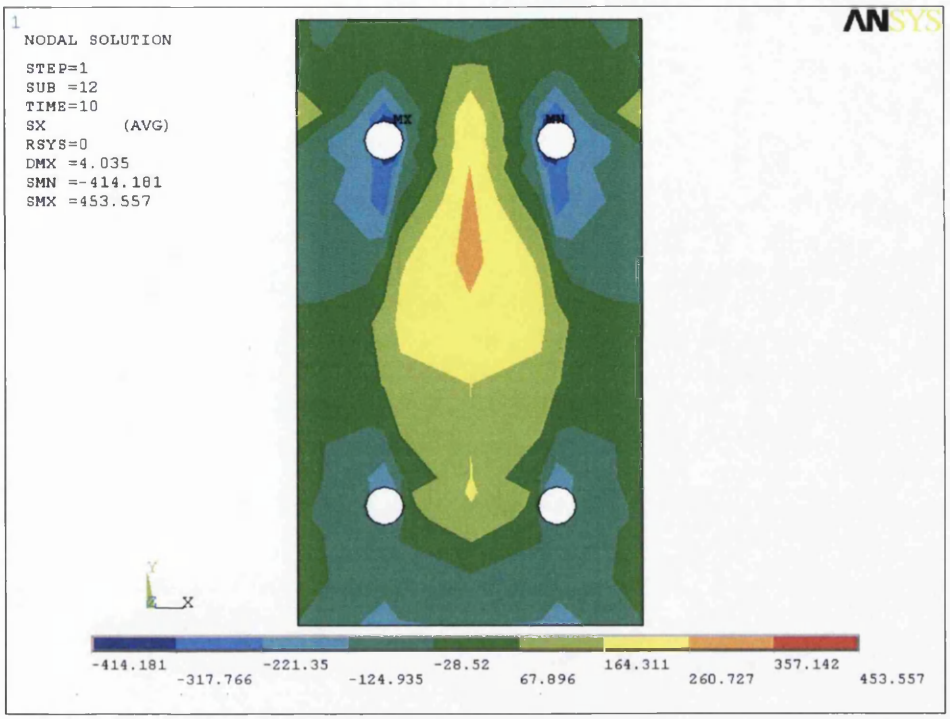

Fig: 5.38: Stress distribution of end plate in x- direction – SJ1 with monotonic loading

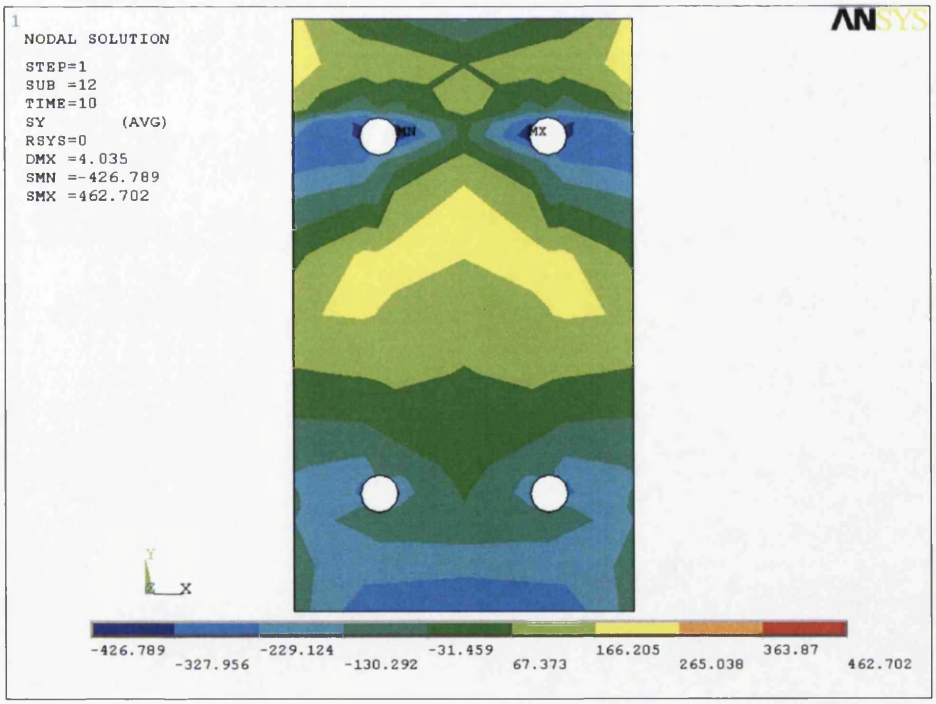

Fig: 5.39: Stress distribution of end plate in y- direction – SJ1 with monotonic loading

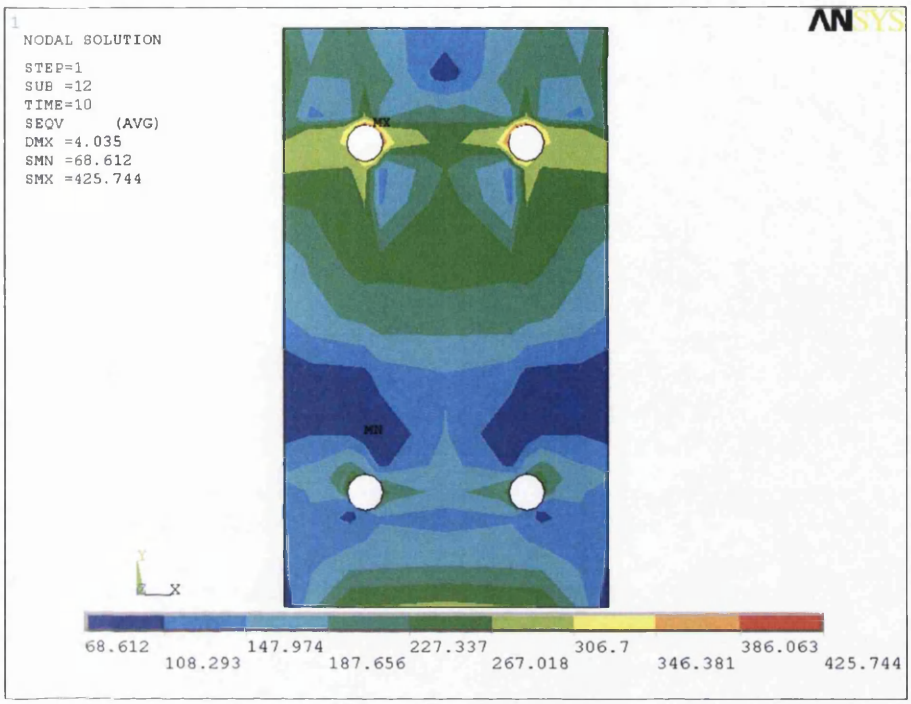

Fig: 5.40: Equivalent von mises Stress distribution of end plate – SJ1 with monotonic loading.

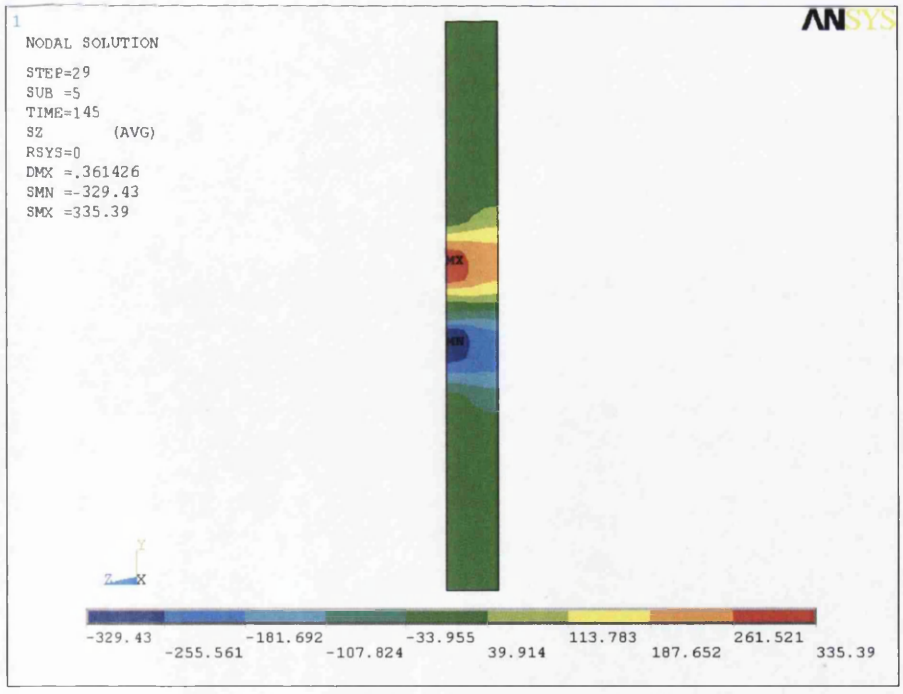

Fig: 5.41: Stress distribution of column web before failure of joint - SJ1 with cyclic loading.

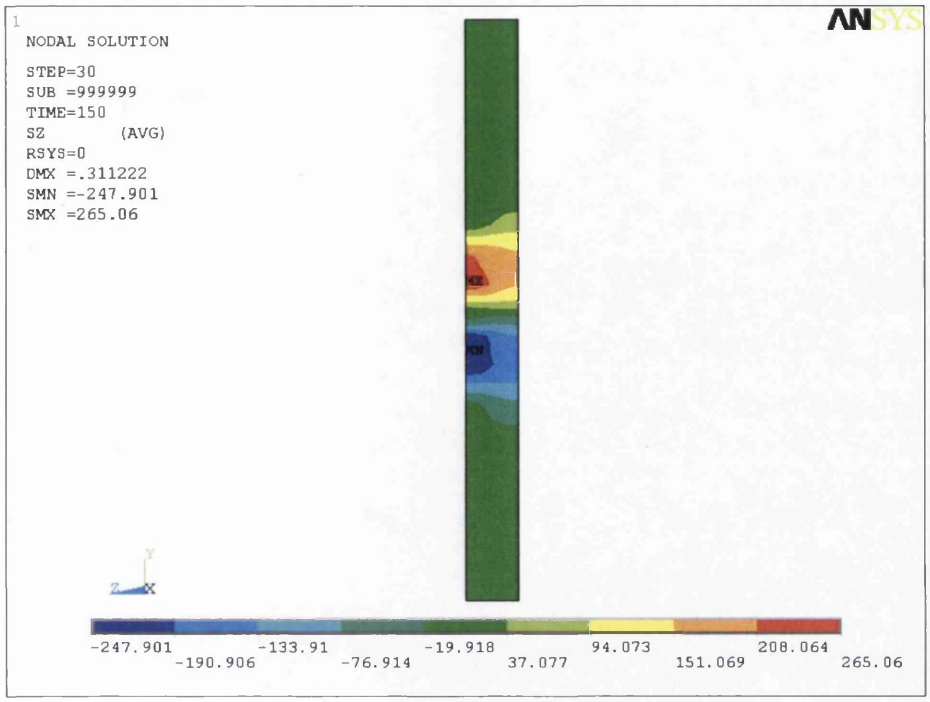

Fig: 5.42: Stress distribution of column web after failure of joint - SJ1 with cyclic loading.

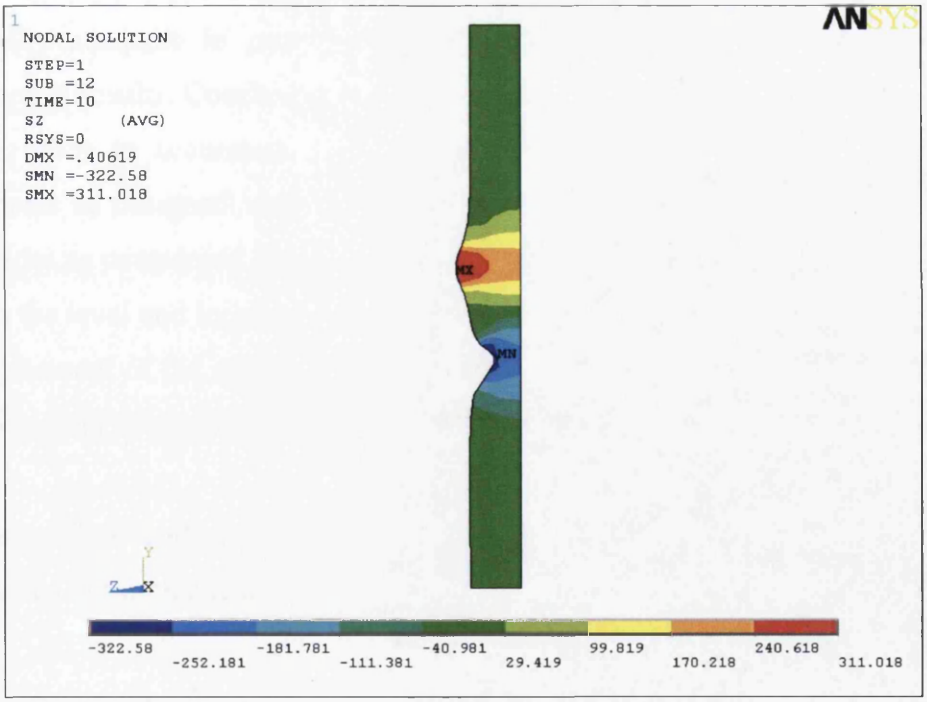

Fig: 5.43: Stress distribution of column web - SJ1 with monotonic loading.

CHAPTER-6

CONCLUSIONS

6.1 CONCLUSIONS

From the results it is concluded that the finite element model is well constructed and to be very adequate in producing results that are in good agreement with the experimental results. Confidence in the FE model is a result of the excellent level of detailing done to accurately reproduce the actual geometry of all the structural components as designed with the experimental setup. Exact material properties of steel grades as considered in the experimental investigation were used. The attention given to the level and location of mesh refinement is adequate and contributed to the good agreement of the results obtained. Special attention is given to the description of the boundary conditions to simulate the experimental setup.

The observations and conclusions arrived based on the results of FEM model has been carried out in this research are as follows.

1. The results obtained from the FEA for the moment-rotation curves of different specimens of flush endplate connection are within the range of 5% to 10% compared to the experimental results as shown in Fig.5.1

2. Waiving of column web stiffeners is not advisable because their absence causes premature failure in the column web. This consequently leads to a drastic drop in moment and rotation capacities. However, connection with column web stiffeners is advisable because their presence increases moment capacity up to 20%.

3. From the Fig 5.7, it can be observed that rotation values from monotonic and cyclic tests were almost identical and the maximum moment capacity in case of cyclic load test is about 183.75 KN-m, where as in case of monotonic test the maximum moment capacity is nearly 205 KN-m. The difference between the both maximum moment capacities is works out to be 10.5% which is less than 12% [10].

4. In case of bare steel joint specimen SJ1, stresses in both the + ve and – ve ranges were almost similar. The joint's moment rotational responses of FEM analysis follows the same trend of experimental investigation as shown in Fig 5.9, which are almost identical in both the positive and negative moment regions because of symmetry of the connection to the mid depth of beam section.

5. It is also observed that during the cyclic load analysis, the stresses are getting relieved (dissipated energy) in joint components due to failure of one of the joint components. But after the failure of joints the stress values were more or less same as monotonic loading in the range of 15 to 20% variation. This is shown in Fig 5.32 to 5.43 stress distribution of endplate before and after failure of joint.

6. The stresses in the endplate attain the maximum values earlier than the column flange both in the case of cyclic loading as well as monotonic loading.

7. In case of composite joint, the results in negative region are higher than the positive region because of increase in stiffness due to composite action as shown in Fig. 5.11 to 5.14.

8. In finite element investigation, it is observed that during cyclic loading, modes of failure of specimens were similar to those displayed with monotonic loads. Also specimens displayed large rotation ductility capacities. This trend is also the same in case of experimental investigation.

9. It is observed that cyclic loading produces much more deterioration of the resistance of the connection than that in the monotonic loading.

10. The moment rotation curve of connections developed with circular hole and hexagonal hole in the endplate of FEM model shows results correlate with each other with marginal difference of 5% to 7% (Fig : 5.21).

11. It is concluded that the moment carrying capacity of composite joint is about 60% to 75% higher than the bare steel joint as shown in Fig 5.24. This is due to strength and position of reinforcement and metal decking.

12 There is about 20% increases in moment capacity in case of four rows of bolts as compare to two rows (Fig: 5.25) and there is not much difference in moment capacity for bolt diameters M20 and M22 as shown in Fig 5.26.

13. From Fig 5.27, it can be observed that if thickness of endplate is higher than the thickness of column flange, the moment capacity of the connection will not increase in higher order due to excessive deformation of column flange and web.

14. It is observed that increase in moment is considerable (about 30%) as reinforcement ratio increases from 0.5% to 1.5% and ductility of connection in terms of rotation increases almost double (Fig:5.28). If the percentage of

reinforcement ratio is increase to 2.0%, ultimate stresses increases beyond the limit due to excessive deflection of column web, flange and endplate.

15. From this research, it can be concluded that detailing of connections should have significant influences on their flexibility, energy absorption, strength and ductility to resist earthquake forces.

From the above observations and conclusions, this work clearly demonstrates that if a proper FE model is constructed as presented in the research, many advantages can be achieved such as tremendous savings in time and cost. The FE model gives flexibility to model different geometries and setups under a variety of loading conditions and different parameters. The FEA provides a full field of results that enables the investigator to view results at any location with ease.

6.2 RECOMMENDATIONS FOR FURTHER RESEARCH

In further research, the proposed finite models and their results described in Chapters 4 and 5 needs to be calibrated against the experimental test results. Unfortunately, in this research the results of the proposed finite element models can not be validated because of non-availability of results from experimental investigations, which will be carried out in Tongji University, China in near future.

Also further investigation would consist of the development of finite element modeling on a series of different types of connections under static and cyclic loading to further enhance the reliability of the finite element approach.

APPENDIX I

CALCULATION PROCEDURE

In the finite element investigation, the bending moment, M, is defined as a moment at the column face, resulting as the product of the applied load and the distance from the centre of the load to the outside surface of the column. The rotation of a joint, Φ is defined according to Fig. A2.1 The rotation of a joint is calculated by dividing the sum of the measured displacements at top and bottom of end plate with distance between the measurement points.

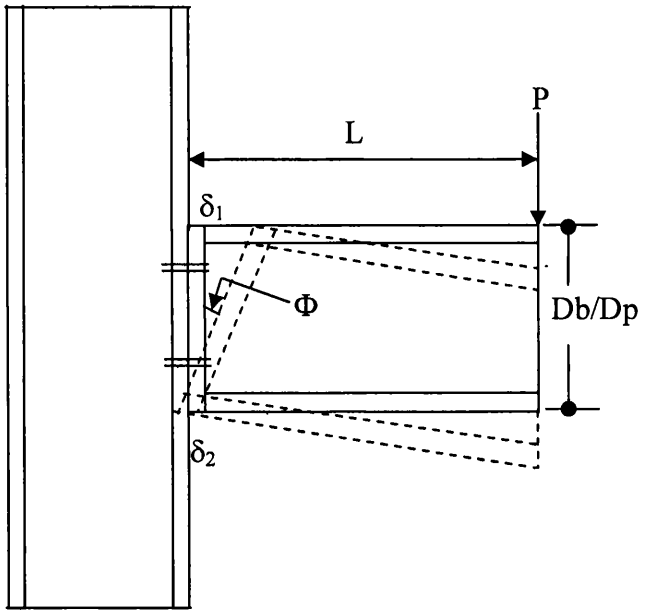

Fig A2.1 – Shows measurement of rotation

Rotation,

$$\Phi = \text{ATAN}\left[\frac{(\delta_1 - \delta_2)}{D_p}\right] = \frac{(\delta_1 - \delta_2)}{D_p} \qquad \text{(Eq A2.1)}$$

Moment,

$$M = P \times L \qquad \text{(Eq A2.2)}$$

δ_1 & δ_2 - Displacements at top and bottom of the end plate

APPENDIX II

INPUT FILE FOR FINITE ELEMENT ANALYSIS USING ANSYS – 8.1

The typical input for flush end plate connection with two rows of bolts developed for experimental investigation conducted by J.Y. Richard Liew, T.H.Teo, N.E.Shanmugam [10] – SJ1 as shown in fig 4.3. Because of symmetry, half model is considered.

```
/Title, static analysis with flush end plate connection
/Units, SI
/prep7
!* Key points for end plate section in column flange        *!
!*step-1-Creating Key points for ends of plate             *!
K,1,0,0,0          K,2,100,0,0          K,3,-100,0,0,          K,4,0,-350.0,0
K,5,100,-350.0,0   K,6,-100,-350.0,0

!*****************************************************************!

!*Step -2 -Modelling of bolt head and bolt hole                    *!
!*creating Key points & areas for bolt head                        *!
!* co-ordinates of first bolt                                       *!
!* Key points for bolt head section & circular bolt hole section.  *!
k,7,40.775,-53.55,0   k,8,31.55,-69.55,0    k,9,40.775,-85.55,0   k,10,59.225,-85.55,0
k,11,68.45,-69.55,0   k,12,59.225,-53.55,0  k,13,36.16250,-61.55,0
k,14,36.16250,-77.55,0      k,15,50.0,-85.55,0      k,16,63.83750,-77.55,0
k,17,63.83750,-61.55,0      k,18,50.0,-53.55,0
!*circular bolt hole
k,19,61.0,-69.550,0.0       k,20,50.0,-58.550,0.0       k,21,59.526,-64.050,0.0
k,22,55.500,-60.024,0.0     k,23,39.0,-69.550,0.0       k,24,44.50,-60.024,0.0
k,25,40.474,-64.050,0.0     k,26,50.0,-80.550,0.0       k,27,40.474,-75.050,0.0
k,28,44.50,-79.076,0.0      k,29,55.50,-79.076,0.0      k,30,59.526,-75.050,0.0
!*creating areas through key points
!* area nos 1 to 12
!*for first bolt and sarrounding
a,24,7,13,25   a,25,13,8,23   a,23,8,14,27   a,27,14,9,28   a,28,9,15,26   a,26,15,10,29
a,29,10,16,30  a,30,16,11,19  a,19,11,17,21  a,21,17,12,22  a,22,12,18,20  a,20,18,7,24

!*****************************************************************!
!*Step -3 Modelling of bolt head and bolt hole on -ve x-direction
!*creating k.p's & areas for bolt head
!* co-ordinates of third bolt
!* key points for bolt head section & circular bolt hole section
!*key points 31 to 54
```

```
k,31,-40.775,-53.55,0        k,32,-31.55,-69.55,0        k,33,-40.775,-85.55,0
k,34,-59.225,-85.55,0        k,35,-68.45,-69.55,0        k,36,-59.225,-53.55,0
k,37,-36.16250,-61.55,0      k,38,-36.16250,-77.55,0     k,39,-50.0,-85.55,0
k,40,-63.83750,-77.55,0      k,41,-63.83750,-61.55,0     k,42,-50.0,-53.55,0
!*circular bolt hole
k,43,-61.0,-69.550,0.0       k,44,-50.0,-58.550,0.0      k,45,-59.526,-64.050,0.0
k,46,-55.500,-60.024,0.0     k,47,-39.0,-69.550,0.0      k,48,-44.50,-60.024,0.0
k,49,-40.474,-64.050,0.0     k,50,-50.0,-80.550,0.0      k,51,-40.474,-75.050,0.0
k,52,-44.50,-79.076,0.0      k,53,-55.50,-79.076,0.0     k,54,-59.526,-75.050,0.0
!*creating areas through key points
!* area nos 13 to 24
!*for third bolt and sarrounding
a,46,36,41,45  a,45,41,35,43  a,43,35,40,54  a,54,40,34,53  a,53,34,39,50  a,50,39,33,52
a,52,33,38,51  a,51,38,32,47  a,47,32,37,49  a,49,37,31,48  a,48,31,42,44  a,44,42,36,46

!*********************************************************************!

!**Step-4
!*copy same set of ares of bolt head and bolt hole in y-direction
!*area nos 25 to 48 and K.p nos 55 to 102 (48 nos)
agen,2,1,24,1,0,-210.90,0, ,0

!*********************************************************************!

!**step-5- creatng k.p's and areas for plates arround bolt head
!*k.p nos 103 to
!* K.p's for beam top flange
k,103,0,-26.65,0             k,104,40.775,-26.65,0       k,105,50.0,-26.65,0
k,106,59.225,-26.65,0        k,107,83.45,-26.65,0        k,108,100.0,-26.65,0
k,109,-40.775,-26.65,0       k,110,-50.0,-26.65,0        k,111,-59.225,-26.65,0
k,112,-83.45,-26.65,0        k,113,-100.0,-26.65,0
!* K.p's for beam bottom flange
k,114,0,-323.35,0            k,115,40.775,-323.35,0      k,116,50.0,-323.35,0
k,117,59.225,-323.35,0       k,118,83.45,-323.35,0       k,119,100.0,-323.35,0
k,120,-40.775,-323.35,0      k,121,-50.0,-323.35,0       k,122,-59.225,-323.35,0
k,123,-83.45,-323.35,0       k,124,-100.0,-323.35,0
!* K.p's for end plate at top
k,125,40.775,0,0             k,126,50.0,0,0              k,127,59.225,0,0
k,128,83.45,0,0              k,129,-40.775,0,0           k,130,-50.0,0,0
k,131,-59.225,0,0            k,132,-83.45,0,0
!* K.p's for end plate at bottom
k,133,40.775,-350.0,0        k,134,50.0,-350.0,0         k,135,59.225,-350.0,0
k,136,83.45,-350.0,0         k,137,-40.775,-350.0,0      k,138,-50.0,-350.0,0
k,139,-59.225,-350.0,0       k,140,-83.45,-350.0,0
!*creating keypoints in y-direction
!* along the centre line of plate
k,141,0.0,-53.55,0    k,142,0.0,-61.55,0    k,143,0.0,-69.55,0    k,144,0.0,-77.55,0
```

```
k,145,0.0,-85.55,0    k,146,0.0,-264.45,0   k,147,0.0,-272.45,0   k,148,0.0,-280.45,0
k,149,0.0,-288.45,0   k,150,0.0,-296.45,0
!*plate end on both sides
k,151,100.0,-53.55,0          k,152,100.0,-61.55,0          k,153,100.0,-69.55
k,154,100.0,-77.55,0          k,155,100.0,-85.55,0          k,156,100.0,-264.45,0
k,157,100.0,-272.45,0         k,158,100.0,-280.45,0         k,159,100.0,-288.45,0
k,160,100.0,-296.45,0         k,161,-100.0,-53.55,0         k,162,-100.0,-61.55,0
k,163,-100.0,-69.55,0         k,164,-100.0,-77.55,0         k,165,-100.0,-85.55,0
k,166,-100.0,-264.45,0        k,167,-100.0,-272.45,0        k,168,-100.0,-280.45,0
k,169,-100.0,-288.45,0        k,170,-100.0,-296.45,0
!* intermidiate kp's beam end on both sides
k,171,83.45,-53.55,0          k,172,83.45,-61.55,0          k,173,83.45,-69.55,0
k,174,83.45,-77.55,0          k,175,83.45,-85.55,0          k,176,83.45,-264.45,0
k,177,83.45,-272.45,0         k,178,83.45,-280.45,0         k,179,83.45,-288.45,0
k,180,83.45,-296.45,0         k,181,-83.45,-53.55,0         k,182,-83.45,-61.55,0
k,183,-83.45,-69.55,0         k,184,-83.45,-77.55,0         k,185,-83.45,-85.55,0
k,186,-83.45,-264.45,0        k,187,-83.45,-272.45,0        k,188,-83.45,-280.45,0
k,189,-83.45,-288.45,0        k,190,-83.45,-296.45,0
!*creating key poins for center of plate
k,191,0,-175.0,0              k,192,40.775,-175.0,0         k,193,50.0,-175.0,0
k,194,59.225,-175.0,0         k,195,83.45,-175.0,0          k,196,100.0,-175.0,0
k,197,-40.775,-175.0,0        k,198,-50.0,-175.0,0          k,199,-59.225,-175.0,0
k,200,-83.45,-175.0,0         k,201,-100.0,-175.0,0
!*creating key poins at 1/3th of dist bet centre of plate and centre of hole
k,202,0,-104.70,0             k,203,40.775,-104.70,0        k,204,50.0,-104.70,0
k,205,59.225,-104.70,0        k,206,83.45,-104.70,0         k,207,100.0,-104.70,0
k,208,-40.775,-104.70,0       k,209,-50.0,-104.70,0         k,210,-59.225,-104.70,0
k,211,-83.45,-104.70,0        k,212,-100.0,-104.70,0
!*creating key poins at 1/2th of dist bet centre of plate and centre of hole
k,213,0,-139.85,0             k,214,40.775,-139.85,0        k,215,50.0,-139.85,0
k,216,59.225,-139.85,0        k,217,83.45,-139.85,0         k,218,100.0,-139.85,0
k,219,-40.775,-139.85,0       k,220,-50.0,-139.85,0         k,221,-59.225,-139.85,0
k,222,-83.45,-139.85,0        k,223,-100.0,-139.85,0
!*creating key poins at 2/3rd of plate below centre of plate
k,224,0,-210.15,0             k,225,40.775,-210.15,0        k,226,50.0,-210.15,0
k,227,59.225,-210.15,0        k,228,83.45,-210.15,0         k,229,100.0,-210.15,0
k,230,-40.775,-210.15,0       k,231,-50.0,-210.15,0         k,232,-59.225,-210.15,0
k,233,-83.45,-210.15,0        k,234,-100.0,-210.15,0
!*creating key poins at 3/4rd of plate below centre of plate
k,235,0,-245.30,0             k,236,40.775,-245.30,0        k,237,50.0,-245.30,0
k,238,59.225,-245.30,0        k,239,83.45,-245.30,0         k,240,100.0,-245.30,0
k,241,-40.775,-245.30,0       k,242,-50.0,-245.30,0         k,243,-59.225,-245.30,0
k,244,-83.45,-245.30,0        k,245,-100.0,-245.30,0
!* creating area through k.ps for plate
!*area nos from 49 to
a,1,103,104,125     a,125,104,105,126     a,126,105,106,127     a,127,106,107,128
a,128,107,108,2     a,1,129,109,103       a,129,130,110,109     a,130,131,111,110
```

```
a,131,132,112,111   a,132,3,113,112     a,103,141,7,104     a,104,7,18,105
a,105,18,12,106     a,106,12,171,107    a,107,171,151,108   a,103,109,31,141
a,109,110,42,31     a,110,111,36,42     a,111,112,181,36    a,112,113,161,181
a,141,142,13,7      a,142,143,8,13      a,143,144,14,8      a,144,145,9,14
a,12,17,172,171     a,17,11,173,172     a,11,16,174,173     a,16,10,175,174
a,171,172,152,151   a,172,173,153,152   a,173,174,154,153   a,174,175,155,154
a,141,31,37,142     a,142,37,32,143     a,143,32,38,144     a,144,38,33,145
a,36,181,182,41     a,41,182,183,35     a,35,183,184,40     a,40,184,185,34
a,181,161,162,182   a,182,162,163,183   a,183,163,164,184   a,184,164,165,185
a,145,202,203,9     a,9,203,204,15      a,15,204,205,10     a,10,205,206,175
a,175,206,207,155   a,145,33,208,202    a,33,39,209,208     a,39,34,210,209
a,34,185,211,210    a,185,165,212,211   a,202,213,214,203   a,203,214,215,204
a,204,215,216,205   a,205,216,217,206   a,206,217,218,207   a,202,208,219,213
a,208,209,220,219   a,209,210,221,220   a,210,211,222,221   a,211,212,223,222
a,213,191,192,214   a,214,192,193,215   a,215,193,194,216   a,216,194,195,217
a,217,195,196,218   a,213,219,197,191   a,219,220,198,197   a,220,221,199,198
a,221,222,200,199   a,222,223,201,200   a,191,224,225,192   a,192,225,226,193
a,193,226,227,194   a,194,227,228,195   a,195,228,229,196   a,191,197,230,224
a,197,198,231,230   a,198,199,232,231   a,199,200,233,232   a,200,201,234,233
a,224,235,236,225   a,225,236,237,226   a,226,237,238,227   a,227,238,239,228
a,228,239,240,229   a,224,230,241,235   a,230,231,242,241   a,231,232,243,242
a,232,233,244,243   a,233,234,245,244   a,235,146,56,236    a,236,56,77,237
a,237,77,75,238     a,238,75,176,239    a,239,176,156,240   a,235,241,99,146
a,241,242,101,99    a,242,243,80,101    a,243,244,186,80    a,244,245,166,186
a,56,146,147,57     a,57,147,148,59     a,59,148,149,61     a,61,149,150,63
a,75,73,177,176     a,73,71,178,177     a,71,69,179,178     a,69,67,180,179
a,176,177,157,156   a,177,178,158,157   a,178,179,159,158   a,179,180,160,159
a,146,99,97,147     a,147,97,95,148     a,148,95,93,149     a,149,93,91,150
a,80,186,187,81     a,81,187,188,83     a,83,188,189,85     a,85,189,190,87
a,186,166,167,187   a,187,167,168,188   a,188,168,169,189   a,189,169,170,190
a,150,114,115,63    a,63,115,116,65     a,65,116,117,67     a,67,117,118,180
a,180,118,119,160   a,150,91,120,114    a,91,89,121,120     a,89,87,122,121
a,87,190,123,122    a,190,170,124,123   a,114,4,133,115     a,115,133,134,116
a,116,134,135,117   a,117,135,136,118   a,118,136,5,119     a,114,120,137,4
a,120,121,138,137   a,121,122,139,138   a,122,123,140,139   a,123,124,6,140
aglue, all

!*********************************************************************!

!*step -6 creating column first flange
!*k.ps'246 to 490  & area nos 197 to 392
!*copying the same set of areas of end plate for first column flange
!*copy 5mm in -ve z direction
agen,2,1,196,1,0,0,-5.0,0,1,0

!*********************************************************************!
```

```
!*step -7
!* line elements to connect plate and col. flange for first plate
!*line nos 889 to  1133

L, 1, 342      L, 125, 345    L, 126, 347    L, 127, 349    L,128, 351     L, 2,  353
L, 129, 354    L, 130, 356    L, 131, 358    L, 132, 360    L, 3, 362      L, 103, 343
L, 104, 344    L, 105, 346    L, 106, 348    L, 107, 350    L, 108, 352    L, 109, 355
L, 110, 357    L, 111, 359    L, 112, 361    L, 113, 363    L, 141, 364    L, 7,   247
L, 18, 268     L, 12, 266     L, 171, 365    L, 151, 366    L, 31, 290     L, 42, 292
L, 36, 271     L, 181, 367    L, 161, 368    L, 13, 248     L, 8, 250      L, 14, 252
L, 9, 254      L, 15, 256     L, 10, 258     L, 16, 260     L, 11, 262     L, 17, 264
L, 41, 272     L, 35, 274     L, 40, 276     L, 34, 278     L, 39, 280     L, 33, 282
L, 38, 284     L, 32, 286     L, 37, 288     L, 24, 246     L, 25, 249     L, 23, 251
L, 27, 253     L, 28, 255     L, 26, 257     L, 29, 259     L, 30, 261     L, 19, 263
L, 21, 265     L, 22, 267     L, 20, 269     L, 46, 270     L, 45, 273     L, 43, 275
L, 54, 277     L, 53, 279     L, 50, 281     L, 52, 283     L, 51, 285     L, 47, 287
L, 49, 289     L, 48, 291     L, 44, 293     L, 142, 369    L, 143, 370    L, 144, 371
L, 145, 372    L, 172, 373    L, 173, 374    L, 174, 375    L, 175, 376    L, 152, 377
L, 153, 378    L, 154, 379    L, 155, 380    L, 182, 381    L, 183, 382    L, 184, 383
L, 185, 384    L, 162, 385    L, 163, 386    L, 164, 387    L, 165, 388    L, 202, 389
L, 203, 390    L, 204, 391    L, 205, 392    L, 206, 393    L, 207, 394    L, 208, 395
L, 209, 396    L, 210, 397    L, 211, 398    L, 212, 399    L, 213, 400    L, 214, 401
L, 215, 402    L, 216, 403    L, 217, 404    L, 218, 405    L, 219, 406    L, 220, 407
L, 221, 408    L, 222, 409    L, 223, 410    L, 191, 411    L, 192, 412    L, 193, 413
L, 194, 414    L, 195, 415    L, 196, 416    L, 197, 417    L, 198, 418    L, 199, 419
L, 200, 420    L, 201, 421    L, 224, 422    L, 225, 423    L, 226, 424    L, 227, 425
L, 228, 426    L, 229, 427    L, 230, 428    L, 231, 429    L, 232, 430    L, 233, 431
L, 234, 432    L, 235, 433    L, 236, 434    L, 237, 435    L, 238, 436    L, 239, 437
L, 240, 438    L, 241, 439    L, 242, 440    L, 243, 441    L, 442, 244    L, 244, 442
L, 245, 443    L, 146, 444    L, 147, 449    L, 148, 450    L, 149, 451    L, 150, 452
L, 176, 445    L, 177, 453    L, 178, 454    L, 179, 455    L, 180, 456    L, 156, 446
L, 157, 457    L, 158, 458    L, 159, 459    L, 160, 460    L, 186, 447    L, 187, 461
L, 188, 462    L, 189, 463    L, 190, 464    L, 166, 448    L, 167, 465    L, 168, 466
L, 169, 467    L, 170, 468    L, 114, 469    L, 115, 470    L, 116, 471    L, 117, 472
L, 118, 473    L, 119, 474    L, 120, 475    L, 121, 476    L, 122, 477    L, 123, 478
L, 124, 479    L, 4,   480    L, 133, 481    L, 134, 482    L, 135, 483    L, 136, 484
L, 5,   485    L, 137, 486    L, 138, 487    L, 139, 488    L, 140, 489    L, 6,   490
L, 56,  295    L, 57,  296    L, 59,  298    L, 61,  300    L, 63,  302    L, 65,  304
L, 67,  306    L, 69,  308    L, 71,  310    L, 73,  312    L, 75,  314    L, 77,  316
L, 80,  319    L, 81,  320    L, 83,  322    L, 85,  324    L, 87,  326    L, 89,  328
L, 91,  330    L, 93,  332    L, 95,  334    L, 97,  336    L, 99,  338    L, 101, 340
L, 55,  294    L, 58,  297    L, 60,  299    L, 62,  301    L, 64,  303    L, 66,  305
L, 68,  307    L, 70,  309    L, 72,  311    L, 74,  313    L, 76,  315    L, 78,  317
L, 79,  318    L, 82,  321    L, 84,  323    L, 86,  325    L, 88,  327    L, 90,  329
L, 92,  331    L, 94,  333    L, 96,  335    L, 98,  337    L, 100, 339    L, 102, 341
```

```
!*creating key points for col flange end
k,491,152.65,0,-5.0          k,492,152.65,-26.65,-5.0     k,493,152.65,-53.55,-5.0
k,494,152.65,-61.55,-5.0     k,495,152.65,-69.55,-5.0     k,496,152.65,-77.55,-5.0
k,497,152.65,-85.55,-5.0     k,498,152.65,-104.70,-5.0    k,499,152.65,-139.85,-5.0
k,500,152.65,-175.0,-5.0     k,501,152.65,-210.15,-5.0    k,502,152.65,-245.30,-5.0
k,503,152.65,-264.45,-5.0    k,504,152.65,-272.45,-5.0    k,505,152.65,-280.45,-5.0
k,506,152.65,-288.45,-5.0    k,507,152.65,-296.45,-5.0    k,508,152.65,-323.35,-5.0
k,509,152.65,-350.0,-5.0     k,510,-152.65,0,-5.0         k,511,-152.65,-26.65,-5.0
k,512,-152.65,-53.55,-5.0    k,513,-152.65,-61.55,-5.0    k,514,-152.65,-69.55,-5.0
k,515,-152.65,-77.55,-5.0    k,516,-152.65,-85.55,-5.0    k,517,-152.65,-104.70,-5.0
k,518,-152.65,-139.85,-5.0   k,519,-152.65,-175.0,-5.0     k,520,-152.65,-210.15,-5.0
k,521,-152.65,-245.30,-5.0   k,522,-152.65,-264.45,-5.0    k,523,-152.65,-272.45,-5.0
k,524,-152.65,-280.45,-5.0   k,525,-152.65,-288.45,-5.0    k,526,-152.65,-296.45,-5.0
k,527,-152.65,-323.35,-5.0   k,528,-152.65,-350.0,-5.0

!*creating areas throuhg key points for col end line
!*area nos  393to 428
a,353,352,492,491    a,352,366,493,492    a,366,377,494,493    a,377,378,495,494
a,378,379,496,495    a,379,380,497,496    a,380,394,498,497    a,394,405,499,498
a,405,416,500,499    a,416,427,501,500    a,427,438,502,501    a,438,446,503,502
a,446,457,504,503    a,457,458,505,504    a,458,459,506,505    a,459,460,507,506
a,460,474,508,507    a,474,485,509,508    a,362,510,511,363    a,363,511,512,368
a,368,512,513,385    a,385,513,514,386    a,386,514,515,387    a,387,515,516,388
a,388,516,517,399    a,399,517,518,410    a,410,518,519,421    a,421,519,520,432
a,432,520,521,443    a,432,520,521,443    a,432,520,521,443    a,443,521,522,448
a,448,522,523,465    a,465,523,524,466    a,466,524,525,467    a,467,525,526,468
a,468,526,527,479    a,479,527,528,490
!*****************
!*copying the key points to top of slab
k,529,0,120.0,-5.0           k,530,40.775,120.0,-5.0      k,531;50.0,120.0,-5.0
k,532,59.225,120.0,-5.0      k,533,83.45,120.0,-5.0       k,534,100.0,120.0,-5.0
k,535,152.65,120,-5.0        k,536,-40.775,120.0,-5.0     k,537,-50.0,120.0,-5.0
k,538,-59.225,120.0,-5.0     k,539,-83.45,120.0,-5.0      k,540,-100.0,120.0,-5.0
k,541,-152.65,120,-5.0

!*creating the areas above top of beam for slab thick
!*area nos 429 to 440
a,529,342,345,530    a,530,345,347,531    a,531,347,349,532    a,532,349,351,533
a,533,351,353,534    a,534,353,491,535    a,529,536,354,342    a,536,537,356,354
a,537,538,358,356    a,538,539,360,358    a,539,540,362,360    a,540,541,510,362

!*creating the key points to top of column above slab
k,542,0,625.0,-5.0           k,543,40.775,625.0,-5.0      k,544,50.0,625.0,-5.0
k,545,59.225,625.0,-5.0      k,546,83.45,625.0,-5.0       k,547,100.0,625.0,-5.0
k,548,152.65,625.0,-5.0      k,549,-40.775,625.0,-5.0     k,550,-50.0,625.0,-5.0
k,551,-59.225,625.0,-5.0     k,552,-83.45,625.0,-5.0      k,553,-100.0,625.0,-5.0
k,554,-152.65,625.0,-5.0
```

```
!*creating the areas to top of column above slab
!*area nos 441 to 452
a,542,529,530,543    a,543,530,531,544    a,544,531,532,545    a,545,532,533,546
a,546,533,534,547    a,547,534,535,548    a,542,549,536,529    a,549,550,537,536
a,550,551,538,537    a,551,552,539,538    a,552,553,540,539    a,553,554,541,540

!*creating the key points to for column below end plate
k,555,0,-975.0,-5.0          k,556,40.775,-975.0,-5.0     k,557,50.0,-975.0,-5.0
k,558,59.225,-975.0,-5.0     k,559,83.45,-975.0,-5.0      k,560,100.0,-975.0,-5.0
k,561,152.65,-975.0,-5.0     k,562,-40.775,-975.0,-5.0    k,563,-50.0,-975.0,-5.0
k,564,-59.225,-975.0,-5.0    k,565,-83.45,-975.0,-5.0     k,566,-100.0,-975.0,-5.0
k,567,-152.65,-975.0,-5.0

!*creating the areas for column below end plate
!*area nos 453 to 464
a,480,555,556,481    a,481,556,557,482    a,482,557,558,483    a,483,558,559,484
a,484,559,560,485    a,485,560,561,509    a,480,486,562,555    a,486,487,563,562
a,487,488,564,563    a,488,489,565,564    a,489,490,566,565    a,490,528,567,566
aglue all
```

!****Modelling of bolt & nutt in end plate**********

```
!**step-1
!*k.p's for shank in first hole in first plate
k,568,60.0,-69.550,0.0       k,569,50.0,-59.550,0.0       k,570,58.660,-64.550,0.0
k,571,55.0,-60.890,0.0       k,572,40.0,-69.550,0.0       k,573,45.0,-60.890,0.0
k,574,41.340,-64.550,0.0     k,575,50.0,-79.550,0.0       k,576,41.340,-74.550,0.0
k,577,45.0,-78.210,0.0       k,578,55.0,-78.210,0.0       k,579,58.66,-74.55,0.0
!*k.p's for shank in third hole in first plate
k,580,-60.0,-69.550,0.0      k,581,-50.0,-59.550,0.0      k,582,-58.660,-64.550,0.0
k,583,-55.0,-60.890,0.0      k,584,-40.0,-69.550,0.0      k,585,-45.0,-60.890,0.0
k,586,-41.340,-64.550,0.0    k,587,-50.0,-79.550,0.0      k,588,-41.340,-74.550,0.0
k,589,-45.0,-78.210,0.0      k,590,-55.0,-78.210,0.0      k,591,-58.66,-74.55,0.0

!* step-2
!*copying the same set of k.p's for shank of first and fifth hole in -ve y-dir
!*k.p' nos 592 to 615
kgen,2,568,591,1,0,-210.9,0, ,0

!*extra key points at the centre of shank
!*k.p's 616 to 619
k,616,50,-69.55, 0     k,617,-50,-69.55, 0
kgen,2,616,617,1,0,-210.9,0, ,0

!*step-3
!*creating the areas bet bolt head and shank for first hole in first plate
!*465 to 477
```

```
a,573,7,13,574      a,574,13,8,572      a,572,8,14,576      a,576,14,9,577
a,577,9,15,575      a,575,15,10,578     a,578,10,16,579     a,579,16,11,568
a,568,11,17,570     a,570,17,12,571     a,571,12,18,569     a,569,18,7,573
a,573,574,572,576,577,575,578,579,568,570,571,569

!*creating the areas bet bolt head and shank for second hole in plate
!*478 to 490
a,597,56,57,598     a,598,57,59,596     a,596,59,61,600     a,600,61,63,601
a,601,63,65,599     a,599,65,67,602     a,602,67,69,603     a,603,69,71,592
a,592,71,73,594     a,594,73,75,595     a,595,75,77,593     a,593,77,56,597
a,597,598,596,600,601,599,602,603,592,594,595,593

!*creating the areas bet bolt head and shank for third hole in plate
!*491 to 503
a,583,36,41,582     a,582,41,35,580     a,580,35,40,591     a,591,40,34,590
a,590,34,39,587     a,587,39,33,589     a,589,33,38,588     a,588,38,32,584
a,584,32,37,586     a,586,37,31,585     a,585,31,42,581     a,581,42,36,583
a,583,582,580,591,590,587,589,588,584,586,585,581

!*creating the areas bet bolt head and shank for fourth hole in plate
!*504 to 516
a,607,80,81,606     a,606,81,83,604     a,604,83,85,615     a,615,85,87,614
a,614,87,89,611     a,611,89,91,613     a,613,91,93,612     a,612,93,95,608
a,608,95,97,610     a,610,97,99,609     a,609,99,101,605    a,605,101,80,607
a,607,606,604,615,614,611,613,612,608,610,609,605
!*area nos for bolt head and shank in plate - 465 to 516

!* step-4
!*copy same set of areas for bolt thickness in x-direction
!* area nos - 517 to 568 and k.p.s 620 to 715 (total no of k.p =96)
agen,2,465,516,1,0,0,13,0,1,0
!*extra key points at the centre of shank
k,716,50,-69.55, 13   k,717,-50,-69.55, 13   k,718,50,-280.45,13   k,719,-50,-280.45,13

!* step-5
!* create/define volume through key points for first bolt
!*volume nos 1 to 12
v,573,7,13,574,620,621,622,623      v,574,13,8,572,623,622,624,625
v,572,8,14,576,625,624,626,627      v,576,14,9,577,627,626,628,629
v,577,9,15,575,629,628,630,631      v,575,15,10,578,631,630,632,633
v,578,10,16,579,633,632,634,635     v,579,16,11,568,635,634,636,637
v,568,11,17,570,637,636,638,639     v,570,17,12,571,639,638,640,641
v,571,12,18,569,641,640,642,643     v,569,18,7,573,643,642,621,620
!* create/define volume through key points for second bolt
!*volume nos 13to 24
v,597,56,57,598,644,645,646,647     v,598,57,59,596,647,646,648,649
v,596,59,61,600,649,648,650,651     v,600,61,63,601,651,650,652,653
```

```
v,601,63,65,599,653,652,654,655   v,599,65,67,602,655,654,656,657
v,602,67,69,603,657,656,658,659   v,603,69,71,592,659,658,660,661
v,592,71,73,594,661,660,662,663   v,594,73,75,595,663,662,664,665
v,595,75,77,593,665,664,666,667   v,593,77,56,597,667,666,645,644
!* create/define volume through key points for third bolt
!*volume nos 25 to 36
v,583,36,41,582,668,669,670,671   v,582,41,35,580,671,670,672,673
v,580,35,40,591,673,672,674,675   v,591,40,34,590,675,674,676,677
v,590,34,39,587,677,676,678,679   v,587,39,33,589,679,678,680,681
v,589,33,38,588,681,680,682,683   v,588,38,32,584,683,682,684,685
v,584,32,37,586,685,684,686,687   v,586,37,31,585,687,686,688,689
v,585,31,42,581,689,688,690,691   v,581,42,36,583,691,690,669,668
!* create/define volume through key points for fourth bolt
!*volume nos 37 to 48
v,607,80,81,606,692,693,694,695   v,606,81,83,604,695,694,696,697
v,604,83,85,615,697,696,698,699   v,615,85,87,614,699,698,700,701
v,614,87,89,611,701,700,702,703   v,611,89,91,613,703,702,704,705
v,613,91,93,612,705,704,706,707   v,612,93,95,608,707,706,708,709
v,608,95,97,610,709,708,710,711   v,610,97,99,609,711,710,712,713
v,609,99,101,605,713,712,714,715  v,605,101,80,607,715,714,693,692

!* step-6
!* create/define volume through key points for shank of first bolt
!*volume nos 49 to 60
v,616,573,574,716,620,623  v,616,574,572,716,623,625  v,616,572,576,716,625,627
v,616,576,577,716,627,629  v,616,577,575,716,629,631  v,616,575,578,716,631,633
v,616,578,579,716,633,635  v,616,579,568,716,635,637  v,616,568,570,716,637,639
v,616,570,571,716,639,641  v,616,571,569,716,641,643  v,616,569,573,716,643,620
!* create/define volume through key points for shank of second bolt
!*volume nos 61 to 72
v,618,597,598,718,644,647  v,618,598,596,718,647,649  v,618,596,600,718,649,651
v,618,600,601,718,651,653  v,618,601,599,718,653,655  v,618,599,602,718,655,657
v,618,602,603,718,657,659  v,618,603,592,718,659,661  v,618,592,594,718,661,663
v,618,594,595,718,663,665  v,618,595,593,718,665,667  v,618,593,597,718,667,644
!* create/define volume through key points for shank of third bolt
!*volume nos 73 to 84
v,617,583,582,717,668,671  v,617,582,580,717,671,673  v,617,580,591,717,673,675
v,617,591,590,717,675,677  v,617,590,587,717,677,679  v,617,587,589,717,679,681
v,617,589,588,717,681,683  v,617,588,584,717,683,685  v,617,584,586,717,685,687
v,617,586,585,717,687,689  v,617,585,581,717,689,691  v,617,581,583,717,691,668
!* create/define volume through key points for shank of fourth bolt
!*volume nos 85 to 96
v,619,607,606,719,692,695  v,619,606,604,719,695,697  v,619,604,615,719,697,699
v,619,615,614,719,699,701  v,619,614,611,719,701,703  v,619,611,613,719,703,705
v,619,613,612,719,705,707  v,619,612,608,719,707,709  v,619,608,610,719,709,711
v,619,610,609,719,711,713  v,619,609,605,719,713,715  v,619,605,607,719,715,692
```

```
!* step-7
!* creating the k.p's for shank in first column flange
!*k.p's for shank in first hole
k,720,60.0,-69.550,-5.0      k,721,50.0,-59.550,-5.0      k,722,58.660,-64.550,-5.0
k,723,55.0,-60.890,-5.0      k,724,40.0,-69.550,-5.0      k,725,45.0,-60.890,-5.0
k,726,41.340,-64.550,-5.0    k,727,50.0,-79.550,-5.0      k,728,41.340,-74.550,-5.0
k,729,45.0,-78.210,-5.0      k,730,55.0,-78.210,-5.0      k,731,58.66,-74.55,-5.0
!*k.p's for shank in third hole in first plate in column flange
k,732,-60.0,-69.550,-5.0     k,733,-50.0,-59.550,-5.0     k,734,-58.660,-64.550,-5.0
k,735,-55.0,-60.890,-5.0     k,736,-40.0,-69.550,-5.0     k,737,-45.0,-60.890,-5.0
k,738,-41.340,-64.550,-5.0   k,739,-50.0,-79.550,-5.0     k,740,-41.340,-74.550,-5.0
k,741,-45.0,-78.210,-5.0     k,742,-55.0,-78.210,-5.0     k,743,-58.66,-74.55,-5.0

!* step-8
!*copying the same set of k.p's for shank of first and fifth hole in -ve y-dir
!* k.p starts from 744 to 767
kgen,2,720,743,1,0,-210.9,0, ,0

!*step-9
!*area no starts from 857 to 904
!*creating the areas bet bolt head and shank for first hole in col. first flange
a,725,247,248,726    a,726,248,250,724    a,724,250,252,728    a,728,252,254,729
a,729,254,256,727    a,727,256,258,730    a,730,258,260,731    a,731,260,262,720
a,720,262,264,722    a,722,264,266,723    a,723,266,268,721    a,721,268,247,725
!*creating the areas bet bolt head and shank for second hole in col. first flange
a,749,295,296,750    a,750,296,298,748    a,748,298,300,752    a,752,300,302,753
a,753,302,304,751    a,751,304,306,754    a,754,306,308,755    a,755,308,310,744
a,744,310,312,746    a,746,312,314,747    a,747,314,316,745    a,745,316,295,749
!*creating the areas bet bolt head and shank for third hole in col. first flange
a,735,271,272,734    a,734,272,274,732    a,732,274,276,743    a,743,276,278,742
a,742,278,280,739    a,739,280,282,741    a,741,282,284,740    a,740,284,286,736
a,736,286,288,738    a,738,288,290,737    a,737,290,292,733    a,733,292,271,735
!*creating the areas bet bolt head and shank for fourth hole in col. first flange
a,759,319,320,758    a,758,320,322,756    a,756,322,324,767    a,767,324,326,766
a,766,326,328,763    a,763,328,330,765    a,765,330,332,764    a,764,332,334,760
a,760,334,336,762    a,762,336,338,761    a,761,338,340,757    a,757,340,319,759
!*area nos for nutt and shank in col flange - 857 to 904

!* step-10
!*modelling of nutt
!*copy same set of areas for nutt thickness in z-direction
!* area nos - 905 to 952 and k.p.s 768 to 863 (total no of k.p =96)
agen,2,857,904,1,0,0,-18,0,1,0

!* step-11
!* create/define volume through key points for first nutt
v,725,247,248,726,768,769,770,771        v,726,248,250,724,771,770,772,773
```

```
v,724,250,252,728,773,772,774,775        v,728,252,254,729,775,774,776,777
v,729,254,256,727,777,776,778,779        v,727,256,258,730,779,778,780,781
v,730,258,260,731,781,780,782,783        v,731,260,262,720,783,782,784,785
v,720,262,264,722,785,784,786,787        v,722,264,266,723,787,786,788,789
v,723,266,268,721,789,788,790,791        v,721,268,247,725,791,790,769,768
!* create/define volume through key points for second nutt
v,749,295,296,750,792,793,794,795        v,750,296,298,748,795,794,796,797
v,748,298,300,752,797,796,798,799        v,752,300,302,753,799,798,800,801
v,753,302,304,751,801,800,802,803        v,751,304,306,754,803,802,804,805
v,754,306,308,755,805,804,806,807        v,755,308,310,744,807,806,808,809
v,744,310,312,746,809,808,810,811        v,746,312,314,747,811,810,812,813
v,747,314,316,745,813,812,814,815        v,745,316,295,749,815,814,793,792
!* create/define volume through key points for third nutt
v,735,271,272,734,816,817,818,819        v,734,272,274,732,819,818,820,821
v,732,274,276,743,821,820,822,823        v,743,276,278,742,823,822,824,825
v,742,278,280,739,825,824,826,827        v,739,280,282,741,827,826,828,829
v,741,282,284,740,829,828,830,831        v,740,284,286,736,831,830,832,833
v,736,286,288,738,833,832,834,835        v,738,288,290,737,835,834,836,837
v,737,290,292,733,837,836,838,839        v,733,292,271,735,839,838,817,816
!* create/define volume through key points for fourth nutt
v,759,319,320,758,840,841,842,843        v,758,320,322,756,843,842,844,845
v,756,322,324,767,845,844,846,847        v,767,324,326,766,847,846,848,849
v,766,326,328,763,849,848,850,851        v,763,328,330,765,851,850,852,853
v,765,330,332,764,853,852,854,855        v,764,332,334,760,855,854,856,857
v,760,334,336,762,857,856,858,859        v,762,336,338,761,859,858,860,861
v,761,338,340,757,861,860,862,863        v,757,340,319,759,863,862,841,840
        !**********modelling of bolt and nutt finished***************
!*step-12
!*creating lines bet bolt head and nutt for shank elements
!*line nos starts from 2055 to 2102
!*for first plate
!* for first hole
!*line nos starts from  2055 to 2066
l,620,768    l,623,771    l,625,773    l,627,775    l,629,777    l,631,779
l,633,781    l,635,783    l,637,785    l,639,787    l,641,789    l,643,791
!* for second hole
!*line nos starts from  2067 to 2078
l,644,792    l,647,795    l,649,797    l,651,799    l,653,801    l,655,803
l,657,805    l,659,807    l,661,809    l,663,811    l,665,813    l,667,815
!* for third hole
!*line nos starts from  2079 to 2090
l,668,816    l,671,819    l,673,821    l,675,823    l,677,825    l,679,827
l,681,829    l,683,831    l,685,833    l,687,835    l,689,837    l,691,839
!* for fourth hole
!*line nos starts from  2091 to 2102
l,692,840    l,695,843    l,697,845    l,699,847    l,701,849    l,703,851
l,705,853    l,707,855    l,709,857    l,711,859    l,713,861    l,715,863
```

```
!**creating k.ps for beam on +ve-z-dir
!*k.p's start from 864 to 896
!* K.p's for beam top flange
k,864,0,-26.65,1595          k,865,40.775,-26.65,1595     k,866,50.0,-26.65,1595
k,867,59.225,-26.65,1595     k,868,83.45,-26.65,1595      k,869,-40.775,-26.65,1595
k,870,-50.0,-26.65,1595      k,871,-59.225,-26.65,1595    k,872,-83.45,-26.65,1595
!* K.p's for beam bottom flange
k,873,0,-323.35,1595         k,874,40.775,-323.35,1595    k,875,50.0,-323.35,1595
k,876,59.225,-323.35,1595    k,877,83.45,-323.35,1595     k,878,-40.775,-323.35,1595
k,879,-50.0,-323.35,1595     k,880,-59.225,-323.35,1595   k,881,-83.45,-323.35,1595
!* K.p's for beam web
k,882,0,-53.55,1595          k,883,0,-61.55,1595          k,884,0,-69.55,1595
k,885,0,-77.55,1595          k,886,0,-85.55,1595          k,887,0,-104.70,1595
k,888,0,-139.85,1595         k,889,0,-175.0,1595          k,890,0,-210.15,1595
k,891,0,-245.30,1595         k,892,0,-264.45,1595         k,893,0,-272.45,1595
k,894,0,-280.45,1595         k,895,0,-288.45,1595         k,896,0,-296.45,1595

!*creating areas for beam top flange
!*area nos 1097 to 1112 for both top and bottom flange
a,1303,864,865,1304  a,1304,865,866,1305  a,1305,866,867,1306  a,1306,867,868,1307
a,1303,1308,869,864  a,1308,1309,870,869  a,1309,1310,871,870  a,1310,1311,872,871
!*creating areas for beam bottom flange
a,1312,873,874,1313  a,1313,874,875,1314  a,1314,875,876,1315  a,1315,876,877,1316
a,1312,1317,878,873  a,1317,1318,879,878  a,1318,1319,880,879  a,1319,1320,881,880
!*creating areas for beam web
!*area nos 1113 to 1128
a,1303,864,882,1321  a,1321,882,883,1322  a,1322,883,884,1323  a,1323,884,885,1324
a,1324,885,886,1325  a,1325,886,887,1326  a,1326,887,888,1327  a,1327,888,889,1328
a,1328,889,890,1329  a,1329,890,891,1330  a,1330,891,892,1331  a,1331,892,893,1332
a,1332,893,894,1333  a,1333,894,895,1334  a,1334,895,896,1335  a,1335,896,873,1312
!* aglue all

!*creating the areas for column web
!* key point for centre of column flange because of symmetry
k,897,0,0,-151.25            k,898,0,-26.65,-151.25       k,899,0,-53.55,-151.25
k,900,0,-61.55,-151.25       k,901,0,-69.55,-151.25       k,902,0,-77.55,-151.25
k,903,0,-85.55,-151.25       k,904,0,-104.70,-151.25      k,905,0,-139.85,-151.25
k,906,0,-175.0,-151.25       k,907,0,-210.15,-151.25      k,908,0,-245.30,-151.25
k,909,0,-264.45,-151.25      k,910,0,-272.45,-151.25      k,911,0,-280.45,-151.25
k,912,0,-288.45,-151.25      k,913,0,-296.45,-151.25      k,914,0,-323.35,-151.25
k,915,0,-350.0,-151.25       k,916,0,120.0,-151.25        k,917,0,625.0,-151.25
k,918,0,-975.0,-151.25

!*area nos 1129 to 1149
a,342,343,898,897    a,343,364,899,898    a,364,369,900,899    a,369,370,901,900
a,370,371,902,901    a,371,372,903,902    a,372,389,904,903    a,389,400,905,904
a,400,411,906,905    a,411,422,907,906    a,422,433,908,907    a,433,444,909,908
```

```
a,444,449,910,909    a,449,450,911,910    a,450,451,912,911    a,451,452,913,912
a,452,469,914,913    a,469,480,915,914    a,480,555,918,915    a,529,342,897,916
a,542,529,916,917

!* Define element type

ET,1,shell143  ! Element type for first end plate
!*
ET,2,shell143  ! Element type for column flange
!*
ET,3,shell143  ! Element type for column web
!*
ET,4,shell143  ! Element type for beam top flange
!*
ET,5,shell143  ! Element type for beam bottom flange
!*
ET,6,shell143  ! Element type for beam web
!*
ET,7,solid185   ! Element type for botls and nutts
!*
ET,8,link8      ! element type for link lines inside bolt and nutts
!*
ET,9,CONTAC52   ! element type for connecting pt to pt bet end plate and col

!* Real constants
R, 1, 12,12,12,12, , ,                ! real constant for shell element type 1
R, 2, 20.5, 20.5, 20.5, 20.5, , ,     ! real constant for shell element type 2
R, 3, 12.7, 12.7, 12.7, 12.7, , ,     ! real constant for shell element type 3
R, 4, 6.8, 6.8, 6.8, 6.8, , ,         ! real constant for shell element type 4
R, 5, 6.8, 6.8, 6.8, 6.8, , ,         ! real constant for shell element type 5
R, 6, 5.7, 5.7, 5.7, 5.7, , ,         ! real constant for shell element type 6
R, 7, 1, , , , , ,                    ! real constant for solid element type 7
R, 8, 26.18, 0.003, ,                 ! real constant for solid element type 8
R, 9,2000000,0,2,2000000,1e-006,0, ! real constant for contact element type 9

!* material property
MPTEMP,,,,,,,,
MPTEMP,1,0
MPDATA,EX,1,,2e5          ! Young's modulus for material ref. no. 1 is 2E5
MPDATA,PRXY,1,,0.3        ! poisson's ratio for material ref. no. 1 is 0.3
MP,DENS,1,78500E-9        ! Density for material ref. no. 1 is 78500E-9

MPTEMP,,,,,,,,
MPTEMP,1,0
MPDATA,EX,2,,2e5          ! Young's modulus for material ref. no. 2 is 2E5
MPDATA,PRXY,2,,0.3        ! poisson's ratio for material ref. no. 2 is 0.3
MP,DENS,2,78500E-9        ! Density for material ref. no. 2 is 78500E-9
```

```
MPTEMP,,,,,,,,
MPTEMP,1,0
MPDATA,EX,3,,2e5          ! Young's modulus for material ref. no. 3 is 2E5
MPDATA,PRXY,3,,0.3        ! poisson's ratio for material ref. no. 3 is 0.3
MP,DENS,3,78500E-9        ! Density for material ref. no. 3 is 78500E-9

MPTEMP,,,,,,,,
MPTEMP,1,0
MPDATA,EX,4,,2e5          ! Young's modulus for material ref. no. 4 is 2E5
MPDATA,PRXY,4,,0.3        ! poisson's ratio for material ref. no. 4 is 0.3
MP,DENS,4,78500E-9        ! Density for material ref. no. 4 is 78500E-9

MPTEMP,,,,,,,,
MPTEMP,1,0
MPDATA,EX,5,,2e5          ! Young's modulus for material ref. no. 5
MPDATA,PRXY,5,,0.3         ! poisson's ratio for material ref. no. 5
MP,DENS,5,78500E-9         ! Density for material ref. no. 5 is 78500e-9

MPTEMP,,,,,,,,
MPTEMP,1,0
MPDATA,EX,6,,2e5          ! Young's modulus for material ref. no. 6
MPDATA,PRXY,6,,0.3        ! poisson's ratio for material ref. no. 6
MP,DENS,6,78500E-9        ! Density for material ref. no. 6 is 78500e-9

MPTEMP,,,,,,,,
MPTEMP,1,0
MPDATA,EX,7,,2e5          ! Young's modulus for material ref. no. 7
MPDATA,PRXY,7,,0.3        ! poisson's ratio for material ref. no. 7
MP,DENS,7,78500E-9        ! Density for material ref. no. 7 is 78500e-9

MPTEMP,,,,,,,,
MPTEMP,1,0
MPDATA,EX,8,,2e5          ! Young's modulus for material ref. no. 8
MPDATA,PRXY,8,,0.3         ! poisson's ratio for material ref. no. 8
MP,DENS,8,78500E-9         ! Density for material ref. no. 8 is 78500e-9

MPTEMP,,,,,,,,
MPTEMP,1,0
MPDATA,EX,9,,2e5          ! Young's modulus for material ref. no. 9
MPDATA,PRXY,9,,0.3        ! poisson's ratio for material ref. no. 9
MP,DENS,9,78500E-9         ! Density for material ref. no. 9 is 78500e-9

!* mesh attributes for areas
!*for first end plate
AATT, 1, 1, 1, 0,
Alist,1,62,1    Alist,64,67,1   Alist,69,160,1 Alist,162,165,1        Alist,167,184,1
```

```
!*for column flange
AATT, 2, 2, 2, 0,                Alist,63,68,161,166          Alist,185,434,1
!*for column web
AATT, 3, 3, 3, 0,                Alist,1094,1112,1
!*for top flange of beam
AATT, 4, 4, 4, 0,                Alist,1067,1072,1
!*for bottom flange of beam
AATT, 5, 5, 5, 0,                Alist,1088,1093,1
!*for web of beam
AATT, 6, 6, 6, 0,                Alist,1073,1087,1
!*for bolt and nutt
VATT, 7, 7, 7, 0,                Vlist,1,144,1
!*for shank
LATT, 8, 8, 8, 0,                Llist,2079,2126,1
!*for contact lines
LATT, 9, 9, 9, 0,                Llist,829,1059,1

!* meshing the areas of end plate (command :- AMESH, NA1 to NA2, NINC)
!* for area nos inside the hole
AATT, 1, 1, 1, 0,     ESIZE,0,1,          MSHAPE,0,2D          MSHKEY,1
Amesh,1,62,1  Amesh,64,67,1  Amesh,69,160,1  Amesh,162,165,1  Amesh,167,184,1

!*for column top flange
AATT, 2, 2, 2, 0,
!* for end plate porion,
!* for area nos inside the hole
ESIZE,0,1,          MSHAPE,0,2D     MSHKEY,1          amesh, 253,348,1
!* for area nos arround hole
ESIZE,0,1,          MSHAPE,0,2D     MSHKEY,1          amesh,349,504,1
!* for area nos along the column end portion
ESIZE,0,1,          MSHAPE,0,2D     MSHKEY,1          amesh,505,548,1
!*area nos above plate for slab portion
ESIZE,0,2,          MSHAPE,0,2D     MSHKEY,1          amesh,549,560,1
!*area nos above slab portion
ESIZE,0,10,         MSHAPE,0,2D     MSHKEY,1          amesh,561,572,1
!*area nos below plate
ESIZE,0,10,         MSHAPE,0,2D     MSHKEY,1          amesh,573,584,1

!*for column web
AATT, 3, 3, 3, 0,
!* for end plate porion
ESIZE,0,4,          MSHAPE,0,2D     MSHKEY,1          amesh,1891,1915,1

!*for beam top flange
AATT, 4, 4, 4, 0,
ESIZE,0,10,         MSHAPE,0,2D     MSHKEY,1          amesh,1849,1858,1
```

```
!*for beam bottom flange
AATT, 5, 5, 5, 0,
ESIZE,0,10,          MSHAPE,0,2D      MSHKEY,1          amesh,1859,1868,1

!*for beam web
AATT, 6, 6, 6, 0,
ESIZE,0,10,          MSHAPE,0,2D      MSHKEY,1          amesh,1869,1890,1

!* meshing the volumes (command :- vMESH, Nv1 to Nv2, NINC)
!with mapped command
!*for first end plate
!*meshing of bolt and nutt
VATT,7,7,7,0
ESIZE,0,1,           MSHAPE,0,3D      MSHKEY,1          vmesh,1,48,1
!*meshing of nutt (peripheral portion)
vmesh,97,144,1
!*for first end plate
!*meshing of bolt (central portion)
VATT,7,7,7,0
ESIZE,0,1,           MSHAPE,0,3D      MSHKEY,1          vmesh,49,96,1

!*for shank
LATT, 8, 8, 8, 0,
ESIZE,0,1,
Lmesh,3343,3438,1

!*for contact elements
LATT, 9, 9, 9, 0,
ESIZE,0,1,
Lmesh,1169,1493,1

Finish
```

REFERENCES:

1. Commission of the European Communities, Eurocode 3: Design of Steel Structures 1992.

2. Commission of the European Communities, Eurocode 4, Design of Composite Steel and Concrete Structures, 1994.

3. Commission of the European Communities, Eurocode 8, Design provisions for earthquake resistance of Structures, 1994.

4. Bjorhovde R., Colson A., Brozzetti J., Classification System for Beam-to-column connections. Journal of Structural Engineering, 1990, Vol. 116, No. 11, pp. 3059-3076.

5. Hubber.G, and Tschemmernegg.F., Modelling of Beam-to-Column Joints. Journal of Constructional Steel Research, Vol.45, No.2, 1998. pp. 199-216.

6. Y.Xiao, B.S. Choo & D.A. Nethercot, Composite Connections in Steel and Concrete. Partl – Experimental behaviour of composite beam - column connections, Journal of Constructional Steel Research, Vol. 31, No. l, 1994. pp. 3-30.

7. Gizejowzski. M.A., Papangelis.J.P. and Parameswar.H.C., Stability design of semi-continuous steel frame structures., journal of Constructional Steel Research, 1998, Vol.46, No.1-3., Paper No. 148.

8. Fabbrocino.G. Manfredi.G, Cosenza.E, Modelling of continuous steel-concrete composite beams: computational aspects, Computers and Structures, Vol.80, 2002, PP. 2241-2251.

9. Calado.L. and Lamas.A., Seismic modelling and behaviour of steel beam-to-column connections., Journal of Constructional Steel Research, Vol.46, 1998, No.,1-3, paper No. 267.

10. J.Y. Richard Liew, T.H. Teo, N.E. Shanmugam, Composite joints subject to reversal of loading— Part 1: experimental study, journal of Constructional Steel Research, 2004, Vol.60, pp. 221 – 246.

11 J.Y. Richard Liew, T.H. Teo, N.E. Shanmugam, Composite joints subject to reversal of loading—Part 2: analytical assessments, journal of Constructional Steel Research, 2004, Vol.60, pp. 247 – 268.

12. T.Q. Li, D.A. Nethercot, & R.M. Lawson., Required rotation of composite connections, Journal of Constructional Steel Research, Vol.56l, 2000. pp. 151-173.

13. G.H. Couchman, Design of Semi-Continuous Braced Frames, first edition, SCI Publication, Silwood Park Ascot Berkshire, 2002.

14. G. Hubber, Semi-continuous beam-to-column joints at the millennium tower in Vienna, Austria.

15. B.M. Broderick, A.W. Thomson, The response of flush end plate joints under earthquake loading, journal of Constructional Steel Research, 2002, Vol.58, pp. 1161 - 1175

16. European Steel Design Education Programme (ESDEP) – WG 11 – Lecture 11.7

17. ANSYS theory reference, Release 8.1. ANSYS Incorporation, Canonsburg, 1999.

18. Mohamed R. Bahaari & Archilbald N. Sherbourne, 3D Simulation of Bolted Connections to Unstiffened Columns – II. Extended Endplate Connections, Journal of Constructional Steel Research, Vol. 40, No. 3, 1996. pp. 189-223.

19. Y.Xiao, B.S. Choo & D.A. Nethercot, Composite Connections in Steel and Concrete. Part2 – Moment capacity of end plate beam to column Connections, Journal of Constructional Steel Research, Vol. 37, No. l, 1996. pp. 63-90

20. Robert Y. Xiao and C.D. Fisher, Site monitoring and Computational analysis of semi-continuous composite steel frame structure, International conference in Connections in steel structure IV: Steel Connections in the new millennium – October 22 – 25, 2000, Roanoke, Virginia, USA

21. European Steel Design Education Programme (ESDEP) – WG 17 – Lecture 17.3 - The Cyclic Behaviour of Steel Elements and Connections.

22. Y.I. Maggi, R.M. Goncalves, R.T. Leon & L.F.L. Ribeiro, Parametric analysis of steel and bolted end plate connections using finite element modelling, Journal of Constructional Steel Research, Vol. 61, 2005. pp. 689-708.

23. Ahmed B, Nethercot DA, Prediction of initial stiffness and available rotation capacity of major axis composite flush end plate connection, Journal of Constructional Steel Research, 1997, Vol.41, pp. 31–60.

24. Cheng-chih chen, Shuan-Wei Chen, Ming-Dar Chung, Ming- Chih Lin, Cyclic behaviour of unreinforced and rib-reinforced moment connections, Journal of Constructional Steel Research, 2005, Vol.61, pp. 1–21.

25 Chandrakant S. Desai John F. Abel, Introduction to the finite element method, Van Nostrand Reinhold Ltd, New York.